2007

THE ROLE OF THE MACROPHAGE IN ASBESTOS INDUCED AUTOANTIBODY PRODUCTION

David J. Blake
The University of Montana

THE ROLE OF THE MACROPHAGE IN

ASBESTOS INDUCED AUTOANTIBODY PRODUCTION

By

David J. Blake Jr.

Master of Science, University of Montana-Missoula, Missoula, Montana, 2005
Bachelor of Arts, University of Pennsylvania, Philadelphia, Pennsylvania, 1999

Dissertation

presented in partial fulfillment of the requirements
for the degree of

Doctor of Philosophy
in Integrated Microbiology and Biochemistry
with an emphasis in Molecular Biology

The University of Montana
Missoula, MT

July 2007

Approved by:

Dr. David A. Strobel, Dean
Graduate School

Michael F. Minnick, Chair
Division of Biological Sciences

Jean C. Pfau
Biomedical and Pharmaceutical Sciences

Jesse Hay
Division of Biological Sciences

Scott Wetzel
Division of Biological Sciences

Jean-Marc Lanchy
Division of Biological Sciences

Blake Jr., David J., PhD, Summer 2007 Biochemistry/Microbiology

The role of the macrophage in asbestos induced autoantibody production

Chairperson: Michael F. Minnick

Environmental exposure to silicate compounds such as silica and asbestos has been associated with increased autoimmune responses and the development of autoimmune disease in humans. Residents of Libby, MT have experienced significant asbestos exposure due to an asbestos contaminated vermiculite mine near the community over several decades. Residents have developed numerous asbestos-related diseases as well as increased autoimmune responses. However, the exact mechanism by which Libby amphibole asbestos generates autoimmune responses is unclear. To elucidate a possible mechanism for asbestos induced autoimmunity, the cellular effects of Libby amphibole asbestos were characterized *in vitro* using a phagocytic murine macrophage cell line, which are characteristic of alveolar macrophages. Our results indicate that Libby amphibole asbestos generates oxidative stress in murine macrophages similar to crocidolite asbestos. However, Libby asbestos induces distinct cellular effects compared to crocidolite asbestos. Therefore, the cellular effects of amphibole asbestos may be a combined consequence of its chemical composition as well as the activation of distinct cellular pathways during exposure. Libby amphibole asbestos also induces apoptosis in murine macrophages resulting in the translocation of SSA/Ro52 to cell surface blebs of apoptotic cells. These apoptotic cell surface blebs are recognized by autoantibodies from mice exposed to amphibole asbestos, suggesting that these cell surface structures may be antigenic when presented in a pro-inflammatory context. These results suggest that the induction of apoptosis may play a key role in environmentally induced autoimmunity. Interestingly, autoantibodies found in the sera of the Libby cohort also recognize the SSA/Ro52 autoantigen, indicating that humans and mice exposed to amphibole asbestos generate similar AA profiles and that the alterations of the immune response by amphibole asbestos may be comparable. We hypothesize that asbestos-induced autoimmunity is generated through a two hit mechanism. First, autoantigens become visible to the immune system during apoptosis, which results in the accumulation of autoantigens on the cell surface. The subsequent uptake and processing of apoptotic cells by antigen-presenting cells in a pro-inflammatory context will activate self-reactive T cells, inducing the loss of tolerance and generate the autoimmune responses.

Acknowledgments

In order to successfully complete a dissertation project one needs to believe in oneself and work diligently to complete the task. I truly enjoyed working on this dissertation and learned more than I thought was possible about science, life and asbestos. One also needs a mentor that will support their student throughout their career. I was fortunate enough to find Jean and I wish to thank Jean for letting me work in her laboratory. Jean is a great person in life and science as well as a great mentor. She supported me without hesitation and was able to make me focus when needed. I truly believe she is and will be always a terrific teacher and hope that she continues to enjoy research and science for a long, long time to come. I also want to thank all the faculty members on my committee. Mike wrote letters of recommendations for me and let me bother him during his sabbatical. Thanks Mike! Scott and Jesse were great resources for any questions I had about cell biology or immunology and were very willing to discuss any problems I had with science. Jean-Marc enabled me to graduate in the summer by filling in for Steve and reading my dissertation. I want to thank Steve too even though he is finishing up in Scotland. He helped me through some of the hardest times of my graduate school career. Finally, I would like to thank Amber for not only dealing with me during graduate school but for providing the emotional support I need in the toughest of times. I love you.

Table of Contents

Table of Figures

Chapter 1

Introduction

Asbestos exposure in humans is associated with the development of malignant and nonmalignant diseases including lung cancer, pulmonary fibrosis (asbestosis) and an increased frequency of autoantibody production (112, 141, 167, 189). Although the commercial use of asbestos has decreased in the United States since the 1970s, asbestos exposure remains a major environmental health concern. More than 30 million tons of asbestos have been mined in the U.S. alone (120) and more than 27 million people have been exposed to asbestos between 1940 and 1979 (126). As late as 1989, the use of asbestos products in the U.S. exceeded 55,000 tons per year (1). Developed countries have restricted the use of asbestos because of its harmful public health effects. However, asbestos is now a major concern in developing countries due to increased marketing and commercial use (85, 91). Additionally, in 2002 the vermiculite mine and community of Libby, MT have been designated as EPA Superfund sites due to the amphibole asbestos contamination of vermiculite, which led to exposure throughout the mine site and surrounding area. Significant health issues have become evident in Libby and many other sites where the vermiculite was shipped for processing. Hence, asbestos exposure remains an immediate environmental health concern not only in Libby, MT but throughout the United States and in developing countries.

Physical characteristics and utility of asbestos

Asbestos is a general term for hydrated silicate fibers that are strong and heat-resistant. Because of its high tensile strength and ability to absorb heat, asbestos has been used extensively as a building material in roofing, siding, fire protection material, heating and electrical wire insulation, appliance components, sheet flooring, ceiling and floor tiles, and drywall.

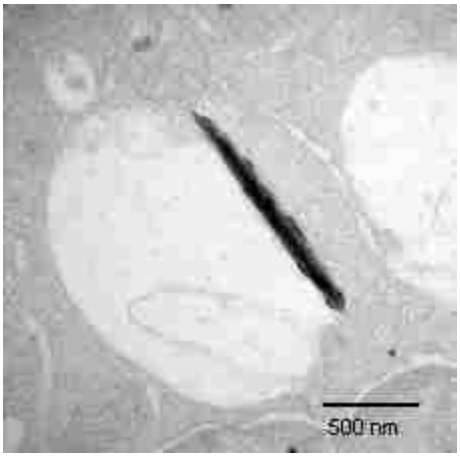

Figure 1.1: Transmission electron micrograph of a Libby amphibole asbestos fiber in a vacuole of a murine macrophage cell. Magnification = 40,000X

Asbestos fibers are categorized into two separate families based on morphology. Amphibole fibers are straight rod-like fibers that include fibers such as amosite, tremolite, crocidolite and Libby amphibole asbestos (Fig. 1.1). In contrast, serpentine fibers are curved pliable fibers. The serpentine fiber family includes a single fiber type, chrysotile, which accounts for 95% of the world's asbestos consumption (95). Chrysotile asbestos fibers are not as biopersistent in the lung and break down into fibrils, which are subsequently destroyed by alveolar macrophages (7). Therefore, exposure to chrysotile asbestos is not associated with lung cancer (198). Amphibole asbestos fibers do not dissolve or breakdown over time. Moreover, amphibole asbestos fibers can remain airborne in contaminated areas and eventually settle into soil, sediment and tree bark (185). Therefore, the toxic potential of asbestos fibers remains constant in contaminated areas once they are introduced into the environment.

Amphibole asbestos contamination in Libby, MT

From 1924 to 1990, Zonolite Mountain in Libby, Montana was the site of a vermiculite mining operation. In 1963, W.R. Grace bought the Zonolite mining operations, which subsequently provided approximately 80% of the world's supply of vermiculite (159). Unfortunately the vermiculite extracted from the Libby mine was contaminated with naturally-occurring asbestos fibers. The mine closed in 1990 after almost 70 years of operation. The first emergency response team from the Environmental Protection Agency (EPA) was sent to Libby, MT in November 1999. The EPA began collecting air, soil and insulation samples over the next few months. In October of 2002 the vermiculite mine and surrounding community of Libby, Montana were designated as EPA Superfund sites due to the asbestos contamination of vermiculite. The various mining, transportation, and processing activities as well as the personal and commercial use of vermiculite in the community led to widespread environmental exposures in the Libby area (43), which resulted in significant asbestos-related diseases even in residents with short exposure times of less than a year (190).

The asbestos contamination of Libby vermiculite has been characterized as both regulated asbestos fibers (e.g., tremolite and other amphibole forms) and unregulated fibers (e.g., winchite and richterite) (113). The mixture of amphibole fibers in the Libby amphibole sample differs in terms of fiber length and metallic cations expressed on the fiber surface. Moreover, these amphibole fibers are thought to be more pathogenic than serpentine asbestos fibers because the longer amphibole fibers cannot be readily cleared from the lung (6).

The extensive asbestos exposure has led to considerable health problems in the community including reduced pulmonary function, enhanced autoimmune responses and increased mortality from lung cancer, malignant mesothelioma and fibrosis (112, 141, 189). Significant health issues have become evident in Libby and many other sites where the vermiculite was shipped for processing (3, 112). The asbestos-related disease (ARD) observed in patients from Libby include interstitial fibrosis, pleural plaques, and mesothelioma, with rapid progression in a subset of patients (189). Although the exact mechanism leading to the progression of ARD has not been fully characterized, recent evidence indicates that these diseases may be immunologically mediated (2, 16, 71).

Occupational asbestos exposure results in a higher prevalence of positive autoantibodies that recognize host derived intracellular antigens (96, 127, 200). Moreover, a positive correlation exists between the development of autoantibodies and the onset of pulmonary fibrosis, which suggests that autoantibodies play a role in asbestos induced lung disease (169). A recent study from our laboratory supported these conclusions and established that a significantly higher proportion of asbestos exposed individuals from Libby, MT exhibit positive autoantibody tests compared to an unexposed control group (141). A murine model of asbestos induced autoimmunity was subsequently generated (140). Asbestos exposed mice developed an increased prevalence of autoantibodies, which preceded symptoms of systemic autoimmunity, such as glomerulonephritis. Autoantibody production in asbestos exposed individuals is known to precede ARD and is correlated with more severe ARD (141, 169). Taken together, these data indicate that autoantibody production may precede and even exacerbate the progression of asbestos-related lung disease (ARD). However, a comprehensive study

focusing on a possible mechanism of asbestos induced autoantibodies has not been performed.

Environmental exposure is associated with systemic autoimmune disease (SAID)

Systemic autoimmune diseases are complex, multisystem diseases that can be life threatening. They are characterized by humoral and cellular immunity to self-antigens and include diseases such as systemic lupus erythematosus (SLE), scleroderma (SSc), Sjogren's syndrome (SS) and rheumatoid arthritis (RA). Although the etiologies of systemic autoimmune diseases remain unknown it is clear that many factors are important in the induction of these diseases including genetic, dietary, hormonal, racial and environmental differences (39, 40).

The importance of hormonal and racial differences in SAID is highlighted by the fact that more than 85% of SLE patients are females and that the incidence of SLE is approximately three times higher among African-Americans than Caucasians (82). Dietary differences are thought to be an important component of SAID because although autoimmune diseases occur predominately in the Western world, immigrants develop the same incidence of SAID as the indigenous population over time (39). A number of environmental factors also activate the immune system and contribute to the development and immunopathology of these diseases.

For example, exposure to silica in "dusty" occupations such as mining, stone cutting or sand blasting can cause chronic pulmonary diseases such as SLE and SSc (36, 136, 150). The mechanism by which silica causes SAID remains unknown, however, evidence suggest that silica particles are phagocytized by alveolar macrophage, which

then interact with immune cells in an inflammatory environment, possibly generating the pathological features observed in silica induced autoimmunity (16, 40).

Mercury is another well recognized environmental factor that generates systemic autoimmunity in humans as well as in mice (32, 64, 143). Occupational exposure to mercury occurs through the mining and processing of raw oil. Environmental exposure is mainly through the ingestion of contaminated fish. Finally, UV radiation is associated with exacerbations in patients with SLE. UV radiation is known to aggravate skin lesions in patients with SLE and exacerbate disease activity (199). Interestingly, patients with autoantibodies to SSA/Ro52 are even more sensitive to UV radiation than typical SLE patient (62).

Taken together, these studies provide a clear link between exposures to certain environmental factors with the exacerbation of a known SAID or the initiation of a disease that resembles traditional SAID. The mechanism and pathological effects of different environmental factors may induce separate SAID, however, all these factors seem to share a common nonspecific adjuvant effect on the immune system, which may be responsible for the development of autoimmunity. Asbestos may function as an environmental adjuvant in the lung initiating a pro-inflammatory condition leading to the loss of tolerance.

Systemic autoimmune disease and autoantibody specificity

Autoantibody production is a key feature of systemic autoimmune disease (SAID) (105). The etiology of SAID is complex and thought to involve multiple pathways, such as increased oxidative stress, elevated levels of apoptosis, disregulated clearance of

apoptotic debris and the redistribution of targeted autoantigens (2, 16, 26, 29, 153, 154). However, all patients diagnosed with SAID share a common clinical manifestation, which is the aberrant production of antibodies against well conserved autoantigens. Autoantibodies (AAs) are specific to nuclear and cytosolic antigens such as double stranded DNA, histones, tRNA synthetase and an E3 ubiquitin ligase.

SAID has been clearly linked to many environmental exposures such as mercury, silica, iodine and possibly asbestos exposure (13, 16, 110, 141). Therefore, it has been proposed that xenobiotics may alter the molecular context or localization of specific autoantigens and lead to the aberrant processing and presentation of these autoantigens on the surface of cells (29). Exposure to xenobiotics, such as asbestos and silica, leads to a chronic inflammatory response (78). Consequently, the altered presentation of antigenic epitopes in the context of a chronic inflammatory response may stimulate tolerance to be broken and thereby generate an immune response against specific autoantigens.

Mercury induced systemic autoimmunity provides an excellent example of how an environmental stimulus can modify cellular autoantigens that generates a specific immune response to the antigenic autoantigen, which can be identified by the specificity of the AA produced. Anti-fibrillarin antibodies are found in SAID such as scleroderma, which has been associated with mercury exposure (110). Therefore, mercury was hypothesized to alter the presentation of fibrillarin so that the protein was recognized as antigenic by the immune system. Mercury was subsequently shown to interact with fibrillarin and lead to its altered presentation to the immune system, which ultimately resulted in the production of anti-fibrillarin AAs (143). In this case, the specificity of the

AA provided valuable information regarding a possible mechanism by which SAID is initiated during mercury exposure.

Exposure to amphibole asbestos induces many clinical features of systemic autoimmunity in C57/BL6 mice, which is a non-autoimmune prone mouse model (140). The AAs generated in response to asbestos, target a specific intracellular antigen, SSA/Ro52. This autoantigen has been recently reported to be a ubiquitously expressed ubiquitin ligase (183). Moreover, this autoantigen is also targeted by AAs obtained from asbestos exposed community members from Libby, MT (141). Therefore, the specificity of the AA in both humans and mice indicate that this protein may be presented as antigenic during the immune response generated by asbestos exposure.

Oxidative stress induced by asbestos exposure

An extensive amount of evidence indicates that cells exposed to amphibole asbestos generate reactive oxygen species (ROS) such as the superoxide anion and the hydroxyl radical (73, 77, 81, 102, 103, 124, 164, 187). Asbestos induced ROS leads to the activation of a number of transcription factors such as AP-1 and NF-KB (30, 51, 53) as well as the release of a number of pro-inflammatory cytokines such as TNF-alpha and IL-1 (46, 100, 138). Therefore, ROS may contribute to the development of an inflammatory state and the subsequent immune response generated by asbestos (8, 124). Interestingly, oxidative stress induced by asbestos fibers has also been postulated to play a key role in the initiation of asbestos induced autoimmunity (162).

ROS generated by asbestos originates from at least three distinct cellular sources. First, asbestos induced ROS functions during the induction of apoptosis in exposed cells. Alveolar epithelial cells exposed to amosite asbestos generate intracellular ROS as a

consequence of mitochondrial DNA damage (135). Amosite induced ROS initiates mitochondrial-regulated apoptosis by activating p53 and caspase 3 and 9 (134). Second, amphibole asbestos fibers, in particular crocidolite and amosite, which contain a high iron content, can spontaneously generate ROS in the presence of hydrogen peroxide through iron catalyzed reactions via the Fenton reaction (88, 188). Crocidolite asbestos triggers cellular toxicity via ROS in macrophages *in vitro*. However, in the presence of iron chelators, asbestos induced cell toxicity is abrogated (67). The importance of fiber chemistry is supported *in vivo* where iron chelators also provide a protective role against pulmonary inflammation and fibrosis (89).

Finally, crocidolite induces ROS production through the release of ROS activating inflammatory cells such as macrophages and neutrophils (88, 123, 124, 178). Crocidolite asbestos fibers have also been shown to stimulate the release of reactive oxygen metabolites from peritoneal macrophages *in vitro* (66). Alveolar macrophages (AMs) that interact with asbestos fibers release ROS extracellularly, specifically the superoxide anion, which is reduced in response to protein kinase C (PKC) and calcium channel inhibitors (87, 151). These results suggest that NADPH oxidase may become activated in response to asbestos, generating ROS *in vitro*.

AMs function to reduce the lung fiber burden by migrating to the site of asbestos deposition and clearing asbestos fibers through phagocytosis (94, 165). Amphibole asbestos fibers, such as crocidolite and tremolite, are straight rod-like fibers that are difficult to phagocytose and clear, leading to "frustrated phagocytosis" and increased oxidative stress for the cell (67). This can result in either cell death or activation of AMs. These events appear to increase antigen presenting cell (APC) activity (70, 71).

Therefore, the alveolar macrophage is a pivotal cell type by which ROS and inflammation can be initiated.

Redistribution of autoantigens involved in systemic autoimmunity

Because antigen processing and presentation constitute the basis for all antigen-driven autoimmune responses, the effects of xenobiotics on the degradation and localization of autoantigens have been characterized to elucidate possible molecular mechanisms of autoimmunity. Xenobiotics have been shown to promote the aberrant redistribution of autoantigens to discrete locations in exposed cells. First, xenobiotics have been shown to alter the localization of nuclear proteins to nucleoplasmic clusters, where they colocalize with proteasomes and are subjected to proteasomal proteolysis. Second, certain autoantigens redistribute themselves to apoptotic blebs at the plasma membrane surface in response to xenobiotics. The uptake and processing of apoptotic cells in a pro-inflammatory context may activate self-reactive T-cells and generate an autoimmune response.

Exposure to xenobiotics such as silica nanoparticles results in the redistribution of the systemic sclerosis (SSc) autoantigen, DNA topoisomerase I (topo-I), to nucleoplasmic clusters that colocalize with the 20S proteasome (27, 29) (Fig. 1.2). The xenobiotic induced redistribution may have important clinical significance, because the colocalization of topo-I and proteasomes occur exclusively in dendritic cells from SSc patients who have developed AAs that specifically recognize DNA topoisomerase I. These data support the hypothesis that the redistribution of nuclear proteins to the

proteasome *in vivo* is correlated with autoimmune responses against specific autoantigens (27-29).

Xenobiotics also redistribute autoantigens to the plasma membrane. Translocation of autoantigens occurs in response to environmental factors known to induce autoimmunity (54, 156). Systemic lupus erythematosus (SLE) is characterized by the production of AAs against certain proteins such as double-stranded DNA (dsDNA) or DNA/RNA/protein complexes. Several lupus autoantigens, which are localized intracellularly in resting cells, are known to translocate to the plasma membrane during environmental exposure (59, 63, 99). UVB radiation on keratinocytes results in the redistribution of Ro52, which is an autoantigen commonly recognized by patients with SLE, to the plasma membrane surface (21, 54, 156). Autoantigens may become 'visible' to the immune system during apoptosis, which results in the accumulation of these antigens at the cell surface (Fig. 2B). Although the redistribution and translocation of intracellular autoantigens have been observed, the manner by which the redistribution occurs in xenobiotically exposed cells may take place through two separate mechanisms.

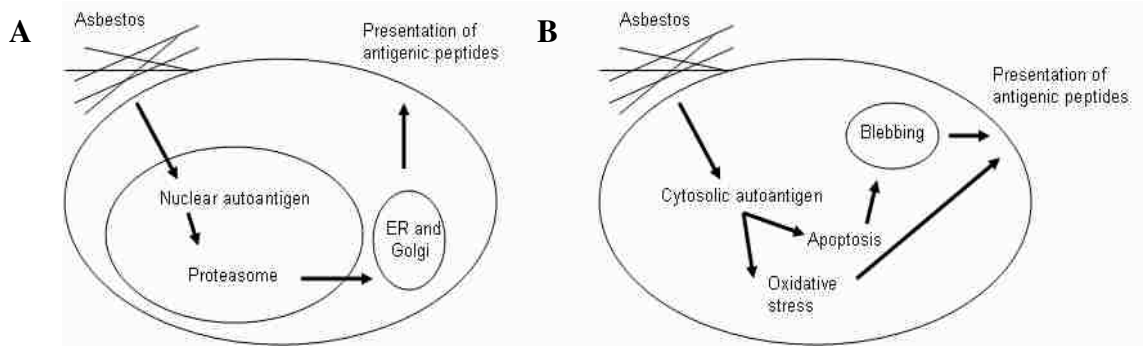

Figure 1.2: Two proposed mechanisms for the aberrant processing and presentation of autoantigens targeted in SAID. In figure 2A, an environmental stimulus, such as asbestos, may result in the redistribution of nuclear autoantigens to the proteasome. In figure 2B, asbestos may lead to the translocation of autoantigens to the cell surface through apoptotic or oxidative stress mechanisms. Both pathways result in the presentation of antigenic epitope to the immune system.

Both oxidative stress and apoptosis have been shown to play a role in the redistribution of autoantigens. For example, the surface expression of the Ro52 autoantigen by UVB radiation has been shown to be independent from apoptosis, which suggests that oxidative stress and not apoptosis induces the alteration of certain nuclear proteins (156). However, other studies indicate that the redistribution of nuclear autoantigens, such as histones, is dependent on programmed cell death and can be blocked with caspase inhibitors as well as with inhibitors of chromatin fragmentation (54). Consequently, it is not clear whether apoptosis or oxidative stress functions as the principle mechanism behind the redistribution of nuclear autoantigens. The possibility exists that different autoantigens become redistributed through separate mechanisms (21). Therefore, since the mechanism involved in the initiation of SAID remains unclear, the redistribution of nuclear autoantigens to the proteasome or to the plasma membrane may occur during asbestos exposure. This premise will be specifically tested in Specific Aim 2 focusing on the intracellular antigen SSA/Ro-52. The aim of this dissertation research concentrates on characterizing the cellular response to asbestos exposure and predicts that an alteration in the host cell environment due to asbestos exposure will lead to a redistribution of nuclear autoantigens.

Possible mechanisms for the initiation of systemic autoimmunity

Two principle immunological events must occur in order for SAID to develop in humans. First, a chronic inflammatory state must be maintained within an individual. Second, tolerance to self-antigens must be broken in order to elicit a humoral immune

response. A chronic inflammatory response and broken tolerance to self-antigens are hypothesized to occur as a result of two main pathways; apoptosis and oxidative stress.

Apoptotic cells generated by environmental exposure such as asbestos may lead to SAID through the presentation of antigenic epitopes not normally seen by the immune system. Apoptotic cells are rapidly removed by professional phagocytotic cells such as dendritic cells and lead to immunosuppresion or lack of an inflammatory response (49, 148). In contrast, secondary necrosis due to overwhelming rates of cellular apoptosis or deficits in apoptotic cell clearance results in inflammation and the release of intracellular antigens to the immune system (191). Indeed, animal models that have abnormal apoptotic cell clearance have a higher prevalence of AAs (72, 119, 161). However, because many redundant mechanisms are involved in the clearance of apoptotic cells, a defect in clearance alone is not sufficient to induce autoimmunity (106).

As previously stated, many intracellular autoantigens targeted by SAID are known to cluster on the surface of apoptotic cells or blebs (153). Asbestos has been shown to lead to apoptosis in exposed cells (70). Many autoantigens have been shown to undergo cleavage and processing during apoptosis. It is thought that these unique cleavage peptides may provide the stimulus for initiating an autoantibody response (129, 153). In fact, some autoantigens involved in SSc are cleaved by metal-catalyzed redox reactions to yield specific targets for the antibodies detected in these patients (22). Therefore, apoptosis may induce novel self-antigens to be presented to an immune system that has not gone through tolerance to these cryptic epitopes (98).

One mechanism by which apoptosis can induce the generation of new epitope is through the activation of granzyme B. Granzyme B is a serine protease found in the

cytoplasm of cytotoxic T-cells and natural killer cells. Granzyme B activation and the subsequent cleavage of B23, which is a nucleolar autoantigen recognized by AAs in SSc patients, generates novel antigens that are distinct from caspase cleaved antigens (176, 177). Moreover, efficient cleavage by granzyme B has been observed for other systemic autoimmune autoantigens (153). Therefore, asbestos exposure may result in an increased rate of apoptosis in exposed cells, which leads to the generation of novel antigenic epitopes that are subsequently recognized by the humoral immune response. Alternatively, autoantigens clustered on the surface of apoptotic cells may be recognized by the immune system. The subsequent processing and presentation of these autoantigens may activate self-reactive T cells to generate an immune response (152).

Oxidative stress induced by ROS has been implicated in the initiation of SAID. ROS are transient high energy molecules, such as the hydroxyl radical or the superoxide anion, with one or more unpaired electrons. ROS are normally produced by cellular metabolism and are detoxified through cellular reducing agents such as glutathione (GSH) and antioxidants such as superoxide dismutase (SOD) or vitamin E. An imbalance in ROS and cellular defenses leads to oxidative stress. Oxidative stress can lead to a myriad of cellular alterations including damage to lipids (lipid peroxidation) and DNA (oxidation of deoxyguanosine (8-oxo-2dG)). Interestingly, lymphocytes isolated from patients with rheumatoid arthritis (RA) and SLE have increased levels of 8-oxo-dG, suggesting that oxidative stress is involved in SAID (104). Although native dsDNA is not immunogenic, dsDNA modified by oxidative stress is highly immunogenic (38, 61). Experimental exposure to ROS-modified DNA generates anti-dsDNA antibodies that cross react with both native and modified DNA (4). Moreover, proteins can be modified

through ROS and promote protein-DNA crosslinking. Therefore, it follows that oxidative stress induced by asbestos exposure may modify DNA or proteins within exposed cells and these novel antigens could be presented to the immune system to generate specific AAs.

Hypothesis and Specific Aims

Asbestos exposure has been shown to generate oxidative stress in exposed cells, which triggers a number of cellular events, including ROS production, DNA damage and apoptosis (9). Therefore, our central hypothesis is that oxidative stress induced by exposure to Libby amphibole asbestos leads to a modified cellular environment, which subsequently generates the aberrant processing and presentation of autoantigens. The specific aims of this proposal test this hypothesis *in vitro* using cultured macrophages as the putative target for oxidative stress, *ex vivo* using primary macrophage from naïve murine lungs as well as *in vivo*. The goal of this research is to identify a possible mechanism by which asbestos induces autoantibody production. This research will add to our understanding of the human health effects of asbestos and has the potential to identify therapeutic targets in asbestos related diseases. The Specific Aims that are addressed in the dissertation research presented here are:

Specific Aim 1: Establish whether Libby asbestos is internalized and results in the activation of the NADPH oxidase complex by murine macrophages.

Specific Aim 2: Determine whether asbestos exposure promotes the redistribution of autoantigens in exposed cells.

Chapter 2

Internalization of Libby amphibole asbestos and induction of oxidative stress in murine macrophages

David J. Blake[*], Celeste M. Bolin[†], David P. Cox[†], Fernando Cardozo-Pelaez[†] and Jean C. Pfau[†]

Division of Biological Sciences[*] and Department of Biomedical & Pharmaceutical Sciences, Center for Environmental Health Sciences[†], University of Montana, Missoula, Montana, 59812

Abstract: The community members of Libby, Montana have experienced significant asbestos exposure and developed numerous asbestos related diseases (ARD) including fibrosis and lung cancer due to an asbestos contaminated vermiculite mine near the community. The form of asbestos in the contaminated vermiculite has been characterized in the amphibole family of fibers. However, the pathogenic effects of these fibers have not been previously characterized. The purpose of this study is to determine the cellular consequences of Libby amphibole exposure in macrophages compared to another well characterized amphibole fiber; crocidolite asbestos. Our results indicate that Libby asbestos fibers are internalized by macrophages and localize to the cytoplasm and cytoplasmic vacuoles similar to crocidolite fibers. Libby asbestos fiber internalization generates a significant increase in intracellular reactive oxygen species (ROS) as determined by DCFDA and DHE fluorescence indicating that the superoxide anion is the major contributing ROS generated by Libby asbestos. Elevated superoxide levels in macrophages exposed to Libby asbestos coincide with a significant suppression of total

SOD activity. Both Libby and crocidolite asbestos generate oxidative stress in exposed macrophages by decreasing intracellular GSH levels. Interestingly crocidolite asbestos, but not Libby asbestos, induces significant DNA damage in macrophages. This study provides evidence that the difference in the level of DNA damage observed between Libby and crocidolite asbestos may be a combined consequence of the distinct chemical compositions of each fiber as well as the activation of separate cellular pathways during asbestos exposure.

Keywords: asbestos, Libby amphibole, murine macrophage, oxidative stress, DNA damage

Introduction

Asbestos exposure in humans is associated with the development of asbestos-related diseases (ARD) such as pulmonary fibrosis and lung cancer. Although the exact mechanism leading to the progression of ARD has not been fully explained, mounting evidence indicates that reactive oxygen species (ROS), such as the superoxide anion and the hydroxyl radical, play a significant role (8, 90). Because airways are continuously exposed to high levels of environmental oxidants, they must maintain the proper balance between pro-oxidants and antioxidants to prevent oxidative stress and cellular damage. Environmental toxicants that alter the cellular redox state in the lung promote oxidative stress and lead to pulmonary injury. Oxidative stress is therefore associated with numerous pulmonary diseases including asthma, chronic obstructive pulmonary disease and pulmonary fibrosis (147).

The vermiculite mine and surrounding community of Libby, Montana were designated as EPA Superfund sites in 2002 due to the asbestos contamination of

vermiculite, which led to significant asbestos exposure throughout the mine site and surrounding area (190). The extensive asbestos exposure has led to considerable health problems in the community including reduced pulmonary function, enhanced autoimmune responses and increased mortality from lung cancer, malignant mesothelioma and fibrosis (112, 141, 189). The form of asbestos in Libby's contaminated vermiculite has been characterized in the amphibole family of fibers and consists of several hydrated silicate fibers, including regulated fibers (tremolite) and unregulated fibers (winchite and richterite) (114). The regulated and unregulated fibers within Libby amphibole asbestos differ in terms of length and in the metallic cations expressed on their surface. Because of their diverse chemical composition Libby amphibole fibers are different from other well studied amphibole fibers, such as crocidolite and amosite, and therefore may induce distinct cellular effects in exposed cells.

Crocidolite asbestos generates an increase in ROS, which leads to a depletion of intracellular glutathione and oxidative damage to DNA and lipids in several cell types (51, 58, 65, 84, 88, 92, 178, 195, 196). Moreover, ROS induced by crocidolite plays an important role in the activation of redox sensitive transcription factors such as NF-KB and AP-1 (51, 53). Because ROS generated by amphibole asbestos results in oxidative stress, the mechanism by which asbestos induces ROS production has been extensively studied. However, the exact source of ROS in response to asbestos fibers is an area of considerable debate and may be due to the unique chemical characteristics of the asbestos fiber (90).

Amphibole asbestos generates increased levels of ROS through at least two independent mechanisms. Amphibole asbestos fibers, specifically crocidolite and amosite, participate in the direct production of ROS via iron-catalyzed reactions due to

their high iron content (90, 122). This mechanism is supported by studies demonstrating that crocidolite asbestos cytotoxicity can be abrogated in the presence of iron chelators (67). The importance of iron in asbestos fiber chemistry is also supported *in vivo* given the fact that iron chelators protect against pulmonary inflammation and fibrosis (89). The second proposed mechanism by which amphibole asbestos generates oxidative stress is through the production of mitochondrial-derived ROS. Alveolar epithelial cells generate intracellular ROS, which results in DNA damage and apoptosis in response to amosite asbestos (134, 135).

The alveolar macrophage is the primary cell type that interacts with inhaled particles and functions to clear particles from the lung. Therefore, our study utilizes primary murine alveolar macrophages and a well characterized macrophage cell line. Our data indicate that Libby amphibole asbestos induces oxidative stress in murine macrophages through increasing ROS levels and suppressing SOD activity. The cellular effects of Libby asbestos exposure appear to be distinct from what is observed with crocidolite asbestos and may be a result of the activation of separate cellular mechanisms within exposed macrophages. This is the first study to elucidate the cellular changes in macrophages as a result of exposure to Libby amphibole asbestos.

Materials and Methods

Cell culture conditions

Mouse macrophages, RAW264.7 cells, (ATCC-2091: American Type Culture Collection, Manassas, VA) were cultured at 37°C in a 5% CO_2 incubator (Thermo Forma, Waltham, MA) in complete media, which contained DMEM media with 4.5 g/L glucose and L-glutamine supplemented with 1.5 mM sodium pyruvate, 20 mM HEPES, 55 μM 2-

mercaptoethanol, 10% fetal bovine serum and antibiotics (100 U/ml penicillin, 100 μg/ml streptomycin and 0.25 μg/ml amphotericin B) (Gibco BRL, Bethesda, MD). Confluent RAW264.7 cells were scraped from T75 flasks, counted with a Z series Coulter Counter (Beckman Coulter, Hialeah, FL) and plated into 96, 12 and 6 well plates or T75 flasks in complete media and allowed to adhere overnight prior to exposure to asbestos fibers. Primary alveolar macrophages were lavaged from C57BL/6 mice as previously described (117), plated, and immediately exposed to asbestos. To elucidate the role of free radical scavengers, cells were incubated with superoxide dismutase (SOD) coupled to methoxypolyethylene glycol overnight at a final concentration of 19.6 Units (U) per ml (Sigma Chemical Co., St. Louis, MO) and concomitantly exposed to asbestos fibers. All experiments were performed using adherent cells only.

Particulate Matter

Three types of fibers were used in this study. Libby asbestos was obtained from the US Geological Survey. The Libby amphibole fibers have been chemically and physically characterized in detail (68, 114, 192). The Libby asbestos sample is chemically representative of the amphibole in the mine and has a particle size distribution that matches the air sample size distribution data (114). Libby asbestos contains six different amphibole fiber types, therefore, the asbestos sample is labeled in this paper as 6-mix. Wollastonite, a non-cytotoxic, non-fibrogenic control fiber, was provided by NYCO Minerals (Willsboro, NY). Crocidolite asbestos was provided by the Research Triangle Institute (RTI, NC). All fibers were dispersed in phosphate buffered saline (pH 7.4) by cup-horn sonication (Misonix, Framingdale, NY) before culturing. Stock concentration suspensions of fibers were prepared fresh immediately prior to their

addition into complete RPMI cell cultures. Fiber concentrations were based on relative mass. The size distributions of all three fiber types are presented in Table 1.1.

Fiber Type	Diameter (microns)	Length (microns)	Aspect Ratio
6-mix	0.61 ± 1.22	7.21 ± 7.01	22.52 ± 22.87
Crocidolite	0.16 ± 0.09	4.59 ± 4.22	34.05 ± 43.29
Wollastonite	0.75 ± 1.02	4.46 ± 5.53	8.48 ± 7.10

Table 2.1: Fiber size distribution data of Libby and crocidolite asbestos and wollastonite fibers. Note: Data are means ± SD.

Transmission Electron Microscopy

RAW264.7 cells were exposed to Libby asbestos fibers at a concentration of 5 μg/cm^2 for 24 h. Cells were washed three times in PBS, detached with a cell scraper and fixed with 4% glutaraldehyde in PBS for 4 h at 25°C. Cells were centrifuged for 5 min at 5000 rpm, washed three times in PBS and the pellet was suspended in low melt agarose. The pellet was post-fixed in 1% osmium tetraoxide in PBS (pH 7.4) for 1 h at 25°C, and washed three times in PBS. The pellet was dehydrated in ethanol and embedded in resin. Ultrathin sections (50 nm) were examined under a Hitachi H-7100 transmission electron microscopy (Hitachi, Ibaraki, Japan) with a tungsten filament and captured with an Advanced Microscopy Techniques digital camera (AMT, Danvers, MA). Sections were viewed at 75 kV. Images were captured with the AMT software version 540.

Cell Viability

RAW264.7 cells were exposed to fiber concentrations and duration stated in the figures. Cells were incubated with trypsin-EDTA (Gibco BRL) for 5 min at room

temperature. Complete media was added to stop the reaction. The cells were washed once and centrifuged at 1000 X g for 10 min. The pellet was resuspended in 200 µl of PBS to obtain a single cell suspension. Cells were permeabilized with 1 ml of 80% ethanol and incubated at -20°C overnight. Cells were washed once in PBS and DNA was stained with 1 ml of PBS containing 0.5% Triton X-100 (Sigma), 50 µg/ml RNase A (Roche, Indianapolis, IN) and 50 µg/ml propidium iodide (PI) (Invitrogen, Carlsbad, CA) then incubated for 40 min at 37°C. Cells were transferred to filter-top polypropylene tubes (BD Labware, Franklin Lakes, NJ) and stored on ice for analysis using the FACS Caliber (BD Biosciences, San Jose, CA) for red fluorescence. Dead and apoptotic cells were identified in the sub-G0/G1 peak determined by PI immunofluorescence. Cell viability was calculated as the percent of viable cells (cells above the sub-G0/G1 phase) divided by the total percent of cells and expressed as percent of control.

Cell viability of RAW264.7 cells after 3 h of exposure to Libby asbestos at a final concentration of 62.5 µg/cm^2 was not significantly different than controls as determined by a one-way ANOVA. These results were confirmed by an LDH-Cytotoxicity Assay (BioVision, Mountain View, CA) and the CellTiter-Blue Reagent assay (Promega, Madison, WI).

Enumeration of internalized fibers

Fiber uptake was quantified as previously described with slight modifications (14). Briefly, RAW264.7 cells were exposed to Libby asbestos for 3 h at a final concentration of 62.5 µg/cm^2. Cells were washed with PBS and detached with trypsin-EDTA (Gibco) for 10 min with gentle rotation at RT to remove any fibers that were adherent but not internalized. Complete media was added to stop the reaction. The cells

were washed in PBS and then examined under phase contrast microscopy to count the number of internalized fibers. The number of fibers per cell was quantified from 0 to 5. Greater than 5 fibers per cell were impossible to differentiate, therefore, the upper limit of detection was 5 fibers per cell. Cells with more than 5 internalized fibers were classified into the upper limit (5). 50 cells were enumerated for each treatment. The experiment was performed twice with similar results.

Quantification of ROS in response to Libby amphibole asbestos

ROS production was measured using dichlorofluorescein diacetate (DCFDA, Molecular Probes, Eugene, OR) and dihydroethidine (DHE, Molecular Probes). DCFDA crosses the cell membrane and is trapped in the cell after deacetylation by intracellular esterases to dichlorofluorescin (DCFH). DCFH is then sensitive to oxidation, forming the fluorescent compound dichlorofluorecein (DCF) (69). DHE is more specific for superoxide than DCFDA and is also oxidized to a fluorescent product (201). Cells were plated in 96-well plates and incubated overnight at 37°C and 5% CO_2. Cells were incubated with 40 μM DCFDA for 1 hr or in 2 μM DHE for 30 min in a 37°C and 5% CO_2 incubator then exposed to fibers at concentrations stated in the figures. The plate was returned to the 37°C, 5% CO_2 incubator between hourly readings on the fluorescent plate reader. Cells without dye were used to subtract background fluorescence. Readings for fluorescence intensity were measured using a SpectraMax fluorescent plate reader set at 485 nm excitation and 530 nm emissions for DCFDA quantification and 518 nm excitation and 605 nm emission for DHE quantification (Molecular Devices, Sunnyvale, CA).

Quantification of total superoxide dismutase (SOD) activity

Total SOD activity was measured as described previously (20). Briefly, RAW264.7 cells were exposed to asbestos for 3, 7, 12 and 24 h at a final concentration of 62.5 μg/cm^2. The cells were washed with PBS and homogenized in 10 mM ethylenediaminetetraacetic acid disodium salt (EDTA) buffer (pH 8.0) by cup-horn sonication. Samples were centrifuged at 20,000 X g at 4°C for 15 min. The supernatants (15 μl) were incubated for 20 min in a 25°C water bath with 150 μl phosphate buffer, 15 μl of 1.5 mM xanthine, and 15 μl of 1.0 mM hydroxylamine chloride. The reaction was initiated by the addition of 75 μl of 0.8 mg protein/ml xanthine oxidase (Sigma). An aliquot of the reaction (100 μl) was added to a mixture of 100 μl of 19 mM sulfanilic acid and 100 μl of 7 mM -napthylamine in a 96-well plate, incubated at room temperature for 20 min, and the absorbance was read at 539 nm using a SpectraMax plate reader (Molecular Devices). The activity of total SOD was determined from a standard curve using known amounts of purified SOD and quantified as Units of SOD activity per milligram of protein. Data are expressed as the percent of total SOD activity compared to time matched controls.

Quantification of reduced glutathione (GSH)

GSH levels were measured using the GSH recycling assay as previously described (160). RAW264.7 cells were exposed to asbestos at concentrations and durations stated in the figures. The cells were washed with PBS and lysed with 2 freeze/thaw cycles in 300 μl of 10 mM HCl. 50 μl aliquots were taken for protein determination. Protein was precipitated by adding 70 μl of 6.5% sulfosalicylic acid,

incubating on ice for 10 min and centrifuging at 2000 X g for 15 min. 200 µl of supernatant was transferred to a 96-well plate for GSH quantification. Total intracellular glutathione was measured using the GSH reductase-DTNB recycling assay, comparing the rate of color formation at 412 nm of the unknowns to a standard curve. Total intracellular GSH levels were determined by quantifying the intracellular GSH levels and dividing by the protein concentration to obtain nmoles of GSH per milligram (mg) protein. Data are expressed as the percent of total glutathione levels compared to time matched controls.

Quantification of 8-hydroxy-2'-deoxyguanosine (8-oxo-dG)

RAW264.7 cells were exposed to asbestos for 12 and 24 h and 8-oxo-dG levels were quantified using the method previously described (11). Briefly, DNA was isolated through phenol-chloroform extraction and digested with nuclease P1 (Roche). 8-oxo-dG and 2-deoxyguanosine (2dG) were resolved by HPLC with a reverse phase YMCBasic column (YMC Inc., Wilmington, NC) and quantified using a CoulArray electrochemical detection system (ESA Inc., Chelmsford, MA). Calibration curves were generated from standards of 2-dG (Sigma) ranging from 100 ng to 2 µg and 8-oxo-dG (Cayman Chemical, Ann Arbor, MI) ranging from 5 to 100 pg. The amount of 2-dG and 8-oxo-dG in control and treated cells was calculated according to the calibration curves. The relative levels of 8-oxo-2dG are expressed as the ratio of 8-oxo-2dG (fmoles) / 2dG (nmoles). Data were recorded, analyzed and stored using CoulArray for Windows data analysis software.

Determination of DNA damage

DNA damage was determined by the comet assay according to previously published methods with minor modifications (174). Briefly, 5ul of the cell suspension was embedded in 75 ul of 0.5% low melt agarose (Bio-Rad) and sandwiched between a layer of 5 ul of 0.5% normal melting agarose and a top layer of 0.5% low melting agarose on conventional microscope slides. To lyse cellular and nuclear membranes of the embedded cells, slides were immersed in ice-cold, freshly prepared, lysis solution (2.5 M NaCl, 100 mM disodium EDTA, 10 mM Tris-Cl and 10% DMSO, pH 13.0) and incubated at 4°C for 1 hour. The slides were incubated in alkaline buffer (0.1% 8-hydroxyquinoline, 10 mM disodium EDTA, 2% DMSO and 200 mM NaOH) for 20 min to allow DNA unwinding. Electrophoresis was performed in alkaline buffer at 300 mA for 20 min. After electrophoresis, the slides were neutralized with 400 mM Tris-Cl, pH 7.4 twice for 20 min. DNA was stained with 100 ul per slide of Hoechst (10 ug/ml) (Molecular Probes). All steps were conducted in darkness to prevent additional DNA damage and samples were analyzed within 4 h.

Microscopic analysis

A laser scanning cytometer (LSC, Compucyte, Cambridge, MA) equipped with a BX50 Olympus microscope and a 407-nm argon laser was used to scan the slides. Hoechst fluorescence was detected with a photomultiplier tube equipped with a 460-485 nm bandpass filter. The embedded cells were focused and scanned on the central portion of each well. The sensitivity threshold was set to contour comet heads only. A threshold value of greater than 3000 provided a good discrimination between nuclear fluorescence and comet tails. Fluorescence was integrated from a region of 6 pixels broader than the threshold around the comet head as previously described (139). For each integration

contour, the integrated fluorescence, maximum pixel and the area were collected. The scanning was run by using a 20x dry objective. Two thousand events were scanned per slide. A histogram of integral fluorescence was compared to that obtained by flow cytometric cell cycle analysis through LSC software (WinCyte, Compucyte). The G1 and G2 phase peak were confirmed by LSC imaging. Cells with damaged DNA contained less DNA and stained with lower fluorescence intensity than the G1 phase cells and therefore appeared in the sub-G1 area of the histogram.

Quantification of 8-oxoguanine-DNA-glycosylase 1 (Ogg1) activity

RAW264.7 cells were exposed to asbestos for 3, 7 and 12 h and Ogg1 activity levels were quantified using the method previously described (11). Briefly, DNA -glycosylase was extracted from the pellets of the EDTA sample buffers, as described above, through homogenization at 4°C in extraction buffer containing 20 mM Trizma-base (pH 8.0), 1 mM EDTA, 0.5 mM spermine, 0.5 mM spermidine, 1 mM DTT, 50% glycerol, and protease inhibitor cocktail (Roche). Following the addition of 2.5 M potassium chloride, the homogenate was incubated at 4°C for 30 min. Aliquots of the supernatant were collected following centrifugation at 20,000 g for 30 min and stored at -80°C. Ogg1 activity was determined using a synthetic probe containing 8-oxo-dG (Trevigen, Gaithersburg, MD) labeled with -^{32}P at the 5'-end, using T4 polynucleotide kinase (Roche). The probe used has the nucleotide sequence 5'-GAACTAGTGXATCCCCCGGGCTGC-3' (X=8-oxo-dG) and was annealed to its corresponding complimentary oligonucleotide before the nicking reaction was preformed. The nicking reaction was initiated by incubating 2.5 μg of protein extract and the double-stranded probe for 30 min at 37°C and stopped by placing the samples on ice. Aliquots of

loading buffer containing 90% formamide, 10 mM NaOH and blue-orange dye (Promega, Madison, WI) were then added to each sample. After 5 min at 95°C, samples were chilled and loaded into a polyacrylamide gel (20%) with 7 M urea and 1X TBE and run at 400 V for 2 h. Gels were quantified using FLA-3000 Series Fuji Film Fluorescent Image Analyzer and analysis software. The capacity of the extract to remove 8-oxo-dG was expressed as a percentage of the cleaved synthetic probe to the total probe used in densitometric units.

Protein Determination

Protein concentrations were determined with the BCA protein assay kit based on the bicinchoninic acid (BCA) method (Pierce, Rockford, IL). The assay, adapted for microtiter plates, was used according to the manufacture's instructions.

Statistical Analysis

Data are given as mean ± standard deviation (SD) or mean ± standard error of the mean (SEM). Analyses were done using the software package GraphPad Prism 3.03 (GraphPad, San Diego, CA). One-way or two-way analysis of variance (ANOVA) was used to compare groups with one independent or two independent variables, respectively. A Bonferroni or Dunnett's post test was used to compare different treatments. Data comparing two group means were analyzed by independent samples *t* test. Significance was noted at $P < 0.05$ and adjusted for the number of comparisons according to Bonferroni's adjustment. Non-parametric analysis of fiber uptake was conducted using the Kruskal-Wallis test. Outliers were detected through Grubb's test from GraphPad Software.

Results

Libby asbestos fibers are internalized by murine macrophages

To determine whether Libby asbestos fibers are internalized *in vitro*, murine macrophages were exposed to Libby asbestos at a concentration of 5 μg/cm^2 for 24 h and analyzed through transmission electron microscopy. After 24 h of asbestos exposure, murine macrophages contained variable numbers of asbestos fibers, which were less than 2 microns in length. The majority of Libby asbestos fibers were observed in cytoplasmic vacuoles or protruding from cytoplasmic vacuoles into the cytosol (Fig. 2.1A and B, respectively), and localized primarily around the nucleus. Libby asbestos fibers were also observed attached to the plasma membrane (Fig. 2.1C) and free within the cytoplasm (Fig. 2.1D). These results indicate that murine macrophages phagocytize Libby asbestos fibers and the internalized fibers localize to cytoplasmic vacuoles and to the cytosol.

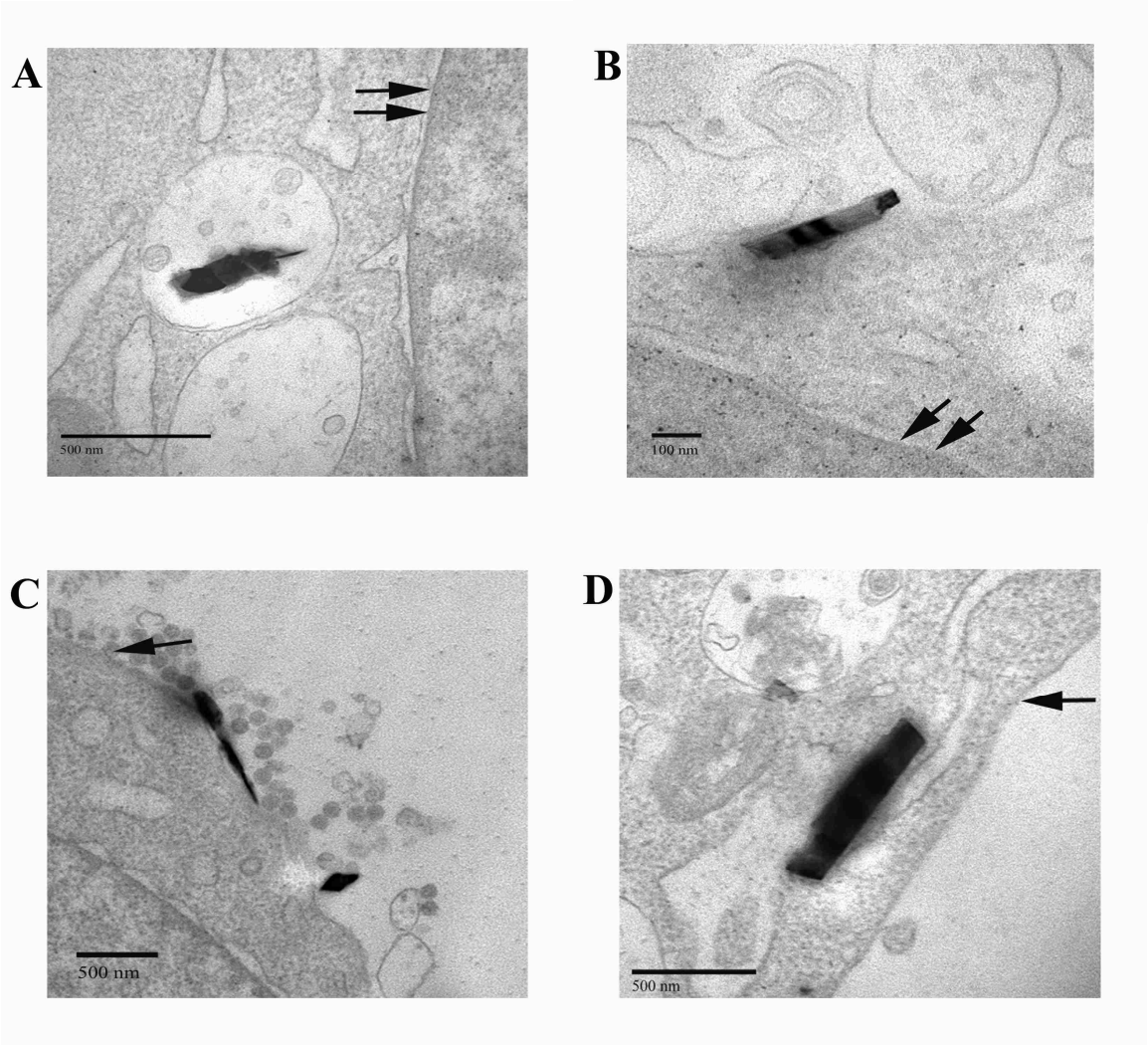

Figure 2.1: Transmission electron microscopy of intracellular Libby asbestos fibers in murine macrophages. RAW264.7 cells were incubated with Libby asbestos (5 μg/cm^2) for 24 h and sections were prepared as described in Materials and Methods. A) Libby asbestos fiber is encompassed by a cytoplasmic vacuole near the nuclear membrane. Magnification 40,000X. B) Libby asbestos fiber near the nuclear membrane protruding from a cytoplasmic vacuole to the cytoplasm. Magnification 60,000X. C) Libby asbestos fibers attached to the plasma membrane. Magnification 15,000X. D) Libby asbestos fiber free in the cytosol of a murine macrophage. Magnification 30,000X. Double arrows denote the nuclear membrane. Single arrows denote the plasma membrane.

Libby asbestos increases intracellular ROS in murine macrophages

To establish whether macrophages produce increased levels of ROS in response to amphibole asbestos, RAW264.7 cells were incubated with 40 μM DCFDA for one hour then exposed to increasing concentrations of Libby asbestos, ranging from 6.25 to 62.5 μg/cm^2. DCFDA is a fluorescent dye used to indirectly quantify the amount of intracellular ROS. Therefore, the relative fluorescence intensity is correlated to the amount of intracellular ROS. Fluorescent readings were taken every hour for 3 h. The relative fluorescence intensities in macrophages over time are shown in Figure 2.2A. Murine macrophages increased intracellular ROS levels in response to Libby asbestos in a dose dependent manner. The lowest concentration of Libby asbestos (6.25 μg/cm^2) significantly increased the relative fluorescence after 3 h of exposure compared to untreated cells ($P < 0.05$). However, higher concentrations of Libby asbestos significantly increased the relative fluorescence after only one hour of exposure ($P < 0.05$). The highest concentration of Libby asbestos (62.5 μg/cm^2) generated the greatest increase in ROS and this concentration of asbestos did not reduce cell viability within 3 h as determined by PI immunofluorescence (Figure 2.2B) and two additional viability assays (see Materials and Methods). The viability of RAW264.7 cells after 3, 7, 12 and 24 h of exposure to Libby and crocidolite asbestos is shown in Figure 2.2B. The viability of RAW264.7 cells after 24 h of exposure to Libby and crocidolite asbestos was 92% and 62%, respectively, compared to untreated cells. Exposure to wollastonite fibers for 24 h did not reduce the viability of RAW264.7 cells compared to untreated controls. Since the highest concentration of asbestos induced the greatest increase in ROS without cell loss, we utilized this fiber concentration for all subsequent experiments.

In order to determine whether the increase in ROS was unique to Libby asbestos, murine macrophages were exposed to equal concentrations of Libby asbestos, wollastonite fibers, a non-fibrogenic control fiber (171), and a well characterized cytotoxic asbestos fiber, crocidolite. As shown in Figure 2.2C, cells exposed to Libby asbestos had a significantly higher relative fluorescence after only one hour of exposure compared to untreated cells ($P < 0.05$). Exposure to wollastonite fibers did not increase the level of fluorescence in macrophages at any time during exposure compared to control cells. Cells exposed to crocidolite increased the level of fluorescence after 3 h of exposure; however, the increase in ROS was lesser in magnitude compared to Libby asbestos exposure. Similar results were obtained using primary alveolar macrophages lavaged from C57BL/6 mice (data not shown). These results demonstrate that exposure to Libby and crocidolite asbestos increases intracellular ROS in murine macrophages and the increase in intracellular ROS occurs in primary alveolar macrophages as well as in macrophage cell line cells.

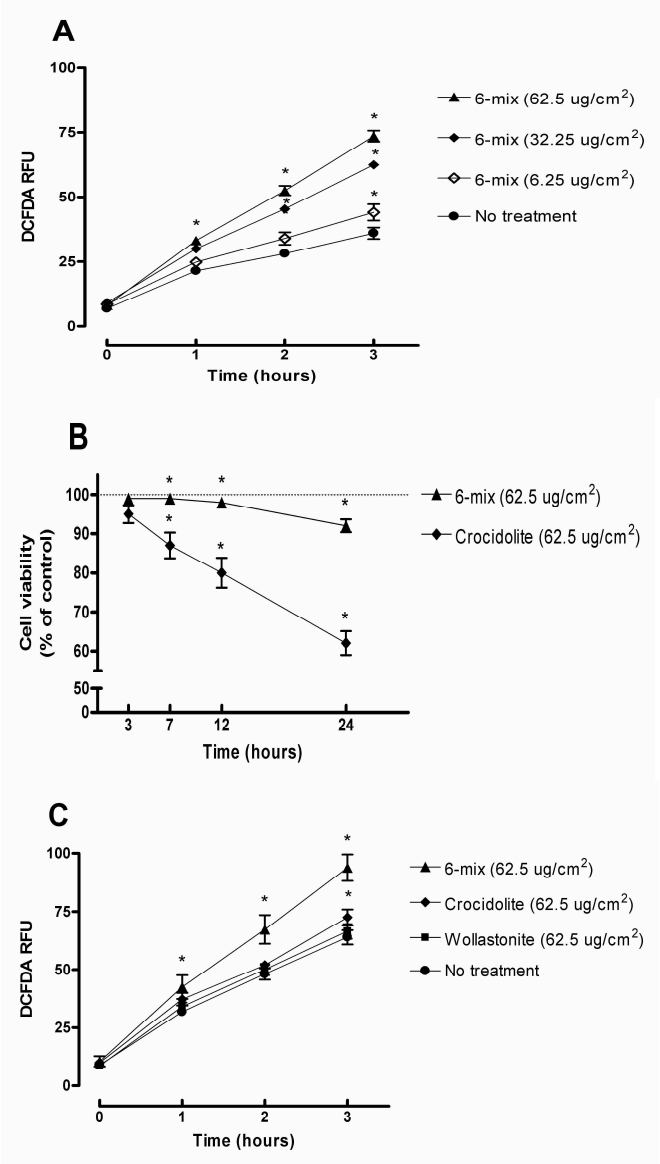

Figure 2.2: Dose-dependent response of Libby asbestos on intracellular ROS levels in RAW264.7 cells. ROS levels were determined by the relative fluorescence units (RFU) of DCFDA as described in Material and Methods. A) Three separate concentrations of Libby asbestos were added to murine macrophages for 3 h. Closed circles denote control cells. Open diamonds denote cells treated with Libby asbestos (6.25 μg/cm^2). Closed diamonds denote cells treated with Libby asbestos (32.25 μg/cm^2). Closed triangles denote cells treated with Libby asbestos (62.5 μg/cm^2). B) RAW264.7 cells were exposed to Libby and crocidolite asbestos for 3, 7 12 and 24 h. Cell viability was determined through PI fluorescence as described in Materials and Methods. Viability was calculated as the percentage of viable cells (cells above the sub-G0/G1 phase) divided by the total percent and expressed as a percent of control. Closed circles denote control cells. Closed triangles denote cells treated with Libby asbestos. Closed diamonds denote cells treated with crocidolite. C) Separate experiment comparing Libby asbestos with wollastonite, a non-fibrogenic control fiber, and crocidolite, a well-characterized cytotoxic fiber. Closed circles denote control cells. Closed rectangles denote cells treated with wollastonite. Closed triangles denote cells treated with Libby asbestos. Closed diamonds denote cells treated with crocidolite. Data are represented as mean ± SD. Single asterisks indicate a significant difference compared to control at each time point through a Bonferonni post-hoc test ($P < 0.05$; n = 3-5) by a two-way ANOVA.

Equivalent number of murine macrophages interact and internalize crocidolite and Libby asbestos fibers

To determine whether the increase in ROS was dependent upon the number of cell-fiber interactions or fiber uptake, we used light microscopy to enumerate the number of cells interacting with asbestos fibers and the number of internalized fibers per cell. To this end, murine macrophages were exposed to equal concentrations of Libby and crocidolite asbestos and wollastonite fibers for 3 h as described above. Cells were washed extensively and examined under phase contrast light microscopy. The number of cells interacting with one or more fibers where enumerated for each treatment. One hundred cells were counted for each treatment.

The preparation of Libby asbestos fibers contained numerous fibers of different lengths and widths. As seen in Figure 2.3A, Libby asbestos fibers visualized through light microscopy were generally less than 100 microns in length. Additionally, all murine macrophages bound or internalized one or more Libby asbestos fibers after 3 h. The preparation of crocidolite asbestos was more homogeneous in morphology and contained longer fibers than the Libby asbestos. All murine macrophages also established multiple interactions with crocidolite asbestos fibers after 3 h (Fig 2.3B). Wollastonite fibers interacted with 25% of macrophages and had fewer fibers in each preparation compared to either amphibole asbestos preparations (Fig 2.3C). These results indicate that equal numbers of murine macrophages bind Libby and crocidolite asbestos fibers after 3 h at the concentrations used in this study.

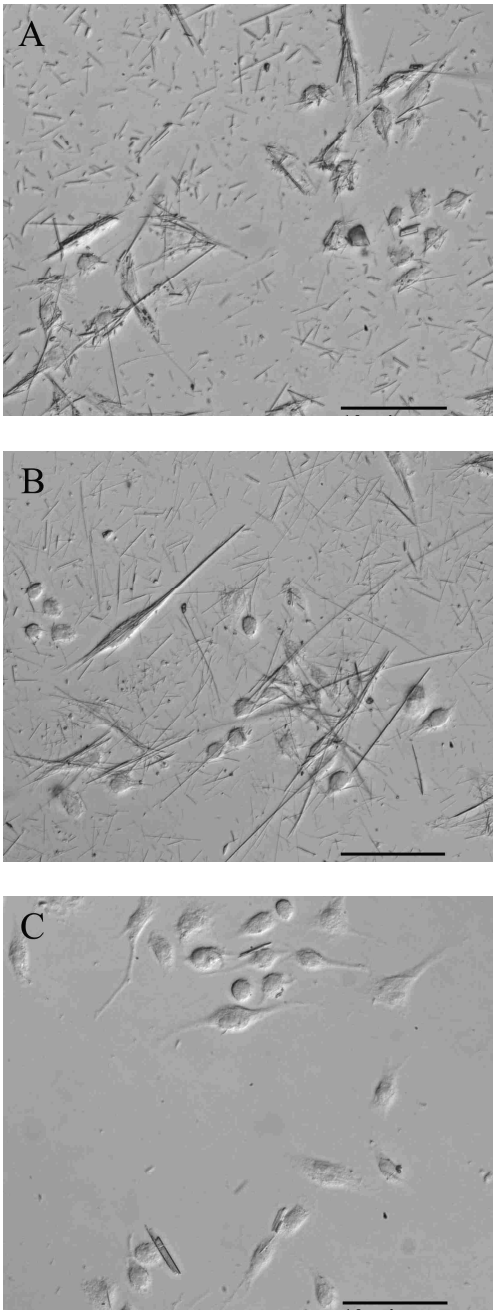

Figure 2.3: Light microscopy of murine macrophages interacting with asbestos and non-asbestos fibers. RAW264.7 cells were incubated with Libby asbestos, crocidolite asbestos and wollastonite fibers at a final concentration of 62.5 μg/cm^2 for 3 h and visualized through phase contrast light microscopy. All RAW264.7 cells bound one or more Libby and crocidolite asbestos fibers (A and B, respectively) while wollastonite fibers interacted with fewer RAW264.7 cells (C). Scale bar = 100 microns.

The number of internalized fibers per cell was quantified as previously described with minor modifications (14). On average, macrophages internalized 4.38 ± 1.06 Libby asbestos fibers per cell and 3.28 ± 1.58 crocidolite asbestos fibers per cell (mean ± SD). The difference between the numbers of Libby and crocidolite asbestos fibers internalized

per cell was not significant. In contrast, macrophages internalized significantly fewer wollastonite fibers per cell (0.88 ± 0.93) compared to the number of amphibole asbestos fibers ($P < 0.05$). Together these data indicate that the increase in the level of ROS in macrophages is not dependent upon the number of cellular interactions with the asbestos fibers nor is it dependent on the number of internalized amphibole fibers.

Increased ROS levels generated by Libby asbestos is suppressed with the addition of exogenous intracellular SOD

To determine whether ROS induced by Libby amphibole asbestos can be inhibited by a free radical scavenger, RAW264.7 cells were incubated overnight with SOD coupled to methoxypolyethylene glycol (PEG). SOD catalyzes the formation of hydrogen peroxide from superoxide anion and the conjugation of PEG leads to the enhanced uptake of exogenous SOD into cells (5). After treatment with PEG-SOD, macrophages were washed and subsequently exposed to Libby asbestos, therefore, the effect of PEG-SOD on asbestos induced ROS production can only be attributed to intracellular SOD activity. As shown in Figure 2.4A, macrophages exposed to Libby asbestos had a significantly higher level of intracellular ROS after 3 h of asbestos exposure ($P < 0.05$). However, macrophages pretreated with PEG-SOD and subsequently exposed to Libby asbestos had significantly lower levels of intracellular ROS compared to macrophages exposed to asbestos alone ($P < 0.05$). Pretreatment of macrophages with PEG-SOD did not change the levels of ROS compared to control cells, indicating that the protective effect of PEG-SOD during asbestos exposure can be attributed to a reduction in superoxide levels. Pretreatment of cells with PEG alone did not inhibit ROS produced by Libby asbestos (data not shown). These data confirm that Libby asbestos induced ROS

is predominately intracellular and can be abrogated by PEG-SOD, suggesting that the superoxide anion is the major contributor to the increased ROS levels.

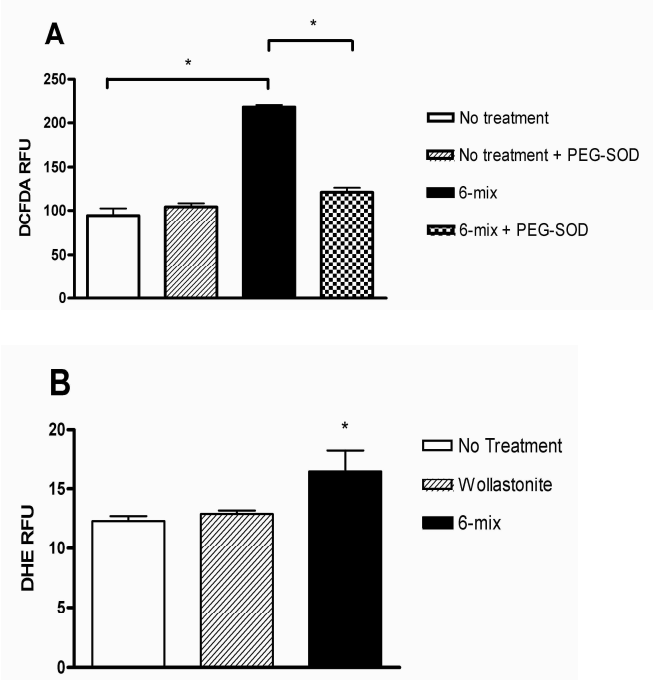

Figure 2.4: Increase in superoxide levels in asbestos exposed macrophages. A) Effect of intracellular superoxide dismutase (SOD) on asbestos-induced ROS in RAW264.7 cells. Cells were incubated overnight at 37°C with SOD conjugated to methoxypolyethylene glycol (11.0 U/ml). Cells were then treated with Libby asbestos (62.5 μg/cm^2). ROS levels were determined by the RFU of DCFDA as described in Material and Methods. Open bars denote control cells. Thatched bars denote control cells pretreated overnight with PEG-SOD (44 U/ml). Black bars denote cells treated with Libby asbestos (62.5 μg/cm^2). Checkered bars denote cells pretreated overnight with PEG-SOD then exposed to Libby asbestos. B) Superoxide levels were determined by the RFU of DHE over 2 h as described in Material and Methods. Open bars denote control cells. Black bars denote cells treated with Libby asbestos (62.5 μg/cm^2). Thatched bars denote cells treated with wollastonite (62.5 μg/cm^2). Data are represented as mean ± SEM. Single asterisks indicate a significant difference through a Bonferonni post-hoc test ($P < 0.05$; $n = 5$) by a one-way ANOVA.

Libby asbestos increases superoxide production in murine macrophages

To provide additional support for the premise that a contributing ROS generated by Libby amphibole asbestos is the superoxide anion, RAW264.7 cells were incubated with 2 μM DHE for 30 min then exposed to Libby asbestos at a final concentration of 62.5 μg/cm^2. DHE is a fluorescent dye used to indirectly quantify the amount of superoxide in cells. Therefore, the relative fluorescent intensity is correlated to intracellular superoxide levels (201). The relative DHE fluorescence intensity of murine macrophages exposed to Libby asbestos and wollastonite fibers is shown in Figure 2.4B. Macrophages exposed to Libby asbestos had a significantly higher relative fluorescence after 2 h of exposure compared to untreated cells ($P < 0.05$). Macrophages exposed to wollastonite fibers did not increase the level of fluorescence compared to control. These data indicate that Libby asbestos exposure increases intracellular levels of superoxide in murine macrophages.

Total intracellular SOD activity is suppressed by Libby amphibole asbestos

Because Libby asbestos exposure increases superoxide levels in murine macrophages, we hypothesized that the increase in superoxide may be due to a modification in SOD activity. Therefore, total intracellular SOD activity was quantified in murine macrophages after 3, 7, 12 and 24 h of exposure as previously described (20). Libby asbestos suppressed total SOD activity by 30% after 3 h of exposure and the reduction in activity was significant compared to untreated controls ($P < 0.05$) (Fig 2.5). However, total SOD activity was not significantly different compared to controls after 7, 12 and 24 h of exposure to Libby asbestos. Total SOD activity was not different in cells exposed to wollastonite compared to time matched controls. Crocidolite asbestos significantly increased total SOD activity by 200% after 24 h of exposure compared to

untreated controls ($P < 0.05$). These results indicate that exposure to Libby asbestos results in an initial suppression of total SOD activity and that exposure to crocidolite asbestos increases total SOD activity after 24 h in murine macrophages.

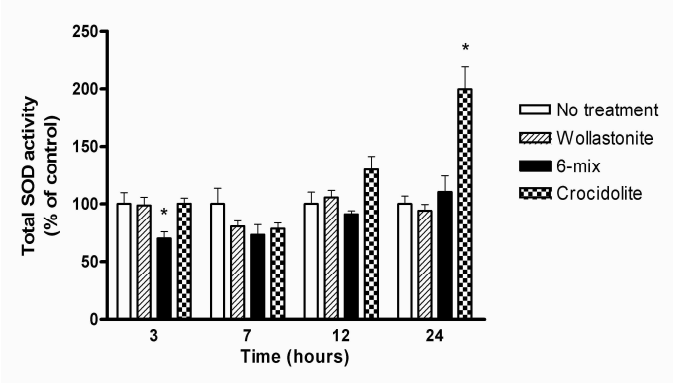

Figure 2.5: Effect of Libby amphibole asbestos on total intracellular SOD activity in RAW264.7 cells. RAW264.7 cells were exposed to fibers as described in Materials and Methods for 3, 7, 12 and 24 h. Total SOD activity levels were quantified as a ratio of Units of SOD activity per mg of protein as previously described (20) and expressed as the percentage of total SOD activity compared to time matched controls. Open bars denote control cells. Thatched bars denote cells treated with wollastonite (62.5 μg/cm^2). Black bars denote cells treated with Libby asbestos (62.5 μg/cm^2). Checkered bars denote cells treated with crocidolite (62.5 μg/cm^2). Data are represented as mean ± SEM. Single asterisks indicate a significant difference compared to time matched controls through an independent *t* test ($P < 0.05$; $n = 4$).

Intracellular glutathione levels are reduced in response to Libby amphibole asbestos

In response to increased levels of ROS, cells utilize GSH to maintain the intracellular redox balance within cells. Reduced levels of intracellular GSH in cells are an indication of oxidative stress. Therefore, intracellular GSH was measured in macrophages after exposure to amphibole asbestos and wollastonite fibers to determine whether exposure results in a decrease in intracellular GSH levels. The intracellular GSH levels were measured through the GSH recycling assay as previously described (160). In response to Libby asbestos, macrophages significantly decreased intracellular GSH levels

compared to untreated cells at 7, 12 and 24 h ($P < 0.05$) (Fig. 2.6). Exposure to crocidolite asbestos also significantly decreased intracellular GSH levels at 7, 12 and 24 h after exposure. However, the decrease in GSH levels was more prominent in response to crocidolite asbestos (average decrease of 55%) at all time points compared to the decrease observed with Libby asbestos (average decrease of 76%). Wollastonite did not decrease the intracellular GSH levels compared to time matched controls. These results indicate that exposure to Libby and crocidolite asbestos induces oxidative stress in murine macrophages.

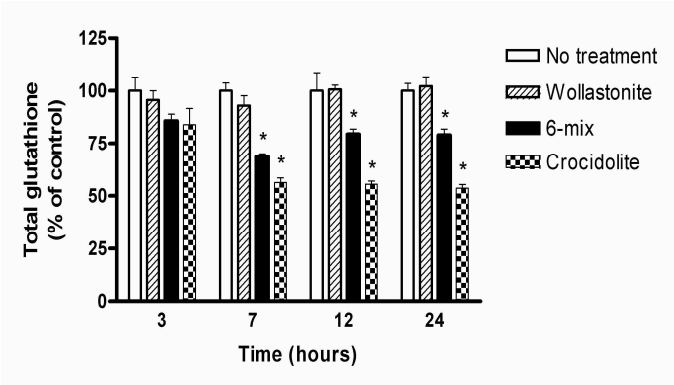

Figure 2.6: Effect of amphibole asbestos on total intracellular glutathione levels in RAW264.7 cells. RAW264.7 cells were exposed to fibers as described in Materials and Methods. GSH levels were quantified as a ratio of GSH in nmoles per mg of protein as previously described (160) and expressed as the percentage of total glutathione levels compared to time matched controls. Open bars denote control cells. Thatched bars denote cells treated with wollastonite (62.5 μg/cm^2). Black bars denote cells treated with Libby asbestos (62.5 μg/cm^2). Checkered bars denote cells treated with crocidolite (62.5 μg/cm^2). Data are represented as mean ± SEM. Single asterisks indicate a significant difference compared to time matched controls through an independent *t* test ($P < 0.05$; n = 3).

Libby amphibole does not promote the formation of 8-oxo-dG or single stranded DNA breaks in macrophages

RAW264.7 cells were exposed to Libby asbestos, crocidolite asbestos and wollastonite fibers and the relative levels of 8-oxo-dG were determined as previously described (11) in order to determine whether the increased levels of ROS generated by Libby and crocidolite asbestos results in oxidative DNA damage. The relative level of 8-oxo-dG is quantified as a ratio of 8-oxo-dG compared to deoxyguanosine. Only adherent cells were included in the DNA damage assay. The levels of 8-oxo-dG in macrophages were significantly elevated in response to crocidolite asbestos at 12 and 24 hr ($P < 0.05$) (Fig. 2.7A). However, in the same cell type, Libby asbestos did not increase the relative levels of 8-oxo-dG at either time 12 or 24 h. Wollastonite, did not increase the relative levels of 8-oxo-dG at either 12 or 24 h. In response to Libby and crocidolite asbestos, the extent of DNA damage, specifically strand breaks, was also quantified at 24 h through the comet assay (Fig. 2.7B). Crocidolite asbestos generated a significantly higher level of DNA damage as determined by the percent of cells in the sub-G1 phase ($P < 0.05$). Libby amphibole did not produce a significant difference in the percentage of cells in the sub-G1 phase. These data indicate that Libby asbestos does not induce oxidative DNA damage in murine macrophage cells and suggests Libby asbestos induces separate cellular responses *in vitro* compared to crocidolite asbestos.

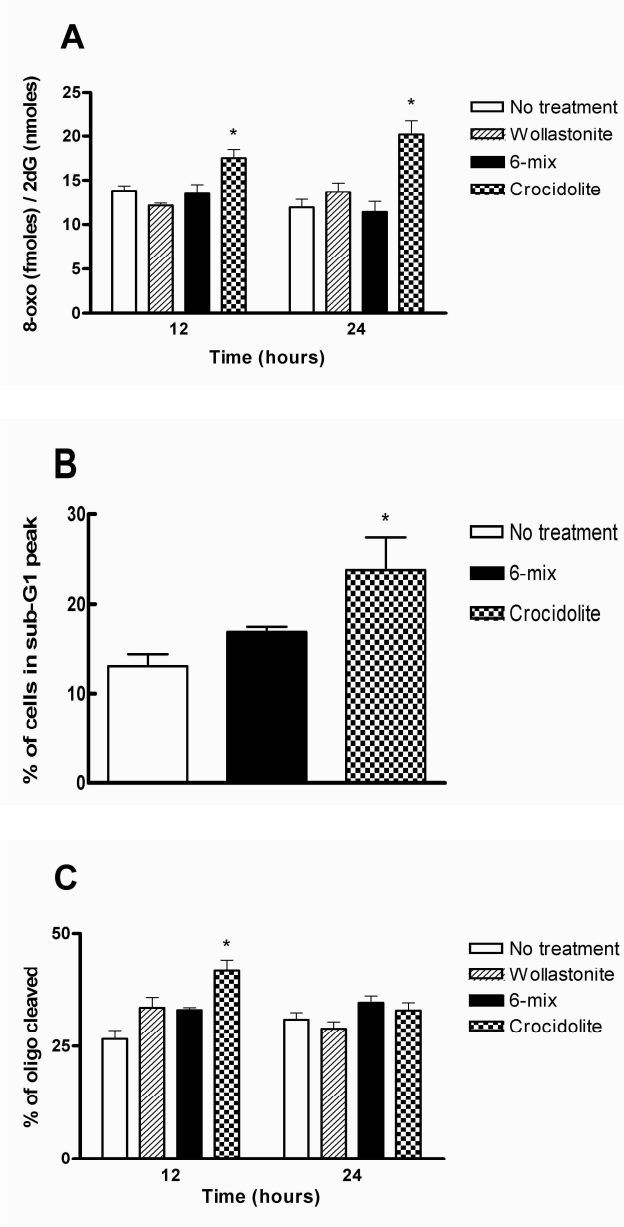

Figure 2.7: Effect of amphibole asbestos on 8-dihydro-8-oxo-2'-deoxyguanosine (8-oxo-dG) levels and Ogg1 activity in RAW264.7 cells. A) RAW264.7 cells were exposed to asbestos as described in Materials and Methods for 12 h and 24 h. The relative levels of 8-oxo-dG in RAW264.7 cells were quantified as previously described (11). The relative level of 8-oxo-dG is calculated as a ratio of 8-oxo-dG compared to 2-deoxyguanosine (2dG). Open bars denote control cells. Thatched bars denote cells treated with wollastonite. Black bars denote cells treated with Libby asbestos. Checkered bars denote cells treated with crocidolite. B) RAW264.7 cells were exposed to amphibole asbestos for 24 h and the percentage of cells that contained damaged DNA, which appeared in the sub-G1 peak, was quantified through the comet assay as described in Materials and Methods. Open bars denote control cells. Black bars denote cells treated with Libby asbestos. Checkered bars denote cells treated with crocidolite asbestos. Single asterisks indicate a significant difference compared to control by Dunnett's test ($P < 0.05$; $n = 4$). C) RAW264.7 cells were exposed to asbestos as described in Materials and Methods. The activity levels of Ogg1 in cells were quantified as the percent of cleaved oligonucleotide as previously described (11). Closed circles denote control cells. Closed rectangles denote cells treated with wollastonite. Closed triangles denote cells treated with Libby asbestos. Closed diamonds denote cells treated with crocidolite. Data are represented as mean ± SEM. Single asterisks indicate a significant difference compared to control by Dunnett's test ($P < 0.05$; $n = 4$).

Effect of Libby asbestos on Ogg1 activity

Ogg1 is an important DNA glycosylase/AP lyase that catalyzes the excision of 8-oxo-dG lesions from damaged DNA and its activity has been shown to increase during oxidative stress (158). To determine whether the lack of DNA damage with Libby asbestos was a result of increased DNA repair generated by asbestos-induced oxidative stress, the activity of Ogg1 was quantified as previously described (11). Murine macrophages were exposed to fibers for 12 and 24 h and the activity of Ogg1 was quantified as the percent of cleaved synthetic oligonucleotide, which contains an 8-oxo-dG residue, compared to the total amount of oligonucleotide. As seen in Figure 2.7C, the activity of Ogg1 in macrophages exposed to Libby asbestos and wollastonite fibers was not different at either time point compared to untreated control cells. Exposure to crocidolite asbestos induces a significant increase in Ogg1 activity in murine macrophages after 12 h, however, Ogg1 activity returns to control levels after 24 h. These results indicate that exposure to Libby asbestos does not increase the activity of Ogg1 in murine macrophages.

Discussion

The community members of Libby, MT have experienced significant exposure to amphibole asbestos and have developed numerous ARD due to the asbestos contaminated vermiculite mine near the community (112, 189). The type of amphibole fiber that residents have been exposed to is a distinct type of amphibole asbestos, which is composed of several different fiber types (114). Because this asbestos type has not been previously studied, we determined the cellular effects of these fibers in order to elucidate a possible cellular mechanism for the initiation of ARD. Our study utilized a phagocytic

cell line that is characteristic of alveolar macrophages as well as primary alveolar macrophages that interact and clear inhaled particles in the lung (193).

Our data indicate that macrophages internalize Libby asbestos fibers and that the fibers localize to the cytosol and to cytoplasmic vacuoles that frequently surround the nucleus. These data are in accordance with previous results that establish crocidolite fibers are internalized through a microtubule dependent mechanism and localize near the nucleus (35). The majority of internalized Libby asbestos fibers are 2 microns or less in length. Libby asbestos fibers of this size have been shown to accumulate in the bark of trees throughout the mine site and surrounding area, indicating these size fibers are respirable and persist in the environment (185). These short, thin fibers are also the predominant asbestos fibers that remain in the tissue of asbestos exposed humans with pleural plaques and malignant mesothelioma (168). Hence, these size fibers play an important role in the development of fibrosis and lung cancer (44).

Exposure to Libby asbestos increases the level of intracellular ROS in murine macrophages and can be significantly reduced by exogenous PEG-SOD. These results suggest that the superoxide anion contributes to ROS generated by Libby asbestos exposure. To support the argument that superoxide contributes to asbestos induced ROS, Libby asbestos exposure also increases DHE fluorescence. DHE is known to preferentially detect superoxide (201). Together these data indicate that Libby asbestos exposure increases intracellular ROS levels in macrophages and that the major contributing ROS is the superoxide anion.

We hypothesized that the increase in superoxide may be due to an alteration of antioxidant concentrations within exposed cells. Therefore, intracellular SOD activity was quantified with an assay that measures total SOD activity and cannot differentiate

between the activity of intracellular copper-zinc SOD and mitochondrial manganese SOD. Exposure to Libby asbestos causes a significant decrease in total SOD activity after 3 h of exposure. The decrease in total SOD activity would consequently generate the observed increase in superoxide levels due to Libby asbestos exposure. The reduction in SOD activity by Libby asbestos may be due to post-translational modifications of SOD as a result of fiber internalization (108). In contrast, crocidolite asbestos increases in total SOD activity after 24 h, which has been previously reported in mesothelial cells (19). Chronic exposure to crocidolite asbestos has also been shown to increase SOD activity *in vivo* and *in vitro* (84, 125). SOD is highly expressed in cells within the lung, such as alveolar macrophages (93). The increased SOD activity observed during amphibole exposure may be a protective antioxidant response in lieu of the increased levels of free radicals generated by amphibole internalization.

Exposure to Libby asbestos results in an increase in ROS in conjunction with a significant decrease in intracellular GSH. The decrease in GSH with Libby asbestos was most notable after 7 h and remained significantly decreased after 24 h of exposure. Crocidolite also significantly decreased GSH levels after 7 h of exposure. These data are in accordance with previously published results that indicate crocidolite asbestos exposure results in a significant decrease in intracellular GSH level in both mesothelial and epithelial cells (65, 83). In the present study, crocidolite asbestos induces a greater decrease in GSH levels than Libby asbestos, which coupled with the increased cytotoxicity of this fiber, correlates to a higher level of oxidative stress in RAW264.7 cells (194).

Unlike previous studies that utilize only a single amphibole fiber, this study utilizes a sample of Libby asbestos that is a mixture of several amphiboles as well as

other fibers not classified in the amphibole family (114). Although exposure to Libby asbestos generates increased levels of ROS, no DNA damage was observed. In contrast, crocidolite asbestos exposure significantly increases DNA damage, which supports previous reports (58, 92). The lack of DNA damage observed with Libby asbestos may be a result of increased DNA repair activity in cells exposed to Libby asbestos. The main defense against oxidative DNA damage is the base excision repair pathway, which is initiated by Ogg1. The activity of Ogg1 significantly increases in murine macrophages in response to crocidolite asbestos, which supports previous *in vitro* results in alveolar epithelial cells (92). However, no difference in Ogg1 activity was observed after exposure to Libby asbestos. Therefore the lack of DNA damage in macrophages in response to Libby asbestos cannot be explained by increased DNA repair activity in these cells.

Although crocidolite and Libby asbestos are both categorized as amphibole fibers, they are chemically distinct. The major difference between these two fibers is that crocidolite contains a high iron content that is greater than 20% (90). The high iron content is known to play a role in crocidolite induced DNA damage (122, 195). On the contrary, Libby amphibole contains less than 5% iron content by weight (114). In addition to differences in chemical composition, this study describes separate cellular consequences of each fiber in the same cell line. DNA damage observed with crocidolite asbestos may be an indirect result of the increased SOD activity observed after 24 h (Figure 2.8). Increased SOD activity produces excess hydrogen peroxide from the dismutation of superoxide. Increased levels of hydrogen peroxide in crocidolite exposed macrophages may interact with the iron associated with crocidolite asbestos fibers and promote the formation of the hydroxyl radical. Indeed crocidolite fibers have been shown

to promote the formation of the hydroxyl radical in the presence of hydrogen peroxide (88, 90). The hydroxyl radical is the most oxidizing ROS in biological systems and promotes the oxidation of 2-dG in DNA generating 8-oxo-dG, which is observed in macrophages in response to crocidolite asbestos (Figure 2.7A) (17). In contrast, Libby asbestos suppresses total SOD activity in macrophages and generates the production of superoxide in exposed cells. The observation that Libby asbestos does not induce DNA damage, may be due to the fact that superoxide has a considerably lower reduction potential and does not participate in the oxidation of 2-dG. Therefore, we hypothesize that the differences in DNA damage observed among Libby and crocidolite asbestos may be a combined consequence of the distinct chemical compositions of each fiber as well as the activation of separate cellular pathways during asbestos exposure (Figure 2.8).

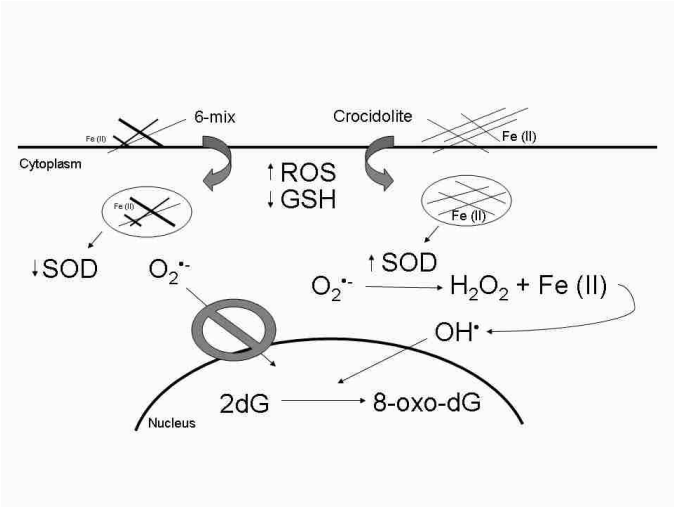

Figure 2.8: Schematic of the proposed mechanisms for Libby and crocidolite asbestos exposure. Internalization of Libby (labeled 6-mix) and crocidolite asbestos generate oxidative stress in RAW264.7 cells through increasing ROS levels and decreasing intracellular GSH levels. Libby asbestos suppresses SOD activity leading to the formation of superoxide ($O_2^{\bullet-}$). Crocidolite asbestos increases SOD activity, which generates hydrogen peroxide (H_2O_2). Hydrogen peroxide can then react with the iron (Fe II) associated with crocidolite fibers to from the reactive hydroxyl radical (OH•), which oxidizes 2-deoxyguanosine (2dG) to 8-hydroxy-2'-deoxyguanosine (8-oxo-dG) in murine macrophages.

In summary, murine macrophages phagocytize Libby amphibole asbestos fibers, which localize to the cytoplasm and cytoplasmic vacuoles. Internalization of Libby asbestos results in an increase in ROS levels, which can be attributed to the suppression of total SOD activity observed subsequent to Libby asbestos exposure. These results are in contrast to what is observed with crocidolite asbestos, which induces oxidative DNA damage. These data support the premise that the cellular effects observed with different asbestos fibers are mediated by their chemical compositions and the activation of separate cellular mechanisms. Finally, this is the first study to characterize the cellular effects of Libby amphibole asbestos, a pathogenic fiber known to cause ARD in humans.

Acknowledgments

The authors thank Ray Hamilton and Sandra Wells, Center for Environmental Health Sciences, University of Montana and James S. Webber, Wadsworth Center, NY for helpful discussions, Pamela Shaw in the CEHS Fluorescence Cytometry Core for assistance with the FACS analysis and Anna Marie Ristich, Microscopy Section Manager, at DataChem Laboratories for assistance with the fiber analysis.

Grants

This work was funded by grants from the NIH P20 NCRR017670 and R21 ES012956.

Chapter 3

Libby amphibole asbestos induces apoptosis and leads to the aberrant translocation of the SSA/Ro52 autoantigen to cell surface blebs

David J. Blake[*] and Jean C. Pfau[†]

Division of Biological Sciences[*] and Department of Biomedical & Pharmaceutical Sciences, Center for Environmental Health Sciences[†], University of Montana, Missoula, Montana, 59812

Abstract: Exposure to asbestos is associated with increased autoimmune responses in humans. For example, the residents of Libby, MT have experienced significant asbestos exposure due to an amphibole asbestos contaminated vermiculite mine near the community. Residents have subsequently developed increased autoimmune responses compared to an unexposed control population. However, the exact mechanism by which Libby amphibole asbestos generates autoimmune responses is unclear. A murine model

of amphibole asbestos induced autoimmunity was recently established and was characterized by the production of autoantibodies that recognized the SSA/Ro52 autoantigen. The purpose of this study was to determine how SSA/Ro52 might become antigenic as a result of asbestos exposure. Our results indicate that Libby 6-mix induces apoptosis in murine macrophages as determined by phosphatidylserine exposure, cleavage of poly (ADP-ribose) polymerase and morphological changes such as nuclear condensation. Asbestos induced apoptosis resulted in the translocation of SSA/Ro52 from the cytosol to apoptotic cell surface blebs. These apoptotic cell surface blebs were recognized by autoantibodies from mice exposed to amphibole asbestos suggesting that these cell surface structures may be antigenic when presented in a pro-inflammatory context. This study supports the premise that the induction of apoptosis may play a key role in environmentally induced autoimmunity.

Keywords: asbestos, macrophage, apoptosis, immunotoxicology

Introduction

Exposure to environmental xenobiotics such as silica, mercury and vinyl chloride is associated with the production of autoantibodies (AAs) and the development of systemic autoimmune disease (SAID) (40, 75). Increased serum immunoglobulins, positive AA tests and immune complexes have also been reported in small cohorts of individuals exposed to asbestos, which is a naturally occurring crystalline silicate fiber (97, 127, 200). The premise that asbestos exposure exacerbates autoimmune responses in humans is supported by a study from an asbestos-exposed population from Libby, MT (141). Residents of Libby, MT have higher frequencies and titers of positive AAs compared to an unexposed control population (141). A significant association was observed between AA titers and both the duration of exposure and lung disease severity.

Residents of Libby, MT also have an increased risk for SAID by more than 50% (128). Although the exact mechanisms that lead to the induction of SAID and AA production as a result of environmental exposure have not been established, evidence supports the role of apoptosis as the potential initiating stimulus (23, 152, 153).

Apoptosis is a regulated and controlled process of cellular destruction that does not elicit inflammation (33, 49). During apoptosis the cellular morphology is dramatically altered leading to the translocation of phosphatidylserine (PS) to the outer leaflet of the cell, nuclear condensation, as well as cellular fragmentation into membrane bound apoptotic blebs (52). These apoptotic blebs contain numerous autoantigens that are targeted by the immune system during autoimmune responses (23). Apoptosis also results in the cleavage of specific autoantigens, which may create neo-epitopes that may be recognized by the immune system as foreign (24, 153). The uptake and processing of apoptotic cells by antigen-presenting cells in a pro-inflammatory context may activate self-reactive T cells, inducing the loss of tolerance and an autoimmune response.

A murine model of asbestos-induced autoimmunity was recently established to investigate the mechanisms by which asbestos triggers systemic autoimmunity (140). Asbestos exposed mice develop positive antinuclear antibody tests and mild glomerulonephritis suggestive of a systemic lupus erythematosus (SLE)-like disease. The asbestos induced SLE-like disease was characterized by the production of AAs that recognize the SSA/Ro52 autoantigen. Autoantibodies against SSA/Ro52 are commonly found in patients with SLE (74, 76, 145, 155). SSA/Ro52 is a newly characterized RING-finger-type E3 ubiquitin ligase (48, 183), which in unstimulated cells localizes to the cytoplasm (132). Exposure to ultraviolet radiation, which is the main environmental factor that exacerbates SLE, has been shown to alter the localization of SSA/Ro52 in

different cell types. Ultraviolet-B (UVB) radiation induces the surface expression of SSA/Ro52 in keratinocytes, which are thought to be the target cells of SLE (59, 99). The translocation of SSA/Ro52 as a result of UVB radiation in keratinocytes has been shown to be independent of apoptosis and mediated through oxidative stress (156). Alternatively, SSA/Ro52 redistributes itself to apoptotic blebs in cardiac monocytes, epithelial cells, salivary gland cells and keratinocytes after exposure to various pro-apoptotic agents (80, 111, 118, 132). Because AAs target SSA/Ro52 during autoimmune responses, the clustering of SSA/Ro52 to small surface blebs of apoptotic cells may be important in the induction of autoimmunity induced by xenobiotics (23, 155).

Clues to the mechanisms connecting environmental exposure and systemic autoimmunity have been identified by characterizing the specific autoantibodies generated by xenobiotics. For example, exposure to mercury is associated with scleroderma (SSc) in humans and leads to the production of AAs in genetically susceptible mouse strains (79, 110). Anti-fibrillarin AAs are found in patients with scleroderma (55) and are the predominant AAs generated in mercury exposed mice (79). Mercury exposure was subsequently found to induce cell death and result in the production of a novel cleavage fragment of fibrillarin (143, 144). Therefore, these novel cleavage fragments of fibrillarin may serve as the antigenic determinants for self-reactive T cells.

Alveolar macrophages are the primary cell type that interact with inhaled particles and function to clear particles from the lung. Therefore, our study utilizes RAW264.7 cells, which is a phagocytic murine cell line that is characteristic of alveolar macrophages (193). Previous results indicate that exposure to Libby amphibole asbestos induces oxidative stress in these cells (9). In this study we test the hypothesis that Libby asbestos

induces apoptosis in macrophages leading to the redistribution of SSA/Ro52 to apoptotic blebs. Moreover, we investigate whether these apoptotic blebs are recognized by AAs generated by asbestos exposed mice. This study helps elucidate a possible mechanism by which environmental exposures like asbestos drive autoimmune responses.

Materials and Methods

Cell culture conditions

Mouse macrophages, RAW264.7 cells, (ATCC-2091: American Type Culture Collection, Manassas, VA) were cultured at 37°C in a 5% CO_2 incubator (Thermo Forma, Waltham, MA) in complete media, which contained DMEM media with 4.5 g/L glucose and L-glutamine supplemented with 1.5 mM sodium pyruvate, 20 mM HEPES, 55 μM 2-mercaptoethanol, 10% fetal bovine serum and antibiotics (100 U/ml penicillin, 100 μg/ml streptomycin and 0.25 μg/ml amphotericin B) (Gibco BRL, Bethesda, MD). Confluent RAW264.7 cells were scraped from T75 flasks, counted with a Z series Coulter Counter (Beckman Coulter, Hialeah, FL) and plated into 12 well plates, 8-well chambered cover glasses (Nalge Nunc International Corp., Rochester, NY) or T75 flasks in complete media and allowed to adhere overnight prior to exposure to asbestos fibers. To induce apoptosis, cells were incubated with 1 μM staurosporine (Sigma-Aldrich, St. Louis, MO) for 6 hours (197).

Particulate Matter

Two types of fibers were used in this study. Libby asbestos was obtained from the US Geological Survey. The Libby amphibole fibers have been chemically and physically characterized in detail (68, 114, 192). Libby asbestos contains six different amphibole

fiber types, including winchite, richterite and tremolite. Therefore the asbestos sample is labeled in this paper as Libby 6-mix. Wollastonite, a non-cytotoxic, non-fibrogenic control fiber, was provided by NYCO Minerals (Willsboro, NY). Both fibers were dispersed in phosphate buffered saline (PBS) (pH 7.4) by cup-horn sonication (Misonix, Framingdale, NY) before culturing. Stock concentration suspensions of fibers were prepared fresh immediately prior to their addition into complete RPMI cell cultures. Fiber concentrations were based on relative mass.

Detection and quantification of apoptosis

RAW264.7 cells were exposed to a final fiber concentration of 62.5 μg/cm^2 for up to 72 h. Apoptosis was quantified using an Annexin V APC conjugated antibody (BD Bioscience, San Jose, CA), as previously described (179). Briefly, cells were exposed to fibers, rinsed with PBS, and incubated in 1X binding buffer containing 0.01 M Hepes (pH 7.4), 0.14 M NaCl and 2.5 mM $CaCl_2$. Staining was performed according to the protocol provided by the manufacturer. Cells were washed then transferred to filter-top polypropylene tubes (BD Labware, Franklin Lanes, NJ) for analysis. Data analysis was performed using FACSDiva software (BD Biosciences) for far red fluorescence. Apoptosis was detected through immunoblotting with an anti-Poly (ADP-ribose) polymerase (PARP) rabbit polyclonal antibody (Biomol, Plymouth Meeting, PA) as described below.

Immunofluorescence

Cells were plated in 8-well chambered cover glass slides and exposed to asbestos fibers. After 48 h, cultures were washed in PBS and fixed with 2% formaldehyde and

0.5% glutaraldehyde for 1 h at 4°C. Following washing, cells were blocked in buffer containing 4% normal goat serum, 0.1% bovine serum albumin and 0.1% sodium azide for 1 h at room temperature. SSA/Ro-52 was detected using a rabbit anti-SSA/Ro52 polyclonal antibody (Chemicon International, Temecula, CA) and an Alexa Fluor 488-conjugated goat anti-rabbit antibody (Molecular Probes, Eugene, OR) in blocking buffer. Antigens recognized by autoantibodies produced from asbestos exposed mice were detected using an Alexa Fluor 647-conjugated goat anti-mouse IgG antibody (Molecular Probes). The plasma membrane was visualized using Alexa Fluor 647 cholera toxin subunit B conjugate (Molecular Probes). The nucleus was visualized with propidium iodide (PI) after treatment with RNase A (Roche, Indianapolis, IN). Chambers were covered with FluoroSave Reagent (EMD Biosciences, San Diego, CA) and visualized using an inverted Nikon TE-300 microscope. Fluorescence was examined using a Bio-Rad Radiance 2000 confocal laser scanning microscope and images were merged using Lasersharp software (Bio-Rad, Hercules, CA).

Colocalization analysis

Confocal microscope images were analyzed for colocalization of SSA/Ro52 proteins with the purified rabbit anti-SSA/Ro52 polyclonal antibody and sera from asbestos-instilled mice by use of ImageJ (W. S. Rasband, National Institutes of Health, Bethesda, Md., 1997-2004, http://rsb.info.nih.gov/ij/). Acquired images were analyzed as individual green and red channels corresponding to anti-SSA/Ro52 protein staining and mouse sera staining, respectively. Background was corrected using the background subtraction function on ImageJ. Regions of interest were selected based on patching patterns in both red and green channels. Areas that contained staining artifacts, as

indicated by intense regions of fluorescence in both channels, were excluded from analysis. Pearson's correlation coefficient and Mander's overlap coefficient, a measure of overlap of the red and green signals were generated using the Intensity Correlation analysis plug-in (107) which is included in the WCIF version of ImageJ (http://www.uhnresearch.ca/facilities/wcif/imagej/), with regions of interest for analysis set for the green channel. Colocalization was defined as regions of interest with Pearson's and Mander's overlap coefficient • 0.65.

Immunoblotting

Cells were lysed in RIPA buffer (50mM Tris-HCl (pH 7.4), 150 mM NaCl, 1mM EDTA, 1% Triton, 1% sodium deoxycholate, 0.1% SDS, complete protease-inhibitor cocktail (Roche, Indianapolis, IN). Cell lysates were sonicated and the total protein content was determined by the bicinchoninic acid (BCA) protein assay (Pierce, Rockford, IL). Equal amounts of total protein (50 µg) were resolved by SDS-PAGE and then transferred to nitrocellulose membranes (Millipore, Marlborough, MA). Non-specific binding sites were blocked by incubation for 1 h at room temperature with PBS containing 0.05% Tween-20 (PBST) and 5% non-fat dry milk. Membranes were exposed to either a rabbit anti-SSA/Ro52 polyclonal antibody (Chemicon), a mouse anti-actin monoclonal antibody (Abcam, Cambridge, MA), a rabbit anti-PARP polyclonal antibody (Biomol) or whole mouse sera in PBST-0.5% milk overnight at 4°C followed by incubation with horseradish peroxidase-conjugated secondary antibodies. Immunoreactivity was visualized by chemiluminescence substrate according to the manufacturer's instructions (Pierce) and was quantified by densitometry using a FugiReader LAS-3000 (Fugifilm, Stamford, CT).

Mice

Eight week old C57Bl/6 (Jackson Laboratories, Bar Harbor, ME) were housed under specific pathogen-free conditions with a 12-hour light and 12-hour dark cycle, constant temperature, and free access to food and water. Euthanasia was performed by ip injection of a lethal dose of sodium pentobarbital, consistent with the recommendations of the Panel on Euthanasia of the American Veterinary Medical Association. All protocols for the use of animals were approved by the University of Montana Institutional Animal Care and Use Committee (IACUC).

Asbestos instillation

C57Bl/6 mice were instilled intra-tracheally with saline, wollastonite (NYCO) or Korean tremolite (NIST) with a total of two doses, each dose being 60 μg of the fibers sonicated in sterile phosphate buffered saline (PBS), given one week apart in the first two weeks of the 7 month experiment as previously described (140). Suspensions of 30 μl were injected into the trachea via 25 gauge needles, and the incision was closed with 3M Vetbond tissue adhesive. The animals were monitored biweekly for autoantibody production. Blood samples were obtained through saphenous vein bleeds, and then by cardiac puncture after euthanization at 7 months after instillation. Serum was collected from the blood by centrifugation following clotting at room temperature. Serum samples were stored at –20°C until analysis.

Detection of autoantibodies

Specific autoimmune targets were identified by immunoblotting on nitrocellulose bound with known nuclear antigens (MarDx Marblot, SLR Research, Carlsbad, CA), according to the manufacturer's instructions, modified to detect mouse IgG using a goat anti-mouse IgG secondary antibody conjugated to alkaline phosphatase (SouthernBiotech, Birmingham AL). Reactivity of murine autoantibodies against SSA/Ro52 was confirmed by an SSA ELISA kit (INOVA Diagnostics, San Diego, CA) modified to detect mouse IgG using goat anti-mouse secondary antibody (Jackson ImmunoResearch, Philadelphia PA).

Statistical Analysis

Data are given as mean ± standard error of the mean (SEM). Analyses were done using the software package GraphPad Prism 3.03 (GraphPad, San Diego, CA). One-way analysis of variance (ANOVA) was used to compare groups with one variable, A Bonferroni post test was used to compare different treatments. Statistical significance was established as a two-tailed probability of type I error occurring at less than 5%.

Results

Libby 6-mix induces apoptosis in murine macrophages

Previous results have shown that exposure to Libby 6-mix decreases cell viability in RAW264.7 cells after 24 h (9). To determine whether the decrease in cell viability is a result of apoptosis, RAW264.7 cells were exposed to Libby 6-mix at a final concentration of 62.5 μg/cm^2 for up to 48 h. Apoptosis was quantified through Annexin V staining as previously described (179). Annexin V staining is a sensitive tool for the detection of

apoptosis because it binds the membrane phospholipid, phosphatidylserine, on the outer leaflet of the cell membrane during early apoptosis. After 24 h of exposure to Libby 6-mix, approximately 10 percent of murine macrophages were positive for Annexin V and therefore apoptotic (Fig. 3.1). The percent of apoptotic cells increased to approximately 20 percent after 48 h of exposure. The increase in apoptosis was statistically significant compared to untreated control cells after 24 and 48 h ($P < 0.05$). Exposure to 1 μM staurosporine for 6 hours induced apoptosis in greater than 50 percent of macrophages. In contrast, exposure to wollastonite fibers, which is a non-cytotoxic, non-fibrogenic control fiber, did not induce apoptosis compared to untreated controls (Fig. 3.1).

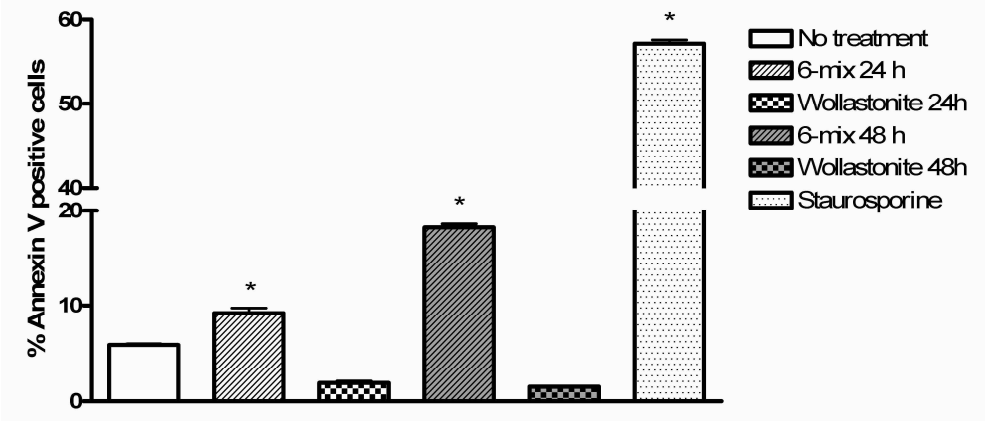

Figure 3.1: Libby 6-mix induces apoptosis in murine macrophages. RAW264.7 cells were exposed to either Libby amphibole asbestos fibers or wollastonite fibers (62.5 μg/cm^2) for 24 and 48 h or 1μM staurosporine for 6 h. Apoptosis was quantified through Annexin V staining as described in Materials and Methods. Apoptosis was quantified as the percent of cells that were positive for Annexin V staining through flow cytometry. Results represent mean percentages ± SEM. Asterisks indicate a significant difference compared to control ($P < 0.05$, $n = 3$).

A second indicator of apoptosis in cells is the cleavage of a select group of nuclear proteins (24). Poly (ADP-ribose) polymerase (PARP) is a 116 kDa nuclear protein that is cleaved into an 89 and 24 kDa fragment in apoptosis (47). Therefore, to confirm that exposure to Libby 6-mix leads to apoptosis in macrophages, RAW264.7 cells were exposed to Libby 6-mix for up to 72 h. Total cell lysates were prepared and analyzed through immunoblotting. In untreated cells, PARP exists primarily as a 116 kDa protein. Treatment of macrophages with 1 μM staurosporine for 6 hours resulted in the cleavage of the full length PARP protein into the 89 kDa fragment (Fig. 3.2), which is consistent with previous results (197). Exposure to Libby 6-mix initially resulted in a reduction of full length PARP protein compared to the total amount of protein as quantified by densitometry (Fig. 3.2). The reduction of full length protein was correlated with an increase in the amount of the 89 kDa fragment after 72 h. Additionally, exposure to either Libby 6-mix or staurosporine did not result in the cleavage of SSA/Ro52 during apoptosis (data not shown), as previously described (24). Together these data clearly indicate that Libby 6-mix induces apoptosis in murine macrophages.

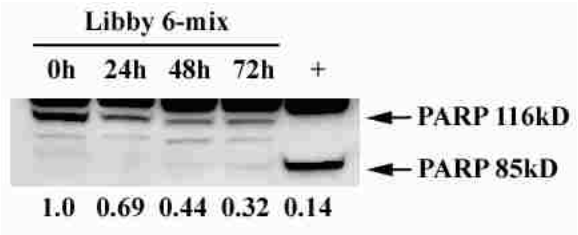

Figure 3.2: Libby 6-mix exposure results in the cleavage of PARP. RAW264.7 cells were exposed to Libby 6-mix fibers at a final concentration of 62.5 μg/cm^2 for 24, 48 and 72 h or to 1 μM staurosporine for 6 h (positive control). Cell lysates were prepared and analyzed through immunoblotting using an anti-PARP rabbit polyclonal that detects the full length protein (116 kDa) and the cleaved fragment (85 kDa). Values below signify the densitometric units determined for the immunoreactive bands of full length PARP divided by the densitometric units determined for the immunoreactive bands of the actin loading control and reported as the fold changed compared to control.

SSA/Ro52 redistributes to apoptotic blebs as a result of exposure to Libby 6-mix

To determine whether SSA/Ro52 localizes to cell surface blebs during asbestos-induced apoptosis, murine macrophages were exposed to Libby 6-mix and the localization of SSA/Ro52 was determined through fluorescence confocal microscopy. Murine macrophages were fixed and immunochemically stained using an anti-SSA/Ro52 rabbit polyclonal antibody and an Alexa Fluor 488-conjugated secondary antibody (Green in Figs. 3.3A, E and I). Nuclei (DNA) were visualized with propidium iodide (Red in Figs. 3.3B, F and J). The plasma membrane was visualized by using an Alexa Fluor 647 cholera toxin subunit B conjugate (Magenta in Figs. 3.3C, G and K).

In normal, unstimulated macrophages, SSA/Ro52 localized to the cytoplasm of cells as shown in Figure 3.3A and 3D. However, asbestos exposure resulted in the redistribution of SSA/Ro52 to surface blebs of apoptotic cells (Figs. 3.3H and L). Apoptosis was defined by morphological changes evident in the nucleus as previously described (129). Briefly, apoptosis was evident where there were distinctive nuclear changes such as elongation, condensation or fragmentation. Distinct nuclear condensation is seen in Figure 33.F. Apoptotic blebs enriched in the SSA/Ro52 autoantigen translocated to the surface of the apoptotic cells and were compartmentalized within membrane bound structures (Fig. 3.3H). Compartmentalization of SSA/Ro52 to membrane bound structures was also confirmed through Z-stack images (data not shown). Apoptotic cells in a more advanced stage of apoptosis also undergo apoptotic membrane blebbing at their surface (Fig. 3.3L). Generally, larger apoptotic blebs contained SSA/Ro52 and DNA whereas smaller apoptotic blebs contained high concentrations of SSA/Ro52 and lacked nuclear material. Similar induction of apoptosis was confirmed in RAW264.7 cells with 1 μM staurosporine treatment of for 6 h

(Supplemental Fig. 3.1). These results clearly show that SSA/Ro52 does redistribute to surface blebs of apoptotic cells after exposure to Libby amphibole asbestos.

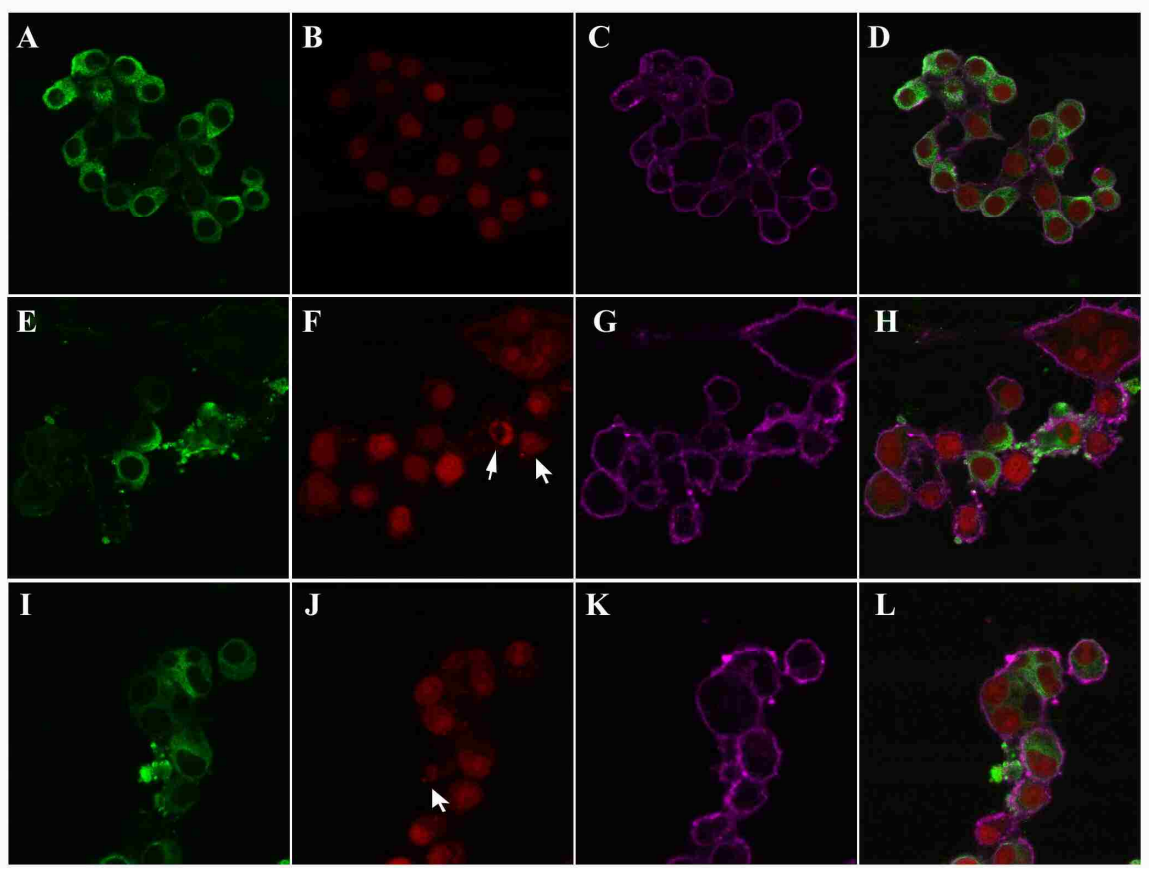

Figure 3.3: Libby 6-mix exposure results in the redistribution of SSA/Ro52 to surface blebs of apoptotic cells. RAW264.7 cells were untreated (Panels A-D) or exposed to Libby asbestos for 48 h (Panels E-L). The distribution of the SSA/Ro52 autoantigen was visualized through confocal microscopy using a rabbit polyclonal anti-SSA/Ro52 and an Alexa Fluor 488 conjugated goat anti-rabbit IgG secondary (Green in panels A, E and I). Nuclei were counterstained with propidium iodide (Red in panels B, F and J). Apoptotic nuclei are indicated by an arrow. The plasma membrane was visualized with Alexa Fluor 647 cholera toxin subunit B conjugate (Magenta in panels C, G and K). Right panels (D, H and L) show merged images.

Apoptotic blebs containing SSA/Ro52 are recognized by autoantibodies from asbestos exposed mice

Sera from tremolite exposed mice have been shown to be positive for anti-SSA/Ro52 autoantibodies through ELISA (140). However, sera from PBS or wollastonite treated animals were negative. To confirm reactivity of murine AAs in RAW264.7 cells, whole cell lysates were prepared and analyzed through immunoblotting with mouse sera. As seen in Figure 3.4, mouse sera from tremolite treated mice recognized SSA/Ro52. However, little or no reactivity was observed with sera from mice treated with PBS or wollastonite fibers, which supports our previous results.

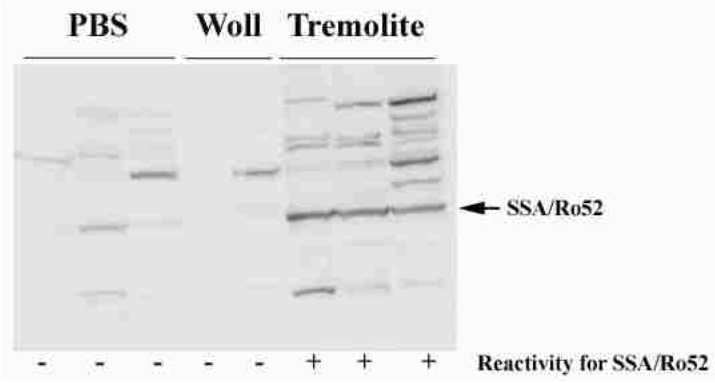

Figure 3.4: Autoantibodies from asbestos-exposed mice specifically recognize the SSA/Ro52 autoantigen. RAW264.7 cell lysates were prepared and reactivity of whole mouse sera from saline, wollastonite or tremolite asbestos exposed animals was analyzed through immunoblotting. Arrow indicates the correct size of the SSA/Ro52 autoantigen. Symbols below indicate which sera were reactive (+) or not reactive (-) to the SSA/Ro52 autoantigen as determined by ELISA as previously reported (140).

To determine whether AAs from asbestos-instilled mice target SSA/Ro52 on the surface of apoptotic cells, murine macrophages were exposed to Libby asbestos as described above, fixed and immunochemically stained using an anti-SSA/Ro52 rabbit polyclonal antibody and an Alexa Fluor 488-conjugated secondary antibody (Green in Fig. 3.5). Nuclei were visualized through propidium iodide (Cyan in Fig. 5). Autoantigens targeted by mouse sera from asbestos-instilled or control mice were visualized with an Alexa Fluor 647-conjugated secondary antibody (Red in Fig. 3.5). Colocalization of SSA/Ro52 with autoantigens recognized by murine AAs is seen as yellow in Figure 3.5.

AAs from asbestos-exposed mice recognized antigens in apoptotic blebs in murine macrophages and resulted in a pattern similar to that of SSA/Ro52, indicating colocalization of SSA/Ro52 with the target of asbestos-induced AAs (Figs. 3.5A-C). A representative confocal microscopy image is shown in Figure 5A with AA staining from a mouse exposed to tremolite asbestos. Figures 3.5B and C include representative confocal microscopy images with AA staining from a different mouse exposed to tremolite asbestos. Colocalization of cell surface blebs with SSA/Ro52 and murine AA staining were visualized on the same plane of focus as apoptotic nuclei (Figs. 3.5A and B) and above the plane of focus of apoptotic nuclei, indicating these blebs are cell surface structures (Fig. 3.5C). Colocalization within regions of interest (ROI) was confirmed by ImageJ using the Intensity Correlation analysis plug-in (see Materials and Methods). Sera from mice exposed to PBS or wollastonite did not recognize apoptotic blebs on the surface of exposed cells (Fig. 3.5D).

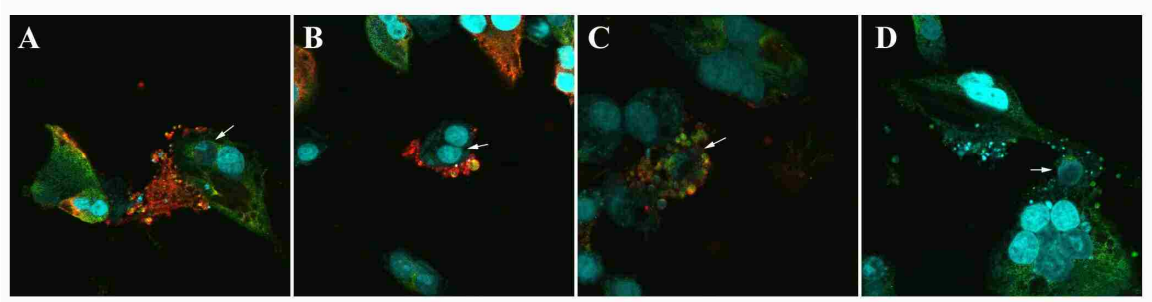

Figure 3.5: Autoantibodies from asbestos-exposed mice recognize apoptotic blebs enriched with the SSA/Ro52 autoantigen. RAW264.7 cells were exposed to Libby asbestos for 48 h (Panels A-D). The SSA/Ro52 autoantigen was visualized through confocal microscopy using a rabbit polyclonal anti-SSA/Ro52 antibody and an Alexa Fluor 488 conjugated goat anti-rabbit IgG secondary (Green in panels A-D). Nuclei were counterstained with propidium iodide (Cyan). Apoptotic nuclei are indicated by an arrow. Binding of mouse autoantibodies were visualized with an Alexa Fluor 647 conjugated goat anti-mouse IgG secondary (Red). Panel A includes AA staining from a mouse exposed to tremolite asbestos. Panels B and C include AA staining from a different mouse exposed to tremolite asbestos. Panel D includes AA staining from a control mouse. Colocalization of SSA/Ro52 and autoantigens recognized by asbestos-induced mouse AAs is visualized in yellow. Colocalization was confirmed through Image J analysis.

Discussion

Environmental exposure to crystalline silicates, such as silica and asbestos, generate the production of AAs and induce autoimmune phenotypes in humans and in mice. Exposure to silica exacerbates autoimmune responses in individuals in 'dusty' trades as well as autoimmune prone mice (15, 136). Likewise, humans exposed to Libby amphibole asbestos have a significantly higher prevalence of AAs (141). AA titers from this cohort correlate with longer exposure times and more severe ARD. Additionally, intra-tracheal amphibole asbestos exposure in mice results in an increase in AA production (140). Together these results provide support for the hypothesis that, like silica, exposure to amphibole asbestos exacerbates autoimmune responses and may lead to the development of autoimmunity. A role for apoptosis in AA responses to silica has

been previously hypothesized (16). However, possible mechanisms for asbestos induced autoimmunity have not been elucidated.

Exposure to Libby amphibole asbestos has been shown to generate in an increase in reactive oxygen species and a decrease in intracellular glutathione levels resulting in oxidative stress in murine macrophages (9). Libby amphibole asbestos also directly affects human alveolar macrophages leading to an increase in lymphocyte derived cytokine production, which suggests that amphibole asbestos fibers can modify immune function by altering antigen presenting cell (APC) activity (71). Increased APC activity due to asbestos exposure may up-regulate the normal lymphocyte response to antigens in the lung leading to a loss of tolerance. We hypothesize that asbestos-induced autoimmunity is generated through a two hit mechanism. First, autoantigens become visible to the immune system during apoptosis, which results in the accumulation of autoantigens on the cell surface. The subsequent uptake and processing of apoptotic cells by antigen-presenting cells in a pro-inflammatory context will activate self-reactive T cells, inducing the loss of tolerance and generate the autoimmune responses observed in humans and mice.

Apoptosis is thought to play a critical role in the development of autoimmunity. Deficiencies in apoptotic cell clearance are associated in humans with the development of autoimmunity (184). Moreover, mice genetically deficient in apoptotic cell recognition molecules have a reduced phagocytic capacity for apoptotic cells and eventually develop autoimmune phenotypes such as immune-complex deposition and the production of AAs (34, 72, 119). However, a defect in apoptotic cell clearance alone is not sufficient to develop an autoimmune phenotype, suggesting that apoptotic cells can persist in the absence of pro-inflammatory consequences (42). Several *in vitro* studies have

demonstrated that the intracellular signals generated by both early and late apoptotic cells are distinct from those generated by necrotic cells. Cellular signals from apoptotic cells are dominant over those of necrotic cells and are not pro-inflammatory even after the loss of membrane integrity (137, 149). Therefore, apoptotic cells alone do not stimulate inflammation to promote autoimmunity.

Cellular antigens targeted by AAs in SAID are expressed intracellularly and are diverse in terms of their localization, structure and function. However, one common factor among autoantigens that are targeted by the immune system is that they are enriched in cell surface blebs of apoptotic cells (23). The present study indicates that Libby amphibole asbestos induces apoptosis in macrophages as determined by several methods including extracellular PS exposure (Fig. 3.1), cleavage of PARP (Fig. 3.2) as well as morphological changes such as nuclear condensation and cell surface blebbing. The cell surface blebs, generated by asbestos induced apoptosis, are enriched in the SSA/Ro52 autoantigen (Fig. 3.3). These cell surface blebs may be the potential stimuli for the initiation of an autoimmune response. Indeed, murine AAs from asbestos exposed mice recognize SSA/Ro52 on the surface of apoptotic macrophages indicating the antigenicity of SSA/Ro52 (Fig. 3.5). The binding of AAs to apoptotic cells has been previously shown to inhibit the clearance of apoptotic cells leading to their accumulation, which promotes inflammation and tissue damage (31, 60, 157). Therefore, AAs induced by asbestos may exacerbate tissue damage in the lung and thereby promote fibrosis in the lung.

Because apoptosis alone does not elicit autoimmunity, a second pro-inflammatory signal such as an adjuvant must be provided in order to generate an immune response (12, 115, 175). Asbestos induces a highly inflammatory state in the lung (50, 89, 170).

Exposure to amphibole asbestos in alveolar macrophages has been previously shown to increase the release of pro-inflammatory cytokines such as TNF- and Il-1 (46). In this environment an increase in apoptosis may lead to excess presentation of autoantigens thereby exacerbating an autoimmune response.

In summary, exposure to Libby amphibole asbestos induces apoptosis in murine macrophages. Apoptosis induces the translocation of SSA/Ro52 from the cytosol to cell surface blebs. These apoptotic blebs containing SSA/Ro52 are recognized by AAs from asbestos exposed mice. This study provides evidence for the role of apoptosis in asbestos induced autoimmune responses and also supports the mechanism of apoptosis in the induction of xenobiotic autoimmunity.

Acknowledgments

The authors thank Scott Wetzel and Sheng'ai Li, University of Montana, for helpful discussions and technical assistance, Pamela Shaw in the CEHS Fluorescence Cytometry Core for assistance with the FACS analysis and Lou Herritt in the CEHS Histology and Imaging Core for assistance with the confocal microscopy analysis.

Grants

This work was funded by grants from the NIH COBRE P20 NCRR017670, R21 ES012956 and from the University of Montana Graduate School.

Supplemental Data

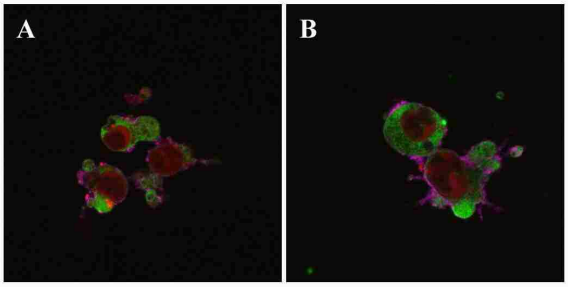

Supplemental Figure 3.1: Staurosporine treatment results in the redistribution of SSA/Ro52 to surface blebs of apoptotic cells. RAW264.7 cells were treated with 1 μM staurosporine for 6 h. The distribution of the SSA/Ro52 autoantigen was visualized through confocal microscopy using a rabbit polyclonal anti-Ro52 and an Alexa Fluor 488 conjugated goat anti-rabbit IgG secondary (Green). Nuclei were counterstained with propidium iodide. Apoptotic nuclei are indicated by an arrow (Red). The plasma membrane was visualized with Alexa Fluor 647 cholera toxin subunit B conjugate (Magenta).

Chapter 4

A characterization of autoantibodies from an asbestos exposed population in Libby, MT is suggestive of a serological autoimmune phenotype similar to systemic lupus erythematosus

David J. Blake[*], Sheng'ai Li[†] and Jean C. Pfau[†]

Division of Biological Sciences[*] *and Department of Biomedical & Pharmaceutical Sciences, Center for Environmental Health Sciences*[†]*, University of Montana, Missoula, Montana, 59812*

Abstract: Residents of Libby, MT have experienced significant exposure to amphibole asbestos due to the mining of asbestos contaminated vermiculite near the community over several decades. Serum samples from these residents have higher frequencies of positive anti-nuclear antibody (ANA) tests compared to those from an unexposed control population. Higher ANA titers correlated with longer exposure times as well as more severe lung disease, suggesting that autoimmune responses may play a role in the progression of ARD. The purpose of this study was to further characterize the serological targets of these autoantibodies (AAs) and determine whether the presence of AAs correlate with particular clinical manifestations. Our results indicate that AAs from amphibole asbestos exposed individuals primarily recognize chromatin, histone and SSA/Ro52, which is similar to patients with systemic lupus erythematosus (SLE). Anti-dsDNA and anti-SSA/Ro52 AAs are also generated in a murine model of asbestos induced autoimmunity, which suggests that similar immunological changes occur in both humans and in mice. Although no correlation was observed between AAs that recognized a specific set of autoantigens and the extent of exposure, this study indicates that human exposed to Libby amphibole asbestos are serologically similar to patients with SLE. These results may aid in the clinical screening, diagnosis and treatment of this asbestos exposed population.

Keywords: asbestos, autoantibodies, environmental autoimmunity, immunotoxicology

Introduction

Environmental asbestos exposure is associated with increased autoimmune responses including increased serum immunoglobulin levels, positive autoantibody (AAs) tests and immune complex deposition, all of which are consistent with the development of autoimmunity (127, 141, 200). The premise that asbestos exposure exacerbates autoimmune responses in humans is supported by two recent studies from an asbestos exposed population in Libby, MT. Residents of Libby, MT have experienced significant exposure to amphibole asbestos due to the mining of asbestos contaminated vermiculite near the community over several decades. Exposure to Libby amphibole asbestos increases the risk for systemic autoimmune disease (SAID) by more than 50% (128). Moreover, residents of Libby, MT have higher frequencies of positive anti-nuclear antibody (ANA) tests compared to those from an unexposed control population (3). Higher ANA titers correlated with longer exposure times as well as more severe lung disease, suggesting that autoimmune responses may play a role in the progression of ARD.

The aberrant production of AAs is a key feature of SAID. Patients with a particular SAID generate AA profiles that recognize specific intracellular components. Therefore, AAs can be used to establish a diagnosis as well as determine the clinical progression of a patient. The prevalence of certain AAs in a particular disease is an important parameter that influences their diagnostic sensitivity and specificity (155). Patients with systemic lupus erythematosus (SLE) generate a number of autoantibodies that react with dsDNA, histones, SSA/Ro52, SSB/La, Sm and ribonucleoprotein (RNP)

(155). Although these AAs can be found in other SAIDs, anti-dsDNA and anti-RNP antibodies are disease markers specific to SLE (37). AAs are also highly correlated with certain clinical disease manifestations. For example, autoantibodies against dsDNA and SSA/Ro correlate to separate clinical disease activities in idiopathic and neonatal lupus patients (146, 172, 173). In contrast, antibodies against histones are correlated to manifestations of drug induced lupus (57).

Exposure to another silicate compound, crystalline silica, is associated with autoimmune diseases such as SLE, scleroderma (SSc) and rheumatoid arthritis (RA) (133, 136). However, it is not known whether a discrete clinical or sub-clinical entity is associated with amphibole asbestos exposure, despite an increased frequency of autoantibody tests in asbestos exposed cohorts (141). Amphibole asbestos exposure increases the risk for SLE, SSc and RA, similar to silica exposure (128). In addition, asbestos exposure leads to clinical manifestations similar to SLE in asbestos exposed mice (140). Therefore, we hypothesize that certain autoimmune diseases may be associated with asbestos exposure in humans. An analysis of the specific targets of AAs from residents in Libby, MT can provide insight and help determine the clinical diagnoses in this exposed population. The spectrum of AAs related to amphibole asbestos exposure may have implications in elucidating the immunologic response to asbestos and provide a biomarker for clinical screening. The objective of this study was to characterize the specific autoantibodies found in serum samples from the Libby cohort and to determine if the presence of autoantibodies correlated with a particular clinical pattern.

Materials and Methods

Human serum samples

All srum samples were acquired according to approved University of Montana institutional review board (IRB) protocols, protecting the well-being and confidentiality of all subjects. Appropriate informed consent was obtained from all subjects, and a questionnaire was administered regarding overall health, smoking status, asbestos exposure, age, and sex. Samples were drawn at the Center for Asbestos Related Diseases Clinic in Libby, MT as previously described (141).

Sample and data collection

The blood samples were collected, and serum samples were obtained and frozen by standardized clinical methods to prevent differences due to handling. The samples were blinded with only sex and age noted, and stored at −80°C until assayed. Coded information regarding disease status and exposure was obtained from a questionnaire and screening data from the Agency for Toxic Substances and Disease Registry (ATSDR), which performed a screening in Libby during 2000-2001 (141).

ARD and asbestos exposure rankings

ARD status, based on data recorded in the database primarily as a result of the ATSDR screenings, was ranked on a scale of 0–3, as previously described (141). Exposure status was ranked on a scale of 0–4, also as previously described (141). The rankings of the Libby subjects were performed independently by two of the researchers.

Detection of serum autoantibodies

A clinical test for autoantibodies to nuclear antigens (ANA assay) was performed at a screening dilution of the sera. All serum samples were diluted 1:40 in phosphate-buffered saline (PBS, pH 7.4) and tested by indirect immunofluorescence (IIF) on a single lot of commercially prepared and fixed HEp-2 cells (ImmunoConcepts Inc., Sacramento, CA), according to manufacturer's instructions. The staining pattern and relative fluorescence intensity were compared with known positive and negative controls using a Zeiss fluorescence microscope with 400× magnification and recorded as positive (1+ to 4+) or negative (0). The staining pattern was also noted and recorded. The same microscope and settings were used for all samples, and the slides were read by two independent readers.

Addressable Laser Bead Immunosorbent Assay (ALBIA)

Analyses of antibodies to eight extractable nuclear antigens (ENAs) and chromatin commonly seen in SAID (Sm, RNP, SS-A 52, SS-A 60, SS-B, Scl-70, Jo-1, Ribosomal P and Chromatin) were performed using an ALBIA kit (QUANTA Plex™ SLE Profile 8; INOVA Diagnostics) according to the manufacturer's instructions, on a Luminex multiplex system (MiraiBio, Alameda, CA). The values were compared by using Starstation 2.0 software (Applied Cytometry Systems, Sacramento, CA) to negative and graduated positive control reagents provided with the kit, and determined to be low or high positive, or negative.

Quantification of IgM rheumatoid factor (RF)

IgM RF in the serum samples was measured with an ELISA kit according to the manufacturer's protocol (INOVA Diagnostics). The plate was read on the SpectraMax

plate reader (Molecular Devices, Sunnyvale, CA) at 450 nm. Optical density (OD) values were compared with known controls provided with the kit and rated as negative or positive.

Histone ELISA

Histone antibodies in the subjects' sera were measured with a QUANTA Lite™ Histone according to the manufacture's protocol (INOVA Diagnostics). Antibodies to H1, H2, H3 and H4 are detected with this assay. The plates were read on the SpectraMax plate reader at 450 nm. Optical density (OD) values were compared with known controls provided with the kit and rated as negative, low positive, high positive.

Statistical Analysis

Serum samples that recognized one of the nine autoantigens as described in Material and Methods were classified as positive and treated as ordinal data. Alternatively, serum samples that were unreactive to the autoantigens were classified as negative. Extent of exposure was classified as ordinal data as 5 point levels. Data were analyzed non-parametrically through two approaches. Data were analyzed using contingency tables using subject scores through the chi-square test. Data was also analyzed using Mann-Whitney analysis using subject scores. Statistical significance was established as a two-tailed probability of type I error occurring at less than 5%. Analysis and graphics were performed on Prism 4.0 software (GraphPad, San Diego, CA).

Results

Frequency of antinuclear antibodies

The 70 randomly chosen serum samples from Libby, MT were tested by IIF for ANA and were determined to be positive or negative based on known controls. 50 of the 70 serum samples (70%) were ANA positive, which is consistent with previously published results (141). The intensity and the staining patterns visible on the ANA tests were also recorded (Table 4.1). The staining patterns that were the most prevalent were homogeneous (indicative of antibodies to chromatin), nucleolar and speckled staining patterns.

Patient	Age	Sex	Disease	Exposure	ANA score and pattern	SLE 9 Profile	RF IgM
1	72	M	3	4	0	0	0
2	59	F	3	3	2, spkl	0	0
3	65	F	3	3	3, hom/spkl	SSB	0
4	48	M	3	1	0	0	0
5	54	M	2	4	1 spkl	SSA-52	0
7	47	F	0	3	3 nuc	Chromatin, Histone	0
8	48	F	1	3	0	RNP	0
9	65	M	2	4	3 hom	0	1
11	48	M	3	4	3 hom	Scl-70	0
14	48	M	2	2	0	0	1
17	43	M	2	2	3 spkl	0	0
18	36	M	2	4	1 nuc	0	0
19	62	F	2	3	2 nuc	0	0
36	57	M	3	3	2 nuc	0	1
38	61	M	3		3 hom	Chromatin	1
39	69	F	3	3	2 nuc	Chromatin, Histone	1
40	78	M	3	4	2 nuc	0	1
41	43	M	3	4	2 cent	0	0
44	51	M	2	1	0	0	0
47	66	M	3	3	4 hom	0	0
49	49	F	1	3	0	0	0
50	63	F	2	3	3 hom	SSA-60	1
53	58	F	1	3	2 nuc/cyto	0	1
58	60	M	3	1	0	RNP	1
60	53	M	1	4	4 hom	Chromatin, Histone	1
65	73	F	3	3	2 hom	0	0
66	52	F	1	1	0	0	0
68	45	F	1	1	0	0	0
70	69	F	2	4	3 hom, cyt	Chromatin	1
73	41	M	1	3	4 hom	0	0
74	44	M	0	3	1 nuc	Scl-70	0
77	55	F	2	3	3 hom/nuc	0	0
79	42	F	0	3	1 spkl	0	0
81	51	F	2	3	4 cent	0	1
83	32	F	1	1	0	0	0
86	59	M	2	3	1 spkl	0	0
89	56	M	2	3	2 hom/spkl	0	0
92	66	M	3	3	3 atyp	0	0
98	52	M			0	0	0
99	71	M	3	4	2 hom	0	0
100	66	M	2	3	1 hom	0	0
102	64	M	2	3	1 spkl	0	0
118	79	F	2	3	4 hom	0	0
119	70	F	3	3	3 hom/nuc	0	1
120	79	M	3	2	2 hom	0	1
121	69	F	0	3	4 nuc	Chromatin, Histone	0
122	39	F	0	1	0	0	0
123	36	M	2	2	1 nuc	0	0
126	75	F	2	3	1 hom	0	1
127	60	F			2 spkl	0	0
129	50	M	0	4	3 spkl	0	0
135	62	M	3	3	3 nuc	0	0
136	44	F		1	4 spkl	0	1
142	62	M	2	0	0	0	1
164	39	F	1	3	3 spkl	0	1
167	33	M	3	4	0	0	1
176	99	F	2	3	0	SSA-52	0
177	79	F	0	1	2spkl	0	1
180	62	F	3	3	2 spkl	0	0
185	49	F	0	4	1 spkl	0	0
190	44	F		3	0	0	1
196	66	M	1	4	0	0	0
198	35	M	1	3	0	0	0
207	69	M	3	3	0	0	0
224	49	F	0	1	2 spkl	0	0
225	41	M	0	1	2 hom	0	1
05-143					1 hom/nuc	0	1
05-145					2 hom/nuc	Chromatin, Histone	1
05-148	71	F	3	1	1 hom	0	0
05-153	53	M	2	4	2 hom/nuc	SSA-52	0

Figure Legend on page 81.

Table 4.1: Complete serological data of all seventy Libby serum samples.
Notes: homo denotes homozygous staining, nuc denotes nuclear staining, spkl denotes speckled staining, cyto denotes cytosolic staining, cent denotes centriolar staining, atyp denotes atypical staining. For SLE 9 and RF IgM classifications 0 denotes a negative test and 1 denotes a positive test.

Autoantibody characterization

An addressable laser bead immunoassay, which detects reactivity to nine autoantigens commonly targeted in SAID, was used to characterize the specific target antigens of the autoantibodies found in the Libby cohort. Sixteen of the seventy total Libby serum samples (23%) had positive autoantigen tests and were all reactive to a single target antigen. The most common autoantibodies detected in the Libby serum samples were autoantibodies to chromatin (44% of the positive samples) and autoantibodies to SSA/52 (19% of the positive samples). Serum samples that were positive against chromatin were further analyzed through a histone ELISA. Of the seven samples that were positive against chromatin, 5 samples tested positive against histones (71%). No serum samples reacted with Jo-1, Sm or Ribo P. Figure 4.1 shows the distribution of positive tests against the target antigens.

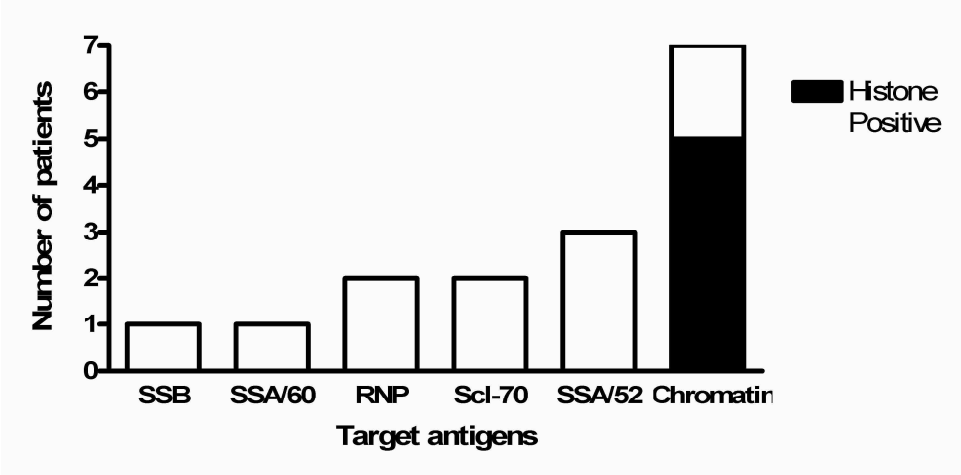

Figure 4.1: Autoantibodies from Libby serum samples recognize multiple autoantigens similar to patients with systemic lupus erythematosus (SLE). 70 Libby serum samples were testedThe specific targets recognized by AAs from Libby serum samples were characterized with an addressable laser bead immunoassay as described in Materials and Methods. Serum samples that tested positive for chromatin were further analyzed for reactivity against histones.

IgM RF frequency

RF is an autoantibody directed at the Fc region of IgG and is usually of IgM isotype. RF is associated with a number of inflammatory diseases and not specific to rheumatoid arthritis (RA) (116). The presence of these AAs may contribute to disease by the formation of immune complexes in tissues. The samples were evaluated for IgM RF by ELISA. 24 of the seventy total Libby serum samples (34%) were positive for RF IgM which is consistent with previously published results (141).

Correlation of assay results with extent of exposure and ARD

In order to improve the power of our statistical analysis, the presence or absence of AAs to one of the nine ENAs was classified as ordinal data and classified as positive or negative, respectively. To determine whether an association exists between the

presence of AAs and the extent of exposure, data were analyzed through a chi-square test. Alternatively, to determine whether the presence of AAs represented a distinct population among the extent of exposure, data were also analyzed through a non-parametric Mann-Whitney U-test. No significant association was observed between the presence of AAs to ENAs and the extent of exposure. Residents with positive ENA tests had a slightly higher exposure status, but this difference was not statistically significant (Fig. 4.2) (P = 0.1312). These results indicate that the presence of AAs to specific ENAs do not correlate to asbestos exposure in this small asbestos exposed cohort.

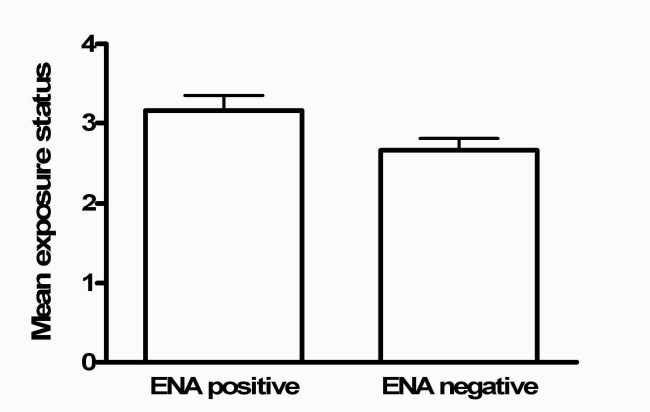

Figure 4.2: Libby serum samples that were ENA positive had a higher exposure status than ENA negative samples. 70 Libby serum samples were determined to be either ENA positive or negative by an addressable laser bead immunoassay as described in Materials and Methods. The exposure score of each serum sample was determined as described in Material and Methods and is indicated in Table 4.1. Serum samples that were positive for the presence of autoantibodies had slightly higher asbestos exposure scores.

Discussion

Environmental exposure to crystalline silicates such as silica and asbestos is associated with the production of AAs and the development of SAID in humans (16, 127, 200). More specifically, exposure to amphibole asbestos in the population of Libby, MT has been shown to increase autoimmune responses (141). The present study looks to

extend these observations by characterizing the specific AA targets in this cohort in order to aid in the screening, diagnosis and treatment of asbestos exposed subjects.

The most useful technique for the detection of AAs is indirect immunofluorescence for ANAs using HEp-2 cells. This screening test offers the appropriate level of sensitivity (182), however, it is not sufficiently specific to establish a diagnosis in patients with SAID. AA tests against ENAs is a more specific and sensitive confirmatory test for the detection and semiquantification of ENA antibodies in human sera (109). With the exception of antibodies to cytoplasmic antigens, such as Jo-1 and SSA/Ro52, it is rare to have a positive anti-ENA antibody test in the absence of a positive ANA test. In order to correctly screen a patient for the presence of AAs, it has been suggested that a two stage testing be performed that includes an initial ANA screening test followed by a confirmatory anti-ENA test (142).

Residents of Libby, MT have higher frequencies and titers of positive ANA tests, which correlated to the extent of exposure and the severity of disease (141). AAs characterized from the Libby cohort were initially described as recognizing more than one ENA (141). The reactivity of serum samples to more than one target antigen makes a serological diagnosis for a specific SAID difficult. In addition, the present characterization indicates that in all cases AAs from the asbestos exposed cohort recognize a single antigen. Reactivity to more than one antigen in the earlier study may have been due to non-specific binding of the serum samples to the beads in the immunoassay. Indeed, some serum samples appear to have high background binding without demonstrating specific binding to any of the cognate antigens (56). Therefore, the present study provides necessary data to enable a more specific assessment of the AAs.

The most common AAs from the Libby cohort were reactive to chromatin, histones and SSA/Ro52. This AA profile is similar to those found in patients with SLE (155). Anti-dsDNA antibodies are found in approximately 70% of patients with SLE and are an important disease marker (37). However, anti-dsDNA antibodies are also found in a small percentage of patients with mixed connective tissue disease (MCTD) disease and RA (37). Anti-histone antibodies are also found in approximately 40% of patients with SLE, but are associated with clinical symptoms of drug-induced lupus (37). Antibodies against certain components of histone, such as H2A-H2B dimer, are thought to be characteristic of drug-induced lupus while reactivity to the H1 and H2B subunits of histones is common in idiopathic SLE (18, 40). Since the assay used to determine anti-histone reactivity was not specific to a certain component of histone, the anti-histone antibodies observed in this study could be directed against the H1, H2, H3 or H4 subunits of histone. Therefore, further characterization is needed to determine the specific epitopes targeted for histones. Finally, anti-SSA/Ro52 AAs have also been identified in patients with idiopathic SLE (74, 145). Although clinical observations are needed to diagnosis a specific autoimmune disease, the serological data presented here heavily supports a SLE-like syndrome in the asbestos exposed cohort from Libby, MT.

A murine model of asbestos-induced autoimmunity was recently established to investigate the mechanisms by which asbestos triggers systemic autoimmunity (140). Asbestos exposed mice develop positive ANA tests and mild glomerulonephritis suggestive of a SLE-like disease. Interestingly, the murine SLE-like disease was characterized by the production of AAs that recognize dsDNA and SSA/Ro52 (140). Anti-chromatin and anti-SSA/Ro52 AA are the predominant AAs characterized in the asbestos exposed cohort. These data support the premise that amphibole asbestos

generates a serological SLE-like disease in both humans and in mice. Moreover, because humans and mice exposed to amphibole asbestos generate similar AA profiles, the alterations of the immune response by amphibole asbestos may be comparable. Therefore, the murine model of asbestos induced autoimmunity is both relevant and useful to study the immunological effects of amphibole asbestos.

Although no correlation was observed between the presence of AAs against a specific set of autoantigens and extent of exposure, our data clearly indicate an autoimmune phenotype in this cohort. The lack of correlation may be a result of the lack of statistical power due to the small numbers of positive samples. Therefore, further characterization studies can enhance this study by analyzing a larger number of serum samples from the Libby cohort. Correlations between autoantibody specificities and exposure or the severity of disease may be elucidated with a larger cohort. Indeed, certain AA profiles have been identified in SLE patients and are associated with specific clinical symptoms such as arthritis (76). Finally, collaboration with medical doctors that treat and advise patients from Libby, MT would provide necessary clinical diagnosis data for this study. Joining clinical observations and the serological characterization presented here has an excellent chance to help accurately characterize clinical autoimmune manifestations of asbestos exposure, and therefore to screen, diagnose and treat asbestos exposed individuals.

Chapter 5

Conclusions and Future Directions

Exposure to Libby amphibole asbestos increases autoimmune responses in humans and in mice (140, 141). The immunological responses induced by asbestos may be a result of the internalization of asbestos fibers by macrophages, which results in oxidative stress and apoptosis in these cells (9, 10). Previous results have shown that the target antigens for autoantibodies elicited by asbestos exposure in C57BL/6 mice are indeed clustered on the surface of apoptotic cell blebs (10). The uptake and processing of apoptotic cells by antigen-presenting cells in a pro-inflammatory context may activate self-reactive T cells, inducing the loss of tolerance and an autoimmune response. In order to more rigorously test this hypothesis three main questions must be answered.

First, are respirable amphibole fibers, which are approximately 1 micron in diameter, more toxic *in vivo* and *in vitro* than other fibers? Second, do apoptotic cells in the presence of amphibole asbestos drive autoimmune responses? Finally, what is the role of antigen presenting cells in the lung in asbestos induced autoantibody production? By addressing these three questions, the mechanisms by which asbestos exposure alters immunological responses in humans will be elucidated. More importantly, understanding the molecular mechanisms by which an environmental exposure generates autoimmune responses may identify important therapeutic targets for environmentally induced autoimmunity in human.

The asbestos used in the studies described previously was provided by the US Geological Survey and is a combination of asbestos samples from 6 separate collection areas. Therefore, the asbestos contamination of Libby vermiculite is chemically and

physically complex. Libby amphibole asbestos has been characterized as both regulated asbestos fibers (e.g., tremolite and other amphibole forms) and unregulated fibers (e.g., winchite and richterite) (113). The mixture of amphibole fibers in the Libby amphibole sample differ in terms of fiber length and metallic cations expressed on the fiber surface. Approximately 5% of the Libby amphibole is non-fibrous material (personal communication - Anna Marie Ristich, DataChem Laboratories). In order to more correctly mimic real life asbestos exposure, respirable fibers can be fractionated from the Libby amphibole stock, which can then be used in future asbestos studies.

Fiber dimension is the most important determinant of fiber pathogenicity in terms of cancer development (130). Early work suggested that fibers longer than 8 microns were more potent inducers of mesothelioma (166). The increased pathogenicity of longer fibers compared to shorter ones has been confirmed *in vivo* (123). Longer fibers also generate enhanced tumor necrosis factor production and an increased level of oxidative stress (45, 66). However, more recent evidence supports the premise that asbestos fibers of all lengths, not simply long fibers, induce pathological responses (44, 168). Indeed, different fiber lengths are thought to induce separate pathological outcomes such as asbestosis, mesothelioma and lung cancer (101).

Inhaled large fibers have sufficient inertia to be deposited in the upper respiratory tract, where they are cleared by the mucociliary escalator and therefore do not contribute to pulmonary diseases caused by asbestos (163). Alternatively, fibers that are small enough to bypass the upper respiratory tract and penetrate deeply into the lungs are termed respirable. These respirable fibers are the ones that produce the pathologies associated with asbestos exposure.

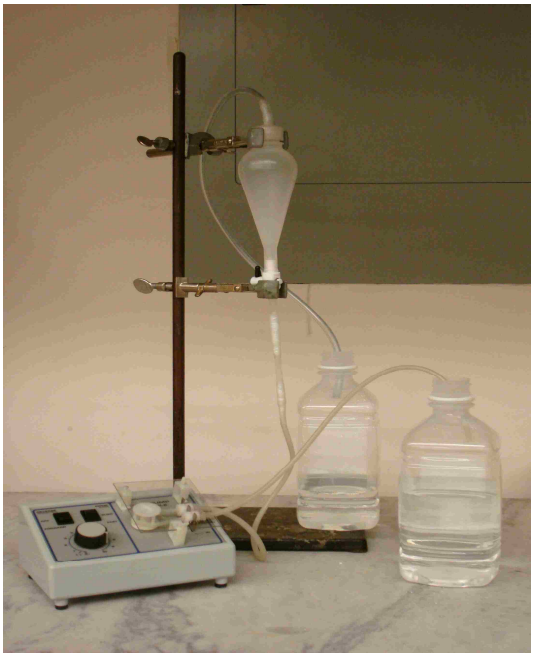

Figure 5.1: A functioning elutriator. Water is drawn from one container and pumped upwards through the funnel, which contains Libby amphibole asbestos fibers. Respirable fibers are eluted out of the top of the funnel, collected in a second container, lyophilized and physically and chemically characterized.

The most important factor of a fiber's respirability is fiber diameter. Fibers that are larger than 5 microns are deposited in the upper respiratory tract and tracheobronchial area (163). The largest alveolar deposition of fibers in the lung occurs when fiber diameters are between 1 and 2 microns (41). Fibers of this size are cleared by alveolar macrophages in the lung (121, 131). Since Libby amphibole asbestos is composed of a diversity of fiber sizes and types, the isolation and utilization of respirable fibers is an important step in mimicking real life asbestos exposure. To this end, the isolation and characterization of respirable Libby amphibole fibers has begun.

With the help of Jim Webber from the Wadsworth Institute in New York, Libby amphibole asbestos fibers have been fractionated according to fiber diameter by subjecting fibers to an elutriation flow, which can separate fibers by aerodynamic diameter. The elutriator (Fig. 5.1) can recover respirable fibers while discarding larger fibers. Taking into account the dimensions of the elutriator, the diameter of respirable fibers (1.5 microns) and the particle density of amphiboles (3.0 grams/cm^2), an elutriation flow rate of 0.6 ml/min will fractionate respirable fibers from the Libby amphibole stock (186). As seen in Figure 5.2, initial fractionations have correctly isolated fibers that are small in diameter and homogenous in morphology. Eluted fibers will be physically and chemically characterized to ensure the correct fiber sizes are recovered during elutriation. A stock of these fibers will then be created and used in all *in vitro* and *in vivo* studies in the Center for Environmental Health Sciences. Moreover, since *in vivo* and *in vitro* exposures are prepared on a per mass basis, fractionation may enhance the amount of biologically active fibers in each exposure.

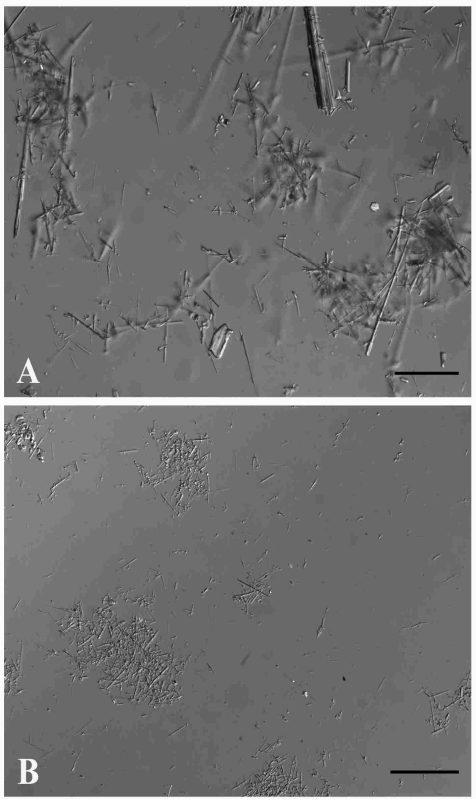

Figure 5.2: Light microscopy picture of two representative fiber fractions. A) Libby amphibole fibers taken from the funnel after elutriation. B) Elutriated (respirable) fibers. Scale bar equals 50 microns.

Another important question that needs to be addressed with respect to asbestos induced autoimmunity is whether apoptotic cells in the presence of amphibole asbestos drive autoimmune responses. Although Libby amphibole induces apoptosis in macrophages, the presence of apoptotic cells alone is not

enough to generate an autoimmune response. Previous studies have shown that intravenous (IV) injections of apoptotic cells (ACs) stimulate the production of autoantibodies only transiently (115). However, ACs coupled with an adjuvant, such as primed dendritic cells or incomplete Freund's adjuvant, generates strong, long-lasting autoimmune responses (12, 175). Therefore, apoptotic cells induced by asbestos, in the presence of amphibole asbestos may stimulate an autoimmune response due to asbestos' ability to serve as an adjuvant, similar to silica (136). To test this hypothesis, bone marrow derived macrophages from C57/BL6 mice can be generated as previously described (25), exposed to Libby amphibole asbestos and subsequently injected IP to produce an immune response. The schedule of IP injections can be similar to a vaccination schedule (Fig. 5.3). The production of antibodies against dsDNA or SSA/Ro52 will be assessed through ELISA. Results from this experiment will indicate whether amphibole asbestos acts as an environmental adjuvant to activate the immune response to target autoantigens usually clustered on the surface of apoptotic cells.

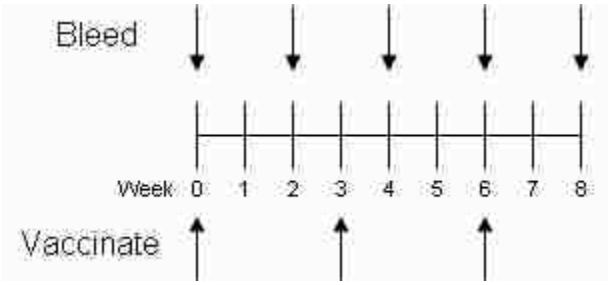

Figure 5.3: Schematic depiction of immunization protocol.

Finally, does the uptake and processing of apoptotic alveolar macrophages by APCs drive asbestos induced autoimmune responses? APC cells, such as dendritic cells (DCs), are necessary in the induction of immune responses. Airway DCs form a network in the bronchial epithelium, capture antigen and migrate to the mediastinal lymph nodes (LNs) where antigen is presented to CD4+ and CD8+ cells (181). Therefore, during

asbestos induced autoimmune responses, airway DCs may play a key role in the uptake of apoptotic alveolar macrophages and the subsequent processing and presentation of antigenic material.

To examine the need for DCs in the induction of autoimmune responses due to asbestos exposure, airway DCs can be conditionally removed from the lung of mice using transgenic mice in which the CD11c promoter element drives the expression of diphtheria toxin receptor (86). Murine cells are normally insensitive to diphtheria toxin because they lack the correct receptor. However, in these transgenic mice, diphtheria toxin can be administered locally to the lungs leading to the ablation of lung CD11c+ cells prior to asbestos exposure. If autoimmune responses in transgenic mice are reduced compared to control mice then airways DCs do play a role in autoimmune responses. To define whether the apoptosis of alveolar macrophages provides antigenic material to elicit autoimmune responses, alveolar macrophages can be depleted from the lung of control and transgenic mice with the use of chlodronate, as previously described (180), then exposed to diphtheria toxin and asbestos as described above. Together these results will provide evidence to either support or challenge the hypothesis that the uptake and processing of apoptotic cells by airway DCs will activate self-reactive T cells, inducing the loss of tolerance and an autoimmune response.

Taking into account the variability of asbestos exposure, the immunological mechanisms at work as well as issues not addressed in this dissertation such as genetic or hormonal predispositions, it is safe to say that the etiology of asbestos induced autoimmunity is extraordinary complicated. Chapter four illustrates that this complexity manifests as an array of autoantibodies that points to, but does not clearly define a clinical autoimmune entity in asbestos exposed individuals. Autoantibodies not only

indicate immune dysfunction, but can also help define both chemical and mechanistic phenomena. Therefore, further characterization of asbestos induced autoimmunity, in collaboration with clinical rheumatologists, is essential. The murine model of asbestos induced autoimmunity also provides an excellent tool to explore the basis of these responses.

The goals of this dissertation were simply 1) to characterize the cellular response by macrophages to Libby amphibole asbestos and 2) to identify a possible molecular mechanism by which autoantigens become immunogenic. This dissertation provides support for the premise that apoptosis may provide the necessary stimulus for environmentally induced autoantibody production.

References

1. 1990. Identifying types of asbestos in the home. United States Environmental Protection Agency.
2. Ahsan, H., A. Ali, and R. Ali. 2003. Oxygen free radicals and systemic autoimmunity. Clin Exp Immunol 131:398-404.
3. Anderson, B. A., S. M. Dearwent, J. T. Durant, J. J. Dyken, J. A. Freed, S. M. Moore, and J. S. Wheeler. 2005. Exposure pathway evaluations for sites that processed asbestos-contaminated vermiculite. Int J Hyg Environ Health 208:55-65.
4. Ashok, B. T., and R. Ali. 1999. Antigen binding characteristics of experimentally-induced antibodies against hydroxyl radical modified native DNA. Autoimmunity 29:11-9.
5. Beckman, J. S., R. L. Minor, Jr., C. W. White, J. E. Repine, G. M. Rosen, and B. A. Freeman. 1988. Superoxide dismutase and catalase conjugated to polyethylene glycol increases endothelial enzyme activity and oxidant resistance. J Biol Chem 263:6884-92.
6. Bernstein, D. M., J. Chevalier, and P. Smith. 2005. Comparison of Calidria chrysotile asbestos to pure tremolite: final results of the inhalation biopersistence and histopathology examination following short-term exposure. Inhal Toxicol 17:427-49.
7. Bernstein, D. M., and J. A. Hoskins. 2006. The health effects of chrysotile: current perspective based upon recent data. Regul Toxicol Pharmacol 45:252-64.
8. Bhattacharya, K., E. Dopp, P. Kakkar, F. N. Jaffery, D. Schiffmann, M. C. Jaurand, I. Rahman, and Q. Rahman. 2005. Biomarkers in risk assessment of asbestos exposure. Mutat Res 579:6-21.
9. Blake, D. J., C. M. Bolin, D. P. Cox, F. Cardozo-Pelaez, and J. C. Pfau. In Press. Internalization of Libby amphibole asbestos and induction of oxidative stress in murine macrophages. Toxicological Sciences.
10. Blake, D. J., and J. C. Pfau. Submitted. Exposure to Libby amphibole asbestos induces apoptosis and the translocation of SSA/Ro52 to cell surface blebs in murine macrophages. Toxicology and Applied Pharmacology.
11. Bolin, C., T. Stedeford, and F. Cardozo-Pelaez. 2004. Single extraction protocol for the analysis of 8-hydroxy-2'-deoxyguanosine (oxo8dG) and the associated activity of 8-oxoguanine DNA glycosylase. J Neurosci Methods 136:69-76.
12. Bondanza, A., V. S. Zimmermann, G. Dell'Antonio, E. D. Cin, G. Balestrieri, A. Tincani, Z. Amoura, J. C. Piette, M. G. Sabbadini, P. Rovere-Querini, and A. A. Manfredi. 2004. Requirement of dying cells and environmental adjuvants for the induction of autoimmunity. Arthritis Rheum 50:1549-60.
13. Bournaud, C., and J. J. Orgiazzi. 2003. Iodine excess and thyroid autoimmunity. J Endocrinol Invest 26:49-56.

14. Boylan, A. M., D. A. Sanan, D. Sheppard, and V. C. Broaddus. 1995. Vitronectin enhances internalization of crocidolite asbestos by rabbit pleural mesothelial cells via the integrin alpha v beta 5. J Clin Invest 96:1987-2001.
15. Brown, J. M., A. J. Archer, J. C. Pfau, and A. Holian. 2003. Silica accelerated systemic autoimmune disease in lupus-prone New Zealand mixed mice. Clin Exp Immunol 131:415-21.
16. Brown, J. M., Pfau, J.C., Pershouse, M.A. and Holian, A. 2004. Silica, Apoptosis and Autoimmunity. Journal of Immunotoxicology 1:177-187.
17. Buettner, G. R. 1993. The pecking order of free radicals and antioxidants: lipid peroxidation, alpha-tocopherol, and ascorbate. Arch Biochem Biophys 300:535-43.
18. Burlingame, R. W., and R. L. Rubin. 1991. Drug-induced anti-histone autoantibodies display two patterns of reactivity with substructures of chromatin. J Clin Invest 88:680-90.
19. Cardinali, G., D. Kovacs, V. Maresca, E. Flori, M. L. Dell'Anna, A. Campopiano, S. Casciardi, G. Spagnoli, M. R. Torrisi, and M. Picardo. 2006. Differential in vitro cellular response induced by exposure to synthetic vitreous fibers (SVFs) and asbestos crocidolite fibers. Exp Mol Pathol 81:31-41.
20. Cardozo-Pelaez, F., S. Song, A. Parthasarathy, C. J. Epstein, and J. Sanchez-Ramos. 1998. Attenuation of age-dependent oxidative damage to DNA and protein in brainstem of Tg Cu/Zn SOD mice. Neurobiol Aging 19:311-6.
21. Caricchio, R., L. McPhie, and P. L. Cohen. 2003. Ultraviolet B radiation-induced cell death: critical role of ultraviolet dose in inflammation and lupus autoantigen redistribution. J Immunol 171:5778-86.
22. Casciola-Rosen, L., F. Wigley, and A. Rosen. 1997. Scleroderma autoantigens are uniquely fragmented by metal-catalyzed oxidation reactions: implications for pathogenesis. J Exp Med 185:71-9.
23. Casciola-Rosen, L. A., G. Anhalt, and A. Rosen. 1994. Autoantigens targeted in systemic lupus erythematosus are clustered in two populations of surface structures on apoptotic keratinocytes. J Exp Med 179:1317-30.
24. Casiano, C. A., S. J. Martin, D. R. Green, and E. M. Tan. 1996. Selective cleavage of nuclear autoantigens during CD95 (Fas/APO-1)-mediated T cell apoptosis. J Exp Med 184:765-70.
25. Celada, A., P. W. Gray, E. Rinderknecht, and R. D. Schreiber. 1984. Evidence for a gamma-interferon receptor that regulates macrophage tumoricidal activity. J Exp Med 160:55-74.
26. Chen, M., A. Dittmann, A. Kuhn, T. Ruzicka, and A. von Mikecz. 2005. Recruitment of topoisomerase I (Scl-70) to nucleoplasmic proteasomes in response to xenobiotics suggests a role for altered antigen processing in scleroderma. Arthritis Rheum 52:877-84.
27. Chen, M., and A. von Mikecz. 2005. Formation of nucleoplasmic protein aggregates impairs nuclear function in response to SiO2 nanoparticles. Exp Cell Res 305:51-62.
28. Chen, M., and A. von Mikecz. 2005. Proteasomal processing of nuclear autoantigens in systemic autoimmunity. Autoimmun Rev 4:117-22.

29. Chen, M., and A. von Mikecz. 2005. Xenobiotic-induced recruitment of autoantigens to nuclear proteasomes suggests a role for altered antigen processing in scleroderma. Ann N Y Acad Sci 1051:382-9.
30. Cheng, N., X. Shi, J. Ye, V. Castranova, F. Chen, S. S. Leonard, V. Vallyathan, and Y. Rojanasakul. 1999. Role of transcription factor NF-kappaB in asbestos-induced TNFalpha response from macrophages. Exp Mol Pathol 66:201-10.
31. Clancy, R. M., P. J. Neufing, P. Zheng, M. O'Mahony, F. Nimmerjahn, T. P. Gordon, and J. P. Buyon. 2006. Impaired clearance of apoptotic cardiocytes is linked to anti-SSA/Ro and -SSB/La antibodies in the pathogenesis of congenital heart block. J Clin Invest 116:2413-22.
32. Clarkson, T. W. 1997. The toxicology of mercury. Critcal reviews in clinical laboratory sciences 34:369-403.
33. Cocco, R. E., and D. S. Ucker. 2001. Distinct modes of macrophage recognition for apoptotic and necrotic cells are not specified exclusively by phosphatidylserine exposure. Mol Biol Cell 12:919-30.
34. Cohen, P. L., R. Caricchio, V. Abraham, T. D. Camenisch, J. C. Jennette, R. A. Roubey, H. S. Earp, G. Matsushima, and E. A. Reap. 2002. Delayed apoptotic cell clearance and lupus-like autoimmunity in mice lacking the c-mer membrane tyrosine kinase. J Exp Med 196:135-40.
35. Cole, R. W., J. G. Ault, J. H. Hayden, and C. L. Rieder. 1991. Crocidolite asbestos fibers undergo size-dependent microtubule-mediated transport after endocytosis in vertebrate lung epithelial cells. Cancer Res 51:4942-7.
36. Conrad, K., J. Mehlhorn, K. Luthke, T. Dorner, and K. H. Frank. 1996. Systemic lupus erythematosus after heavy exposure to quartz dust in uranium mines: clinical and serological characteristics. Lupus 5:62-9.
37. Conrad, K., W. Schlosler, F. Hiepe, and M. J. Fritzler. 2002. Autoantibodies in systemic autoimmune disease. A diagnostic reference. Pabst Science Publishers, Berlin.
38. Cooke, M. S., N. Mistry, C. Wood, K. E. Herbert, and J. Lunec. 1997. Immunogenicity of DNA damaged by reactive oxygen species--implications for anti-DNA antibodies in lupus. Free Radic Biol Med 22:151-9.
39. Cooper, G. S., M. A. Dooley, E. L. Treadwell, E. W. St Clair, C. G. Parks, and G. S. Gilkeson. 1998. Hormonal, environmental, and infectious risk factors for developing systemic lupus erythematosus. Arthritis Rheum 41:1714-24.
40. D'Cruz, D. 2000. Autoimmune diseases associated with drugs, chemicals and environmental factors. Toxicol Lett 112-113:421-32.
41. Dai, Y. T., and C. P. Yu. 1998. Alveolar deposition of fibers in rodents and humans. J Aerosol Med 11:247-58.
42. Devitt, A., K. G. Parker, C. A. Ogden, C. Oldreive, M. F. Clay, L. A. Melville, C. O. Bellamy, A. Lacy-Hulbert, S. C. Gangloff, S. M. Goyert, and C. D. Gregory. 2004. Persistence of apoptotic cells without autoimmune disease or inflammation in CD14-/- mice. J Cell Biol 167:1161-70.

43. Dixon, G., Doria, J., Freed, J., Wood, P., May, I., Chambers, T. 1985. Exposure Assessment for Asbestos-Contaminated Vermiculite. U.S. Environmental Protection Agency, Office of Pesticides and Toxic Substances.

44. Dodson, R. F., M. A. Atkinson, and J. L. Levin. 2003. Asbestos fiber length as related to potential pathogenicity: a critical review. Am J Ind Med 44:291-7.

45. Dogra, S., and K. Donaldson. 1995. Effect of long and short fibre amosite asbestos on in vitro TNF production by rat alveolar macrophages: the modifying effect of lipopolysaccharide. Ind Health 33:131-41.

46. Driscoll, K. E., J. K. Maurer, J. Higgins, and J. Poynter. 1995. Alveolar macrophage cytokine and growth factor production in a rat model of crocidolite-induced pulmonary inflammation and fibrosis. J Toxicol Environ Health 46:155-69.

47. Duriez, P. J., and G. M. Shah. 1997. Cleavage of poly(ADP-ribose) polymerase: a sensitive parameter to study cell death. Biochem Cell Biol 75:337-49.

48. Espinosa, A., W. Zhou, M. Ek, M. Hedlund, S. Brauner, K. Popovic, L. Horvath, T. Wallerskog, M. Oukka, F. Nyberg, V. K. Kuchroo, and M. Wahren-Herlenius. 2006. The Sjogren's syndrome-associated autoantigen Ro52 is an E3 ligase that regulates proliferation and cell death. J Immunol 176:6277-85.

49. Fadok, V. A., D. L. Bratton, A. Konowal, P. W. Freed, J. Y. Westcott, and P. M. Henson. 1998. Macrophages that have ingested apoptotic cells in vitro inhibit proinflammatory cytokine production through autocrine/paracrine mechanisms involving TGF-beta, PGE2, and PAF. J Clin Invest 101:890-8.

50. Fattman, C. L., R. J. Tan, J. M. Tobolewski, and T. D. Oury. 2006. Increased sensitivity to asbestos-induced lung injury in mice lacking extracellular superoxide dismutase. Free Radic Biol Med 40:601-7.

51. Faux, S. P., and P. J. Howden. 1997. Possible role of lipid peroxidation in the induction of NF-kappa B and AP-1 in RFL-6 cells by crocidolite asbestos: evidence following protection by vitamin E. Environ Health Perspect 105 Suppl 5:1127-30.

52. Fink, S. L., and B. T. Cookson. 2005. Apoptosis, pyroptosis, and necrosis: mechanistic description of dead and dying eukaryotic cells. Infect Immun 73:1907-16.

53. Flaherty, D. M., M. M. Monick, A. B. Carter, M. W. Peterson, and G. W. Hunninghake. 2002. Oxidant-mediated increases in redox factor-1 nuclear protein and activator protein-1 DNA binding in asbestos-treated macrophages. J Immunol 168:5675-81.

54. Frisoni, L., L. McPhie, L. Colonna, U. Sriram, M. Monestier, S. Gallucci, and R. Caricchio. 2005. Nuclear autoantigen translocation and autoantibody opsonization lead to increased dendritic cell phagocytosis and presentation of nuclear antigens: a novel pathogenic pathway for autoimmunity? J Immunol 175:2692-701.

55. Fritzler, M. J. 1993. Autoantibodies in scleroderma. J Dermatol 20:257-68.

56. Fritzler, M. J., F. Behmanesh, and M. L. Fritzler. 2006. Analysis of human sera that are polyreactive in an addressable laser bead immunoassay. Clin Immunol.
57. Fritzler, M. J., and E. M. Tan. 1978. Antibodies to histones in drug-induced and idiopathic lupus erythematosus. J Clin Invest 62:560-7.
58. Fung, H., Y. W. Kow, B. Van Houten, and B. T. Mossman. 1997. Patterns of 8-hydroxydeoxyguanosine formation in DNA and indications of oxidative stress in rat and human pleural mesothelial cells after exposure to crocidolite asbestos. Carcinogenesis 18:825-32.
59. Furukawa, F., M. Kashihara-Sawami, M. B. Lyons, and D. A. Norris. 1990. Binding of antibodies to the extractable nuclear antigens SS-A/Ro and SS-B/La is induced on the surface of human keratinocytes by ultraviolet light (UVL): implications for the pathogenesis of photosensitive cutaneous lupus. J Invest Dermatol 94:77-85.
60. Gandhi, R., E. Hussain, J. Das, R. Handa, and R. Pal. 2006. Anti-idiotype-mediated epitope spreading and diminished phagocytosis by a human monoclonal antibody recognizing late-stage apoptotic cells. Cell Death Differ 13:1715-26.
61. Garg, D. K., and R. Ali. 1998. Reactive oxygen species modified polyguanylic acid: immunogenicity and implications for systemic autoimmunity. J Autoimmun 11:371-8.
62. Gilliam, J. N., and R. D. Sontheimer. 1982. Skin manifestations of SLE. Clin Rheum Dis 8:207-18.
63. Golan, T. D., K. B. Elkon, A. E. Gharavi, and J. G. Krueger. 1992. Enhanced membrane binding of autoantibodies to cultured keratinocytes of systemic lupus erythematosus patients after ultraviolet B/ultraviolet A irradiation. J Clin Invest 90:1067-76.
64. Goldman, M., P. Druet, and E. Gleichmann. 1991. TH2 cells in systemic autoimmunity: insights from allogeneic diseases and chemically-induced autoimmunity. Immunol Today 12:223-7.
65. Golladay, S. A., S. H. Park, and A. E. Aust. 1997. Efflux of reduced glutathione after exposure of human lung epithelial cells to crocidolite asbestos. Environ Health Perspect 105 Suppl 5:1273-7.
66. Goodglick, L. A., and A. B. Kane. 1990. Cytotoxicity of long and short crocidolite asbestos fibers in vitro and in vivo. Cancer Res 50:5153-63.
67. Goodglick, L. A., and A. B. Kane. 1986. Role of reactive oxygen metabolites in crocidolite asbestos toxicity to mouse macrophages. Cancer Res 46:5558-66.
68. Gunter, M. E., D. M. Dyar, B. Twamley, F. F. Foit Jr, and S. Cornelius. 2003. Composition, Fe+3/Fe and crystal structure of non-asbestiform and asestiform amphiboles from Libby, Montana, USA. American Mineralogist 89:1579.
69. Halliwell, B., and M. Whiteman. 2004. Measuring reactive species and oxidative damage in vivo and in cell culture: how should you do it and what do the results mean? Br J Pharmacol 142:231-55.

70. Hamilton, R. F., L. L. Iyer, and A. Holian. 1996. Asbestos induces apoptosis in human alveolar macrophages. Am J Physiol 271:L813-9.
71. Hamilton, R. F., Jr., A. Holian, and M. T. Morandi. 2004. A comparison of asbestos and urban particulate matter in the in vitro modification of human alveolar macrophage antigen-presenting cell function. Exp Lung Res 30:147-62.
72. Hanayama, R., M. Tanaka, K. Miyasaka, K. Aozasa, M. Koike, Y. Uchiyama, and S. Nagata. 2004. Autoimmune disease and impaired uptake of apoptotic cells in MFG-E8-deficient mice. Science 304:1147-50.
73. Hansen, K., and B. T. Mossman. 1987. Generation of superoxide (O2-.) from alveolar macrophages exposed to asbestiform and nonfibrous particles. Cancer Res 47:1681-6.
74. Hassan, A. B., I. E. Lundberg, D. Isenberg, and M. Wahren-Herlenius. 2002. Serial analysis of Ro/SSA and La/SSB antibody levels and correlation with clinical disease activity in patients with systemic lupus erythematosus. Scand J Rheumatol 31:133-9.
75. Hess, E. V. 2002. Environmental chemicals and autoimmune disease: cause and effect. Toxicology 181-182:65-70.
76. Hoffman, I. E., I. Peene, L. Meheus, T. W. Huizinga, L. Cebecauer, D. Isenberg, K. De Bosschere, F. Hulstaert, E. M. Veys, and F. De Keyser. 2004. Specific antinuclear antibodies are associated with clinical features in systemic lupus erythematosus. Ann Rheum Dis 63:1155-8.
77. Hogg, B. D., P. K. Dutta, and J. F. Long. 1996. In vitro interaction of zeolite fibers with individual cells (macrophages NR8383): measurement of intracellular oxidative burst. Anal Chem 68:2309-12.
78. Holian, A., M. O. Uthman, T. Goltsova, S. D. Brown, and R. F. Hamilton, Jr. 1997. Asbestos and silica-induced changes in human alveolar macrophage phenotype. Environ Health Perspect 105 Suppl 5:1139-42.
79. Hultman, P., S. Enestrom, K. M. Pollard, and E. M. Tan. 1989. Anti-fibrillarin autoantibodies in mercury-treated mice. Clin Exp Immunol 78:470-7.
80. Igarashi, T., Y. Itoh, Y. Fukunaga, and M. Yamamoto. 1995. Stress-induced cell surface expression and antigenic alteration of the Ro/SSA autoantigen. Autoimmunity 22:33-42.
81. Ishizaki, T., E. Yano, and P. H. Evans. 1997. Cellular mechanisms of reactive oxygen metabolite generation from human polymorphonuclear leukocytes induced by crocidolite asbestos. Environ Res 75:135-40.
82. Jacobson, D. L., S. J. Gange, N. R. Rose, and N. M. Graham. 1997. Epidemiology and estimated population burden of selected autoimmune diseases in the United States. Clin Immunol Immunopathol 84:223-43.
83. Janssen, Y. M., N. H. Heintz, and B. T. Mossman. 1995. Induction of c-fos and c-jun proto-oncogene expression by asbestos is ameliorated by N-acetyl-L-cysteine in mesothelial cells. Cancer Res 55:2085-9.
84. Janssen, Y. M., J. P. Marsh, M. P. Absher, D. Hemenway, P. M. Vacek, K. O. Leslie, P. J. Borm, and B. T. Mossman. 1992. Expression of antioxidant

enzymes in rat lungs after inhalation of asbestos or silica. J Biol Chem 267:10625-30.
85. Joshi, T. K., and R. K. Gupta. 2004. Asbestos in developing countries: magnitude of risk and its practical implications. Int J Occup Med Environ Health 17:179-85.
86. Jung, S., D. Unutmaz, P. Wong, G. Sano, K. De los Santos, T. Sparwasser, S. Wu, S. Vuthoori, K. Ko, F. Zavala, E. G. Pamer, D. R. Littman, and R. A. Lang. 2002. In vivo depletion of CD11c(+) dendritic cells abrogates priming of CD8(+) T cells by exogenous cell-associated antigens. Immunity 17:211-20.
87. Kalla, B., R. F. Hamilton, R. K. Scheule, and A. Holian. 1990. Role of extracellular calcium in chrysotile asbestos stimulation of alveolar macrophages. Toxicol Appl Pharmacol 104:130-8.
88. Kamp, D. W., P. Graceffa, W. A. Pryor, and S. A. Weitzman. 1992. The role of free radicals in asbestos-induced diseases. Free Radic Biol Med 12:293-315.
89. Kamp, D. W., V. A. Israbian, A. V. Yeldandi, R. J. Panos, P. Graceffa, and S. A. Weitzman. 1995. Phytic acid, an iron chelator, attenuates pulmonary inflammation and fibrosis in rats after intratracheal instillation of asbestos. Toxicol Pathol 23:689-95.
90. Kamp, D. W., and S. A. Weitzman. 1999. The molecular basis of asbestos induced lung injury. Thorax 54:638-52.
91. Kazan-Allen, L. 2005. Asbestos and mesothelioma: worldwide trends. Lung Cancer 49 Suppl 1:S3-8.
92. Kim, H. N., Y. Morimoto, T. Tsuda, Y. Ootsuyama, M. Hirohashi, T. Hirano, I. Tanaka, Y. Lim, I. G. Yun, and H. Kasai. 2001. Changes in DNA 8-hydroxyguanine levels, 8-hydroxyguanine repair activity, and hOGG1 and hMTH1 mRNA expression in human lung alveolar epithelial cells induced by crocidolite asbestos. Carcinogenesis 22:265-9.
93. Kinnula, V. L., and J. D. Crapo. 2003. Superoxide dismutases in the lung and human lung diseases. Am J Respir Crit Care Med 167:1600-19.
94. Koerten, H. K., J. Hazekamp, M. Kroon, and W. T. Daems. 1990. Asbestos body formation and iron accumulation in mouse peritoneal granulomas after the introduction of crocidolite asbestos fibers. Am J Pathol 136:141-57.
95. Landrigan, P. J. 1998. Asbestos--still a carcinogen. N Engl J Med 338:1618-9.
96. Lange, A. 1980. An epidemiological survey of immunological abnormalities in asbestos workers. I. Nonorgan and organ-specific autoantibodies. Environ Res 22:162-75.
97. Lange, A. 1980. An epidemiological survey of immunological abnormalities in asbestos workers. II. Serum immunoglobulin levels. Environ Res 22:176-83.
98. Lanzavecchia, A. 1995. How can cryptic epitopes trigger autoimmunity? J Exp Med 181:1945-8.
99. LeFeber, W. P., D. A. Norris, S. R. Ryan, J. C. Huff, L. A. Lee, M. Kubo, S. T. Boyce, B. L. Kotzin, and W. L. Weston. 1984. Ultraviolet light induces binding of antibodies to selected nuclear antigens on cultured human keratinocytes. J Clin Invest 74:1545-51.

100. Li, X. Y., D. Lamb, and K. Donaldson. 1993. The production of TNF-alpha and IL-1-like activity by bronchoalveolar leucocytes after intratracheal instillation of crocidolite asbestos. Int J Exp Pathol 74:403-10.
101. Lippmann, M. 1990. Effects of fiber characteristics on lung deposition, retention, and disease. Environ Health Perspect 88:311-7.
102. Long, J. F., P. K. Dutta, and B. D. Hogg. 1997. Fluorescence imaging of reactive oxygen metabolites generated in single macrophage cells (NR8383) upon phagocytosis of natural zeolite (erionite) fibers. Environ Health Perspect 105:706-11.
103. Lund, L. G., and A. E. Aust. 1991. Iron-catalyzed reactions may be responsible for the biochemical and biological effects of asbestos. Biofactors 3:83-9.
104. Lunec, J., K. Herbert, S. Blount, H. R. Griffiths, and P. Emery. 1994. 8-Hydroxydeoxyguanosine. A marker of oxidative DNA damage in systemic lupus erythematosus. FEBS Lett 348:131-8.
105. Lyons, R., S. Narain, C. Nichols, M. Satoh, and W. H. Reeves. 2005. Effective use of autoantibody tests in the diagnosis of systemic autoimmune disease. Ann N Y Acad Sci 1050:217-28.
106. Mahoney, J. A., and A. Rosen. 2005. Apoptosis and autoimmunity. Curr Opin Immunol 17:583-8.
107. Manders, E. M. M., F. J. Verbeek, and J. A. Aten. 1993. Measurement of co-localisation of objects in dual-colour confocal images. J. Microsc. 169:375-382.
108. Marks-Konczalik, J., A. Gillissen, M. Jaworska, S. Loseke, B. Voss, A. Fisseler-Eckhoff, I. Schmitz, and G. Schultze-Werninghaus. 1998. Induction of manganese superoxide dismutase gene expression in bronchoepithelial cells after rockwool exposure. Lung 176:165-80.
109. Martins, T. B., R. Burlingame, C. A. von Muhlen, T. D. Jaskowski, C. M. Litwin, and H. R. Hill. 2004. Evaluation of multiplexed fluorescent microsphere immunoassay for detection of autoantibodies to nuclear antigens. Clin Diagn Lab Immunol 11:1054-9.
110. Mayes, M. D. 1999. Epidemiologic studies of environmental agents and systemic autoimmune diseases. Environ Health Perspect 107 Suppl 5:743-8.
111. McArthur, C., Y. Wang, P. Veno, J. Zhang, and R. Fiorella. 2002. Intracellular trafficking and surface expression of SS-A (Ro), SS-B (La), poly(ADP-ribose) polymerase and alpha-fodrin autoantigens during apoptosis in human salivary gland cells induced by tumour necrosis factor-alpha. Arch Oral Biol 47:443-8.
112. McDonald, J. C., J. Harris, and B. Armstrong. 2004. Mortality in a cohort of vermiculite miners exposed to fibrous amphibole in Libby, Montana. Occup Environ Med 61:363-6.
113. Meeker, G., A. Bern, I. Brownfield, H. Lowers, S. Sutley, T. Hoefen, and J. Vance. 2003. The Composition and morphology of amphiboles from the Rainy Creek Complex, near Libby, Montana. American Mineralogist 88:1955-1969.

114. Meeker, G. P., A. M. Bern, I. K. Brownfield, H. A. Lowers, S. J. Sutley, T. M. Hoefen, and J. S. Vance. 2003. The Composition and Morphology of Amphiboles from the Rainy Creek Complex, Near Libby, Montana. American Mineralogist 88:1955-1969.

115. Mevorach, D., J. L. Zhou, X. Song, and K. B. Elkon. 1998. Systemic exposure to irradiated apoptotic cells induces autoantibody production. J Exp Med 188:387-92.

116. Mewar, D., and A. G. Wilson. 2006. Autoantibodies in rheumatoid arthritis: a review. Biomed Pharmacother 60:648-55.

117. Migliaccio, C. T., R. F. Hamilton, Jr., and A. Holian. 2005. Increase in a distinct pulmonary macrophage subset possessing an antigen-presenting cell phenotype and in vitro APC activity following silica exposure. Toxicol Appl Pharmacol 205:168-76.

118. Miranda, M. E., C. E. Tseng, W. Rashbaum, R. L. Ochs, C. A. Casiano, F. Di Donato, E. K. Chan, and J. P. Buyon. 1998. Accessibility of SSA/Ro and SSB/La antigens to maternal autoantibodies in apoptotic human fetal cardiac myocytes. J Immunol 161:5061-9.

119. Mitchell, D. A., M. C. Pickering, J. Warren, L. Fossati-Jimack, J. Cortes-Hernandez, H. T. Cook, M. Botto, and M. J. Walport. 2002. C1q deficiency and autoimmunity: the effects of genetic background on disease expression. J Immunol 168:2538-43.

120. Mossman, B. T., J. Bignon, M. Corn, A. Seaton, and J. B. Gee. 1990. Asbestos: scientific developments and implications for public policy. Science 247:294-301.

121. Mossman, B. T., and A. Churg. 1998. Mechanisms in the pathogenesis of asbestosis and silicosis. Am J Respir Crit Care Med 157:1666-80.

122. Mossman, B. T., and J. B. Gee. 1997. Asbestos-related cancer and the amphibole hypothesis. The hypothesis is still supported by scientists and scientific data. Am J Public Health 87:689-90; author reply 690-1.

123. Mossman, B. T., K. Hansen, J. P. Marsh, M. E. Brew, S. Hill, M. Bergeron, and J. Petruska. 1989. Mechanisms of fibre-induced superoxide release from alveolar macrophages and induction of superoxide dismutase in the lungs of rats inhaling crocidolite. IARC Sci Publ:81-92.

124. Mossman, B. T., and J. P. Marsh. 1989. Evidence supporting a role for active oxygen species in asbestos-induced toxicity and lung disease. Environ Health Perspect 81:91-4.

125. Mossman, B. T., J. P. Marsh, and M. A. Shatos. 1986. Alteration of superoxide dismutase activity in tracheal epithelial cells by asbestos and inhibition of cytotoxicity by antioxidants. Lab Invest 54:204-12.

126. Nicholson, W. J., G. Perkel, and I. J. Selikoff. 1982. Occupational exposure to asbestos: population at risk and projected mortality--1980-2030. Am J Ind Med 3:259-311.

127. Nigam, S. K., A. M. Suthar, M. M. Patel, A. B. Karnik, S. K. Dave, S. K. Kashyap, and K. Venkaiah. 1993. Humoral immunological profile of workers exposed to asbestos in asbestos mines. Indian J Med Res 98:274-7.

128. Noonan, C. W., J. C. Pfau, T. C. Larson, and M. R. Spence. 2006. Nested case-control study of autoimmune disease in an asbestos-exposed population. Environ Health Perspect 114:1243-7.
129. Nozawa, K., C. A. Casiano, J. C. Hamel, C. Molinaro, M. J. Fritzler, and E. K. Chan. 2002. Fragmentation of Golgi complex and Golgi autoantigens during apoptosis and necrosis. Arthritis Res 4:R3.
130. Oberdorster, G. 2000. Determinants of the pathogenicity of man-made vitreous fibers (MMVF). Int Arch Occup Environ Health 73 Suppl:S60-8.
131. Oberdorster, G. 1994. Macrophage-associated responses to chrysotile. Ann Occup Hyg 38:601-15, 421-2.
132. Ohlsson, M., R. Jonsson, and K. A. Brokstad. 2002. Subcellular redistribution and surface exposure of the Ro52, Ro60 and La48 autoantigens during apoptosis in human ductal epithelial cells: a possible mechanism in the pathogenesis of Sjogren's syndrome. Scand J Immunol 56:456-69.
133. Oliver, J. E., and A. J. Silman. 2006. Risk factors for the development of rheumatoid arthritis. Scand J Rheumatol 35:169-74.
134. Panduri, V., S. Surapureddi, S. Soberanes, S. A. Weitzman, N. Chandel, and D. W. Kamp. 2006. P53 mediates amosite asbestos-induced alveolar epithelial cell mitochondria-regulated apoptosis. Am J Respir Cell Mol Biol 34:443-52.
135. Panduri, V., S. A. Weitzman, N. S. Chandel, and D. W. Kamp. 2004. Mitochondrial-derived free radicals mediate asbestos-induced alveolar epithelial cell apoptosis. Am J Physiol Lung Cell Mol Physiol 286:L1220-7.
136. Parks, C. G., and G. S. Cooper. 2005. Occupational exposures and risk of systemic lupus erythematosus. Autoimmunity 38:497-506.
137. Patel, V. A., A. Longacre, K. Hsiao, H. Fan, F. Meng, J. E. Mitchell, J. Rauch, D. S. Ucker, and J. S. Levine. 2006. Apoptotic cells, at all stages of the death process, trigger characteristic signaling events that are divergent from and dominant over those triggered by necrotic cells: Implications for the delayed clearance model of autoimmunity. J Biol Chem 281:4663-70.
138. Perkins, R. C., R. K. Scheule, R. Hamilton, G. Gomes, G. Freidman, and A. Holian. 1993. Human alveolar macrophage cytokine release in response to in vitro and in vivo asbestos exposure. Exp Lung Res 19:55-65.
139. Petersen, A. B., R. Gniadecki, and H. C. Wulf. 2000. Laser scanning cytometry for comet assay analysis. Cytometry 39:10-5.
140. Pfau, J. C., J. J. Sentissi, D. J. Blake, S. Li, L. Calderon-Garciduenas, and J. M. Brown. In Press. Asbestos-Induced Autoimmunity in C57Bl/6 Mice. Journal of Immunotoxicology.
141. Pfau, J. C., J. J. Sentissi, G. Weller, and E. A. Putnam. 2005. Assessment of autoimmune responses associated with asbestos exposure in Libby, Montana, USA. Environ Health Perspect 113:25-30.
142. Phan, T. G., R. C. Wong, and S. Adelstein. 2002. Autoantibodies to extractable nuclear antigens: making detection and interpretation more meaningful. Clin Diagn Lab Immunol 9:1-7.
143. Pollard, K. M., D. K. Lee, C. A. Casiano, M. Bluthner, M. M. Johnston, and E. M. Tan. 1997. The autoimmunity-inducing xenobiotic mercury interacts

with the autoantigen fibrillarin and modifies its molecular and antigenic properties. J Immunol 158:3521-8.
144. Pollard, K. M., D. L. Pearson, M. Bluthner, and E. M. Tan. 2000. Proteolytic cleavage of a self-antigen following xenobiotic-induced cell death produces a fragment with novel immunogenic properties. J Immunol 165:2263-70.
145. Popovic, K., S. Brauner, M. Ek, M. Wahren-Herlenius, and F. Nyberg. 2007. Fine specificity of the Ro/SSA autoantibody response in relation to serological and clinical findings in 96 patients with self-reported cutaneous symptoms induced by the sun. Lupus 16:10-7.
146. Provost, T. T., A. Razzaque, P. J. Maddison, and M. Reichlin. 1977. Antibodies to cytoplasmic antigens in lupus erythematosus. Serologic marker for systemic disease. Arthritis Rheum 20:1457-63.
147. Rahman, I., S. K. Biswas, and A. Kode. 2006. Oxidant and antioxidant balance in the airways and airway diseases. Eur J Pharmacol 533:222-39.
148. Ravichandran, K. S. 2003. "Recruitment signals" from apoptotic cells: invitation to a quiet meal. Cell 113:817-20.
149. Reddy, S. M., K. H. Hsiao, V. E. Abernethy, H. Fan, A. Longacre, W. Lieberthal, J. Rauch, J. S. Koh, and J. S. Levine. 2002. Phagocytosis of apoptotic cells by macrophages induces novel signaling events leading to cytokine-independent survival and inhibition of proliferation: activation of Akt and inhibition of extracellular signal-regulated kinases 1 and 2. J Immunol 169:702-13.
150. Rodnan, G. P., T. G. Benedek, T. A. Medsger, Jr., and R. J. Cammarata. 1967. The association of progressive systemic sclerosis (scleroderma) with coal miners' pneumoconiosis and other forms of silicosis. Ann Intern Med 66:323-34.
151. Roney, P. L., and A. Holian. 1989. Possible mechanism of chrysotile asbestos-stimulated superoxide anion production in guinea pig alveolar macrophages. Toxicol Appl Pharmacol 100:132-44.
152. Rosen, A., and L. Casciola-Rosen. 2004. Altered autoantigen structure in Sjogren's syndrome: implications for the pathogenesis of autoimmune tissue damage. Crit Rev Oral Biol Med 15:156-64.
153. Rosen, A., and L. Casciola-Rosen. 1999. Autoantigens as substrates for apoptotic proteases: implications for the pathogenesis of systemic autoimmune disease. Cell Death Differ 6:6-12.
154. Rosen, A., and L. Casciola-Rosen. 2001. Clearing the way to mechanisms of autoimmunity. Nat Med 7:664-5.
155. Routsias, J. G., P. G. Vlachoyiannopoulos, and A. G. Tzioufas. 2006. Autoantibodies to intracellular autoantigens and their B-cell epitopes: molecular probes to study the autoimmune response. Crit Rev Clin Lab Sci 43:203-48.
156. Saegusa, J., S. Kawano, M. Koshiba, N. Hayashi, H. Kosaka, Y. Funasaka, and S. Kumagai. 2002. Oxidative stress mediates cell surface expression of SS-A/Ro antigen on keratinocytes. Free Radic Biol Med 32:1006-16.
157. Salomonsson, S., S. E. Sonesson, L. Ottosson, S. Muhallab, T. Olsson, M. Sunnerhagen, V. K. Kuchroo, P. Thoren, E. Herlenius, and M. Wahren-

Herlenius. 2005. Ro/SSA autoantibodies directly bind cardiomyocytes, disturb calcium homeostasis, and mediate congenital heart block. J Exp Med 201:11-7.

158. Sava, V., D. Mosquera, S. Song, F. Cardozo-Pelaez, and J. R. Sanchez-Ramos. 2004. Effects of melanin and manganese on DNA damage and repair in PC12-derived neurons. Free Radic Biol Med 36:1144-54.

159. Schneider, A. 1999. Deadly orse was shipped around US, Canada, Seattle Post-Intelligencer, Seattle, WA.

160. Schneider, J. C., G. L. Card, J. C. Pfau, and A. Holian. 2005. Air pollution particulate SRM 1648 causes oxidative stress in RAW 264.7 macrophages leading to production of prostaglandin E2, a potential Th2 mediator. Inhal Toxicol 17:871-7.

161. Scott, R. S., E. J. McMahon, S. M. Pop, E. A. Reap, R. Caricchio, P. L. Cohen, H. S. Earp, and G. K. Matsushima. 2001. Phagocytosis and clearance of apoptotic cells is mediated by MER. Nature 411:207-11.

162. Shukla, A., M. Ramos-Nino, and B. Mossman. 2003. Cell signaling and transcription factor activation by asbestos in lung injury and disease. Int J Biochem Cell Biol 35:1198-209.

163. Shusterman, D. 2003. Toxicology of nasal irritants. Curr Allergy Asthma Rep 3:258-65.

164. Simeonova, P. P., and M. I. Luster. 1995. Iron and reactive oxygen species in the asbestos-induced tumor necrosis factor-alpha response from alveolar macrophages. Am J Respir Cell Mol Biol 12:676-83.

165. Sjostrand, M., R. Rylander, and R. Bergstrom. 1989. Lung cell reactions in guinea pigs after inhalation of asbestos (amosite). Toxicology 57:1-14.

166. Stanton, M. F., M. Layard, A. Tegeris, E. Miller, M. May, E. Morgan, and A. Smith. 1981. Relation of particle dimension to carcinogenicity in amphibole asbestoses and other fibrous minerals. J Natl Cancer Inst 67:965-75.

167. Sullivan, P. A. 2007. Vermiculite, respiratory disease, and asbestos exposure in Libby, Montana: update of a cohort mortality study. Environ Health Perspect 115:579-85.

168. Suzuki, Y., S. R. Yuen, and R. Ashley. 2005. Short, thin asbestos fibers contribute to the development of human malignant mesothelioma: pathological evidence. Int J Hyg Environ Health 208:201-10.

169. Tamura, M., T. Tokuyama, H. Kasuga, T. Yoneda, R. Miyazaki, and N. Narita. 1996. [Study on correlation between chest X-P course findings and change in antinuclear antibody in asbestos plant employees]. Sangyo Eiseigaku Zasshi 38:138-41.

170. Tan, R. J., C. L. Fattman, S. C. Watkins, and T. D. Oury. 2004. Redistribution of pulmonary EC-SOD after exposure to asbestos. J Appl Physiol 97:2006-13.

171. Tatrai, E., Z. Kovacikova, M. Brozik, and E. Six. 2004. Pulmonary toxicity of wollastonite in vivo and in vitro. J Appl Toxicol 24:147-54.

172. ter Borg, E. J., G. Horst, E. J. Hummel, P. C. Limburg, and C. G. Kallenberg. 1990. Measurement of increases in anti-double-stranded DNA

antibody levels as a predictor of disease exacerbation in systemic lupus erythematosus. A long-term, prospective study. Arthritis Rheum 33:634-43.

173. Thompson, D., A. Juby, and P. Davis. 1993. The clinical significance of autoantibody profiles in patients with systemic lupus erythematosus. Lupus 2:15-9.

174. Tice, R. R., P. W. Andrews, O. Hirai, and N. P. Singh. 1991. The single cell gel (SCG) assay: an electrophoretic technique for the detection of DNA damage in individual cells. Adv Exp Med Biol 283:157-64.

175. Tzeng, T. C., J. L. Suen, and B. L. Chiang. 2006. Dendritic cells pulsed with apoptotic cells activate self-reactive T-cells of lupus mice both in vitro and in vivo. Rheumatology (Oxford) 45:1230-7.

176. Ulanet, D. B., N. A. Flavahan, L. Casciola-Rosen, and A. Rosen. 2004. Selective cleavage of nucleolar autoantigen B23 by granzyme B in differentiated vascular smooth muscle cells: insights into the association of specific autoantibodies with distinct disease phenotypes. Arthritis Rheum 50:233-41.

177. Ulanet, D. B., M. Torbenson, C. V. Dang, L. Casciola-Rosen, and A. Rosen. 2003. Unique conformation of cancer autoantigen B23 in hepatoma: a mechanism for specificity in the autoimmune response. Proc Natl Acad Sci U S A 100:12361-6.

178. Vallyathan, V., J. F. Mega, X. Shi, and N. S. Dalal. 1992. Enhanced generation of free radicals from phagocytes induced by mineral dusts. Am J Respir Cell Mol Biol 6:404-13.

179. van Engeland, M., F. C. Ramaekers, B. Schutte, and C. P. Reutelingsperger. 1996. A novel assay to measure loss of plasma membrane asymmetry during apoptosis of adherent cells in culture. Cytometry 24:131-9.

180. Van Rooijen, N., and A. Sanders. 1996. Kupffer cell depletion by liposome-delivered drugs: comparative activity of intracellular clodronate, propamidine, and ethylenediaminetetraacetic acid. Hepatology 23:1239-43.

181. Vermaelen, K. Y., I. Carro-Muino, B. N. Lambrecht, and R. A. Pauwels. 2001. Specific migratory dendritic cells rapidly transport antigen from the airways to the thoracic lymph nodes. J Exp Med 193:51-60.

182. von Muhlen, C. A., and E. M. Tan. 1995. Autoantibodies in the Diagnosis of Systemic Rheumatic Diseases. Seminars in Arthritis and Rheumatism 24:323-358.

183. Wada, K., and T. Kamitani. 2006. Autoantigen Ro52 is an E3 ubiquitin ligase. Biochem Biophys Res Commun 339:415-21.

184. Walport, M. J., K. A. Davies, and M. Botto. 1998. C1q and systemic lupus erythematosus. Immunobiology 199:265-85.

185. Ward, T. J., T. Spear, J. Hart, C. Noonan, A. Holian, M. Getman, and J. S. Webber. 2006. Trees as reservoirs for amphibole fibers in Libby, Montana. Sci Total Environ 367:460-5.

186. Webber, J. S. 1999. A Paleolimnological Reconstruction of Airbourne Asbestos Concentrations in the Fibrous-Talc Region of St. Lawrence County, New York from 1872 to 1998. The State University of New York (SUNY) - Albany, Albany, NY.

187. Weitzman, S. A., J. F. Chester, and P. Graceffa. 1988. Binding of deferoxamine to asbestos fibers in vitro and in vivo. Carcinogenesis 9:1643-5.
188. Weitzman, S. A., and P. Graceffa. 1984. Asbestos catalyzes hydroxyl and superoxide radical generation from hydrogen peroxide. Arch Biochem Biophys 228:373-6.
189. Whitehouse, A. C. 2004. Asbestos-related pleural disease due to tremolite associated with progressive loss of lung function: serial observations in 123 miners, family members, and residents of Libby, Montana. Am J Ind Med 46:219-25.
190. Wright, R. S., J. L. Abraham, P. Harber, B. R. Burnett, P. Morris, and P. West. 2002. Fatal asbestosis 50 years after brief high intensity exposure in a vermiculite expansion plant. Am J Respir Crit Care Med 165:1145-9.
191. Wu, X., C. Molinaro, N. Johnson, and C. A. Casiano. 2001. Secondary necrosis is a source of proteolytically modified forms of specific intracellular autoantigens: implications for systemic autoimmunity. Arthritis Rheum 44:2642-52.
192. Wylie, A. G., and J. R. Verkouteren. 2000. Amphibole asbestos from Libby, Montana, aspects of nomenclature. American Mineralogist 85:1540-1542.
193. Xia, T., M. Kovochich, J. Brant, M. Hotze, J. Sempf, T. Oberley, C. Sioutas, J. I. Yeh, M. R. Wiesner, and A. E. Nel. 2006. Comparison of the abilities of ambient and manufactured nanoparticles to induce cellular toxicity according to an oxidative stress paradigm. Nano Lett 6:1794-807.
194. Xiao, G. G., M. Wang, N. Li, J. A. Loo, and A. E. Nel. 2003. Use of proteomics to demonstrate a hierarchical oxidative stress response to diesel exhaust particle chemicals in a macrophage cell line. J Biol Chem 278:50781-90.
195. Xu, A., H. Zhou, D. Z. Yu, and T. K. Hei. 2002. Mechanisms of the genotoxicity of crocidolite asbestos in mammalian cells: implication from mutation patterns induced by reactive oxygen species. Environ Health Perspect 110:1003-8.
196. Yamaguchi, R., T. Hirano, Y. Ootsuyama, S. Asami, Y. Tsurudome, S. Fukada, H. Yamato, T. Tsuda, I. Tanaka, and H. Kasai. 1999. Increased 8-hydroxyguanine in DNA and its repair activity in hamster and rat lung after intratracheal instillation of crocidolite asbestos. Jpn J Cancer Res 90:505-9.
197. Yamaki, K., J. Hong, K. Hiraizumi, J. W. Ahn, O. Zee, and K. Ohuchi. 2002. Participation of various kinases in staurosporine induced apoptosis of RAW 264.7 cells. J Pharm Pharmacol 54:1535-44.
198. Yarborough, C. M. 2007. The risk of mesothelioma from exposure to chrysotile asbestos. Curr Opin Pulm Med 13:334-8.
199. Zamansky, G. B., D. F. Minka, C. L. Deal, and K. Hendricks. 1985. The in vitro photosensitivity of systemic lupus erythematosus skin fibroblasts. J Immunol 134:1571-6.
200. Zerva, L. V., S. H. Constantopoulos, and H. M. Moutsopoulos. 1989. Humoral immunity alterations after environmental asbestos exposure. Respiration 55:237-41.

201. Zhao, H., S. Kalivendi, H. Zhang, J. Joseph, K. Nithipatikom, J. Vasquez-Vivar, and B. Kalyanaraman. 2003. Superoxide reacts with hydroethidine but forms a fluorescent product that is distinctly different from ethidium: potential implications in intracellular fluorescence detection of superoxide. Free Radic Biol Med 34:1359-68.